

OCS Study  
BOEM 2018-024

# Marine Arctic Ecosystem Study— Biophysical and Chemical Observations From Glider and Benthic Surveys in 2016



US Department of the Interior  
Bureau of Ocean Energy Management  
Alaska Region

**BOEM**  
BUREAU OF OCEAN ENERGY MANAGEMENT

# Marine Arctic Ecosystem Study— Biophysical and Chemical Observations From Glider and Benthic Surveys in 2016

April 2018

Authors:

Francis K. Wiese – MARES Technical Director (Stantec)  
H. Rodger Harvey – Biogeochemistry Lead (ODU)  
Rachel McMahon – Biogeochemistry Team (ODU)  
Pam Neubert – Benthic Taxonomy Lead (Stantec)  
Donglai Gong – Glider Lead (VIMS)  
Haixing Wang – Glider Team (VIMS)  
Jeanna Hudson – Glider Team (VIMS)  
Robert Pickard – Moorings Lead (WHOI)  
Ed Ross – Moorings Lead (ASL)  
Matt Charette – Nutrient Analysis Lead (WHOI)  
Michael Fabijan – Consultations and Permitting Lead (Kavik-Stantec)  
Rowenna D. Gryba – MARES Task Order Manager (Stantec)

Prepared under BOEM Award  
M14PC00008 – Task Order No. M15PD00012

By  
Stantec Consulting Services Inc.  
4500 Daley Dr., Suite 100  
Chantilly, VA 20151-3724





## **DISCLAIMER**

Study concept, oversight, and funding were provided by the US Department of the Interior, Bureau of Ocean Energy Management (BOEM), Environmental Studies Program, Washington, DC, under Contract Number M14PC00008. This report has been technically reviewed by BOEM, and it has been approved for publication. The views and conclusions contained in this document are those of the authors and should not be interpreted as representing the opinions or policies of the US Government, nor does mention of trade names or commercial products constitute endorsement or recommendation for use.

## **REPORT AVAILABILITY**

To download a PDF file of this report, go to the US Department of the Interior, Bureau of Ocean Energy Management [Data and Information Systems webpage \(http://www.boem.gov/Environmental-Studies-EnvData/\)](http://www.boem.gov/Environmental-Studies-EnvData/), click on the link for the Environmental Studies Program Information System (ESPIS), and search on 2018-024. The report is also available at the National Technical Reports Library at <https://ntrl.ntis.gov/NTRL/>.

## **CITATION**

Wiese FK, Harvey HR, McMahon R, Neubert P, Gong D, Wang H, Hudson J, Pickard R, Ross E, Fabijan M, Gryba RD. 2018. Marine Arctic Ecosystem Study—Biophysical and chemical observations from glider and benthic surveys in 2016. Anchorage (AK): US Department of the Interior, Bureau of Ocean Energy Management. OCS Study BOEM 2018-024. 98 p.

## **ABOUT THE COVER**

Photo Credit: J. Bartlett, ASL

## **ACKNOWLEDGMENTS**

We would like to acknowledge the support provided by the Stantec MARES team: Diane Ingraham, Jeff Green, Cathy Finnie, Barry Keough, Melissa Gandy and Ally Sullivan. We would like to also acknowledge COR, Guillermo Auad, and the contributions of John Nelson, Dave Fissel, and Carin Ashjian on the mooring array design and location.

# Contents

List of Figures.....	iii
List of Tables.....	v
List of Abbreviations and Acronyms.....	vi
1 Overview .....	1
1.1 Background .....	1
1.2 Biophysical and Chemical Program Goals and Objectives.....	1
1.3 Study Design and Implementation .....	1
1.3.1 Study Design .....	1
1.3.2 Implementation 2015.....	2
1.3.3 Implementation 2016.....	2
1.4 Community Consultations .....	3
1.5 Permitting .....	3
2 AUV Glider Component .....	4
2.1 Introduction.....	4
2.2 Methods.....	4
2.2.1 Glider Setup and Sensor Suite.....	4
2.2.2 Glider Preparation for 2016 .....	5
2.2.3 2016 Glider Survey Plan .....	5
2.2.4 Glider Deployment.....	6
2.2.5 Piloting.....	7
2.2.6 Glider Recovery.....	7
2.2.7 MARES Glider Data Management and QA/QC .....	7
2.2.8 Ocean Data and Ocean Model Output Used for Analysis .....	8
2.3 Results .....	9
2.3.1 Characterization of the Physical Oceanographic Setting.....	9
2.3.2 Hydrography & Water Masses .....	13
2.3.3 Circulation Based on Glider Observations .....	16
2.3.4 Characterization of the Bio-Optical Conditions .....	16
2.3.5 Variability of Hydrography and Circulation .....	18
2.3.6 Wind-Driven Circulation .....	22
2.4 Discussion .....	28
2.4.1 Connection Between Beaufort Shelf and Beaufort Gyre .....	29
2.4.2 Multi-Year Variability of Zonal Winds in the Beaufort Sea .....	29

2.4.3	Fate of the Mackenzie Plume.....	30
2.5	Conclusions.....	30
2.6	Limitations of the MARES Glider Survey .....	31
2.7	Future Research .....	31
3	Mooring Array.....	33
3.1	Introduction.....	33
3.2	Methods.....	33
3.2.1	Field Methods and Equipment .....	33
3.3	Results and Conclusions.....	39
4	Linking Organic Carbon Sources with Meiofauna Abundance and Diversity .....	43
4.1	Introduction.....	43
4.2	Methods.....	43
4.2.1	Sampling Locations .....	43
4.2.2	Water Column Particles .....	44
4.2.3	Sediments .....	44
4.2.4	Total Organic Carbon.....	45
4.2.5	Grain Size.....	45
4.2.6	Meiofaunal Abundance and Diversity .....	45
4.2.7	Organic Biomarkers.....	45
4.2.8	Lipid Markers.....	46
4.3	Results .....	47
4.3.1	Water Structure Across the Shelf.....	47
4.3.2	Total Carbon and Grain Size.....	51
4.3.3	Organic Markers.....	52
4.3.4	Fatty Acids and Sterol Biomarkers.....	55
4.3.5	Meiofaunal Community .....	56
4.4	Discussion .....	59
4.5	Summary.....	62
4.6	Future Research .....	62
5	Conclusions.....	63
6	References.....	64
	Appendix A: 2015 Post-Cruise Report.....	67
	Appendix B: Feeding Guilds and Abundance .....	95

## List of Figures

Figure 1. Slocum G2 Glider.....	5
Figure 2. Planned 2016 glider mission, showing locations of proposed moorings.....	6
Figure 3. Map of the Mackenzie Trough. Bathymetry from the National Oceanic and Atmospheric Administration (NOAA) and bathymetry contours from Geological Survey of Canada.....	10
Figure 4. Climatology plot of Mackenzie River discharge for the period 1973 to 2011. ....	11
Figure 5. Wind rose histograms for Herschel Island (2006–2017) for August, September, and October. .	12
Figure 6. Plot of wind vectors and speed.....	13
Figure 7. Map of the Mackenzie Trough region overlaid with glider tracks (purple) and depth-average velocity estimates (blue arrows).....	14
Figure 8. Plots of potential temperature (left) and salinity (right) versus days of deployment (August 15–October 6, 2016). ....	15
Figure 9. Temperature-Salinity (T/S) plot for MARES 2016 glider deployment.....	16
Figure 10. Plots of: (a) chlorophyll-a fluorescence, (b) CDOM fluorescence, (c) dissolved oxygen saturation, and (d) optical backscattering for the MARES glider study from August 15, 2016, to October 6, 2016. ....	17
Figure 11. Time series of the photosynthetically available radiation (PAR). ....	18
Figure 12. Satellite MODIS remote sensing true color images of the Mackenzie Trough region from late August to early October 2016. ....	19
Figure 13. Mixed layer depth (MLD) during the glider deployment.....	20
Figure 14. Sub-mesoscale variability in the along-canyon axis transect from Sept.11–16, 2016. ....	21
Figure 15. Plot of temperature and salinity as well as heat and salt fluxes for two along-canyon axis glider transects.....	22
Figure 16. NARR daily composite of surface vector winds for the Mackenzie Trough region.....	23
Figure 17. Glider path (blue) and glider estimated depth-averaged velocities (red arrows) overlaid on top of HYCOM sea surface height field and depth-averaged currents (upper 200 m of the water column).....	24
Figure 18. Cross-shelf glider sections of temperature and salinity showing the hydrographic responses during strong eastward flow (left panel) and strong westward flow (right panel) conditions. ....	25
Figure 19. Top panels: NARR monthly mean surface winds for September 2011 (left) and September 2016 (right). Bottom panels: HYCOM depth-averaged currents and sea surface heights for September 2011 (left) and September 2016 (right).....	26
Figure 20. Climatological NARR winds for (a) July, (b) August, (c) September, and (d) October. ....	27
Figure 21. Average NARR surface summer (July–October) winds for (a) 2012–2017, (b) 2005–2011, (c) 2000–2004. (d) An illustration of the major currents in the Chukchi and Beaufort Seas (adopted from Schulze et al. 2013). ....	28

Figure 22. Summertime zonally averaged wind speed for the Chukchi-Beaufort shelf and slope region (1948 to 2017 NCEP reanalysis). .....	30
Figure 23. Profile plot of glider temperature (red), chlorophyll-a (green), light (blue), and density (black) measurements for two glider transects during MARES 2016. ....	32
Figure 24. Locations of the moorings comprising the composite MARES/UAF/DFO array (see the legend). Also shown are the locations of the CTD stations occupied during the deployment cruise. ....	33
Figure 25. WHOI moorings M1 and M2. ....	35
Figure 26. Mooring M3 and M4 (ASL). ....	36
Figure 27. Instrumentation on the UAF, WHOI, and ASL moorings. ....	37
Figure 28. Vertical section of potential temperature ( $^{\circ}\text{C}$ , color), as estimated from the CTD casts, overlain by potential density ( $\text{kg}/\text{m}^3$ , contours), occupied during the deployment cruise. ....	40
Figure 29. Vertical section of potential salinity, as estimated from the CTD casts, and locations of the UAF, WHOI, and ASL moorings. ....	41
Figure 30. Profiles of water data collected at the mooring locations and at the midpoint along the MARES mooring line in October 2016 (note different y-axis scales for each row of data). ....	42
Figure 31. Physical parameters of station M1 at the time of sampling. ....	48
Figure 32. Physical parameters of station M2 at the time of sampling. ....	49
Figure 33. Physical parameters of station M3 at the time of sampling. ....	50
Figure 34. Physical parameters of station M4 at the time of sampling. ....	51
Figure 35. Grain size across the four shelf stations of the Mackenzie shelf transect. ....	52
Figure 36. Measure of total hydrolysable amino acids (THAA) normalized to organic carbon microgram in particles and sediments across the Mackenzie shelf. ....	53
Figure 37. Distribution of individual amino acids in each sample represented in a unit of relative abundance, percent of each amino acid that contributes toward the total sum of all amino acids in that sample. ....	54
Figure 38. A) The % GABA as fraction of total amino acids in surface sediments across the MARES transect plus the AIM pelagic site for comparison. B) The % GABA as fraction of amino acids in POM collected at the fluorescence maximum at available water column sites. ....	55
Figure 39. The distribution and abundance of major sterol markers plus phytol across the Mackenzie shelf transect. ....	56
Figure 40: Meiofaunal abundances and biomass that represent the majority of the benthic community in the meio size range. ....	59
Figure 41. Lipid and amino acid biomarkers of marine origin (panel A) verses summed organic markers both of terrestrial and marine organic matter (panel B). ....	61

## List of Tables

Table 1. UAF, WHOI, and ASL moorings deployed on the CCGS <i>Sir Wilfrid Laurier</i> cruise.....	38
Table 2. List of the instrumentation contained on the WHOI and ASL moorings. ....	38
Table 3. Sampling locations for water and sediment collections. ....	44
Table 4. Water column sample collection and depths (m) at each station. ....	44
Table 5. Locations of sediment collections for organic and meiofaunal analysis .....	45
Table 6. Organic carbon content of all samples from the water column and surface sediments. ....	52
Table 7. Calculated wet and dry weight biomass (grams) based on literature values for major meiofaunal taxonomic groups identified from MARES cross-shelf transect.....	58



## List of Abbreviations and Acronyms

ADCP	acoustic doppler current profiler
AEWC	Alaska Eskimo Whaling Commission
AIM	artic ice monitoring
AOOS	Alaska Ocean Observing System
ASCII	American Standard Code for Information Interchange
ASL	ASL Environmental Science, LLC
AURAL	aural whale recorder
AUV	autonomous underwater vehicle
AZFP	acoustic zooplankton fish profiler
BOEM	Bureau of Ocean Energy Management
CCGS	Canadian Coast Guard Ship
CDOM	colored dissolved organic matter
CO	Contracting Officer
COR	Contracting Officer's Representative
CTD	conductivity-temperature-depth
db	decibar
DBD	Dinkum Binary Data (other file formats: SBD, EBD, TBD)
DFO	Department of Fisheries and Oceans, Canada
DIC	dissolved inorganic carbon
DO	dissolved oxygen
EOSDIS	Earth Observing System Data and Information System
ESI	electrospray ionization
FJMC	Fisheries Joint Management Council
g/OC	gram per organic carbon
GABA	gamma aminobutyric acid
GC-MS	gas chromatography-mass spectrometry
GOFS	Global Ocean Forecast System
GPS	global positioning system
HCl	hydrogen chloride
HTC	Hunters and Trappers Committee
HYCOM	Hybrid Coordinate Ocean Model
IBCAO	International Bathymetric Chart of the Arctic Ocean
IGC	Inuvialuit Game Council
IOS	Institute of Ocean Sciences
IPS	ice profiling sonar
LC-MS	liquid chromatography-mass spectrometry
M	mol
MARES	Marine Arctic Ecosystem Study
mg/L	milligrams/liter
MLD	mixed layer depth
µm	micron
µmol/L	micro-mol/Liter

MODIS	Moderate Resolution Imaging Spectroradiometer
MS	Mass Selective
Mt	metric ton
m/z	mass divided by charge number
N	normal
NaOH	sodium hydroxide (a salt)
NARR	North Atlantic Regional Reanalysis
NCEP	National Centers for Environmental Prediction
NCODA	Navy Coupled Ocean Data
nm	nautical miles
NOAA	National Oceanic and Atmospheric Administration
ODU	Old Dominion University
ORE PORT	acoustic release
PAR	photosynthetically active radiation
PFTBA	perfluorotributylamine
PI	Principal Investigator
POC	particulate organic carbon
POM	particulate organic matter
ppb	parts per billion
psu	practical salinity unit
PUFA	polyunsaturated fatty acid
QA/QC	quality assurance and quality control
RGB	red-green-blue color space
RO	reverse osmosis
RSLC	rapid separation liquid chromatography
SOP	synthetic ocean profile
Sv	salt transport; 1 Sv=10 <sup>6</sup> m <sup>3</sup> /s
THAA	total hydrolysable amino acids
TOC	total organic carbon
T/S	temperature/salinity
T/S/P	temperature/salinity/pressure
TW	terrawatt
TWR	Teledyne Web Research
UAF	University of Alaska Fairbanks
ULS	upward looking sonar
USCGC	United States Coast Guard Cutter
UV	ultraviolet
V	volt
VIMS	Virginia Institute of Marine Science
WHOI	Woods Hole Oceanographic Institute
XBT	expendable bathythermograph

# 1 Overview

## 1.1 Background

The Department of the Interior, Bureau of Ocean Energy Management (BOEM) and its partners, ONR, NOPP, Shell, USARC, US Coast Guard, seek to advance knowledge of the Arctic marine ecosystem. The Marine Arctic Ecosystem Study (MARES) arose from increased attention on climate change, energy development, and related sustainability issues in the Arctic. Results from this study are intended to inform government, industry, and communities on regulatory needs, operational challenges, and resource management and provide important context for economic development, environmental protection, sustainability of local communities, and health and safety.

The focus area of MARES is the eastern Beaufort Sea shelf from Kaktovik to the Mackenzie Delta coastline to a depth of 1,000 m. The overarching scientific goal of MARES, as initially envisioned, was to increase our understanding of the impact of physical drivers (ocean, ice, atmosphere) on the trophic structure and function of the marine ecosystem on the Beaufort shelf with special attention to the implications on marine mammals and local communities. The intent was to implement an integrated, multidisciplinary study combining retrospective analyses, field studies, modeling, and synthesis spanning atmosphere, ice, physical, chemical, and biological oceanography from benthos to fish, marine mammals, and people.

## 1.2 Biophysical and Chemical Program Goals and Objectives

The *Biophysical and Chemical Program* is one component implemented to support the broader MARES objectives. The goals of this component were to:

- Collect physical, biological, and chemical observations in the Eastern Beaufort Sea from moving and moored platforms
- Describe and analyze physical, biological, and chemical observations acquired from the moving platforms
- Simultaneously with the mooring deployment operation, gather water and sediment samples at the mooring locations and process and analyze these samples to estimate the carbon budget and describe carbon cycling processes

These objectives were implemented through a field program conducted in 2016 and took advantage of some new partnership opportunities fostered by Stantec.

## 1.3 Study Design and Implementation

### 1.3.1 Study Design

Stantec partnered with Old Dominion University (ODU), Woods Hole Oceanographic Institution (WHOI), ASL Environmental Sciences (ASL), Virginia Institute of Marine Sciences (VIMS), Department of Fisheries and Ocean Canada (DFO), University of Washington (UW), University of Alaska Fairbanks (UAF), and Kavik-Stantec Inc. to conduct community consultations and collect and analyze biophysical and chemical data needed to fulfill the objectives and goals of this study. Field and analytical study components developed were:

- Deployment of a glider to profile transects in the same region as the mooring deployment and provide high resolution biophysical and chemical data
- Deployment of moorings to acquire biophysical and chemical time series in the study region
- Sampling benthic carbon near the moorings that transected the Mackenzie River-Yukon Shelf region.

These three field and study components provided an integrated approach to describe the biogeochemical impact of the Mackenzie River plume in the study area. A total of five moorings (three on the shelf and two on the shelfbreak) were deployed for approximately 12 months. These provided a continuous biophysical and chemical time series, as well as calibration data for the glider sensors. The moorings were equipped with a combination of sensors to measure fluorescence, conductivity, temperature, depth, current velocities, abundance of zooplankton and fish, and passive acoustics. To provide additional, high resolution data in the region of the moorings, an autonomous glider was equipped with similar sensors to measure oxygen, fluorescence, conductivity, temperature, depth, current velocities, and abundance of zooplankton and fish. The glider collected data along the mooring array and along the shelf and shelfbreak. The benthic carbon sampling was intended to provide estimates on carbon cycling processes associated with the Mackenzie River plume.

### **1.3.2 Implementation 2015**

There was an initial field effort in 2015 that planned for deployment of an autonomous glider between Kaktovik, AK, and the McKenzie Delta for approximately six weeks starting in mid-August, and deployment of a biophysical and chemical mooring array in the eastern US Beaufort Sea along the US-Canada border.

The United States Coast Guard Cutter (USCGC) *Sycamore* was loaded with mooring equipment in Cordova, AK, and arrived at the study location on September 1, 2015, with all mooring devices on board. To avoid interfering with subsistence whaling activities, BOEM and the Alaskan Eskimo Whaling Commission agreed on August 21, 2015, to proceed with mooring deployment when the communities of Nuiqsut and Kaktovik had completed their annual harvest of bowhead whales. On station, the USCGC *Sycamore* waited for the completion of the harvest. Due to deteriorating sea conditions and much prolonged subsistence whaling activities, the vessel was eventually forced to return to port, leaving the area on September 22, 2015, without deploying the mooring devices. The 2015 post-cruise report summarizing all events during the 2015 field season is available in Appendix A.

The AUV Slocum G2 Glider equipped with Seabird pumped CTD, WETLabs ECO Triplet, Aanderaa dissolved oxygen optode, and Imagenex Model 853 scientific echo sounder was deployed from USCGC *Sycamore* on September 21, 2015, immediately east of Kaktovik. The field crew stayed with the glider for the first 24 hours as planned and detected a leak during its first dive to 200 m. The glider was immediately recovered. Unfortunately, the leak could not be repaired in the field, and the mission was aborted. Later investigations found that the leak was caused by a manufacturing error, which was resolved, and the equipment was re-tested (see Appendix A).

### **1.3.3 Implementation 2016**

After the aborted 2015 field season, the scope of the component was changed to reflect lessons learned and to take advantage of some new partnership opportunities Stantec had fostered in the interim. Specifically, the 2016 field program added partnerships with the Department of Fisheries and Oceans (DFO) Canada and the University of Alaska Fairbanks (UAF). It included a six-week deployment of an autonomous glider between mid-August and early October 2016 in the eastern Beaufort Sea centered on the Mackenzie Trough, the deployment of four MARES plus two partner moorings in early October 2016

in the eastern Beaufort Sea just east of Hershel Island, and carbon cycling measurements at the mooring sites.

## **1.4 Community Consultations**

### 2015 Consultations

In 2015, BOEM conducted all consultations with the Alaska Eskimo Whaling Commission (AEWC) regarding the 2015 field program. The BOEM Contracting Officer's Representative (COR) described the mooring deployment plans that were to take place on board the USCGC *Sycamore* and associated timing and communications protocols with the AEW. After the field program was amended to 2016 deployments, consultations, conducted by Kavik-Stantec Inc. with the Inuvialuit Game Council (IGC), were held on December 18, 2015, in Aklavik, Northwest Territories, to introduce the program and gain feedback. The IGC had no concerns with the mooring program.

### 2016 Consultations

In Winnipeg, Manitoba, Canada, in February 2016, the Fisheries Joint Management Committee (FJMC) held a meeting where Stantec presented the field program planned for 2016 to get feedback. The FJMC expressed support for the mooring, glider, and benthic program.

Kavik-Stantec Inc. held consultation meetings with the Inuvik Hunters and Trappers Committee (HTC), Tuktoyaktuk HTC, and the Aklavik HTC, on June 22, 23, and 24, 2016, respectively, regarding the 2016 field program. Each HTC supported the program and were interested in seeing results from the study.

A project summary was submitted to the Inuvialuit Settlement Region Environmental Impact Screening Committee to determine if the project required an Environmental Screening. On August 2, 2016, the Environmental Impact Screening Committee (AEWC) determined that the project does not meet the definition of development as defined under the Inuvialuit Final Agreement, and as a result would not require an Environmental Impact Screening.

BOEM conducted consultations with the AEW, and presented the field program at the AEW meeting held February 1–5, 2016 in Utqiagvik, Alaska.

### 2017 Consultations

Kavik-Stantec Inc. consulted with the Tuktoyaktuk HTC on April 12, 2017, the Aklavik HTC on April 13, 2017 and the Inuvik HTC on April 20, 2017 concerning the 2017 field program and as a follow up to the 2016 program. The HTCs did not have any concerns with the programs.

Stantec submitted a Memo to the IGC on June 9, 2017, which provided information on the Alaska Ocean Observing System (AOOS) and access to the data.

## **1.5 Permitting**

Stantec and Kavik-Stantec Inc. gathered all necessary permits and permissions as outlined in the contract agreement including applicable permits from the Northwest Territories (Aurora Research Institute [ARI]). The program was conducted by adding MARES to a cooperative agreement with DFO Canada previously held by ASL to conduct oceanographic research in the Canadian Beaufort Sea. Confirmation to conduct all activities under Task Order 3 were received.

## 2 AUV Glider Component

### 2.1 Introduction

An underwater autonomous vehicle—Slocum G2 Glider—was deployed in the summer of 2016 to advance our understanding of the exchange processes between the Mackenzie River, the shelf, and the eastern Beaufort Sea, and the impact of these exchanges on the ecosystem.

We aimed to test the following hypotheses:

- The Mackenzie River plume strongly affects the stratification and bio-optical properties of the surface mixed layer on both Canadian and US continental shelves
- River-shelf-basin exchange is strongly affected by seasonal heating and cooling, wind-driven advection, and interaction with shelfbreak frontal currents
- In the absence of strong wind forcing, buoyancy-driven shelf flow and the shelfbreak jet advects fresh Mackenzie River water eastward toward the Amundsen Gulf. Under moderate to strong easterly winds, however, the Mackenzie River plume is advected westward toward the Alaskan Beaufort Sea
- The Mackenzie River plume and wind forcing vary on time scale of 1 to 2 weeks driven by regional weather and variability of shelf and shelfbreak circulation

Working toward the scientific objectives of MARES, Principal Investigator (PI) Gong of the VIMS led the effort to prepare, deploy, and recover one Teledyne Webb Research (TWR) Slocum G2 Glider in the eastern Beaufort Sea. The glider study complemented the ongoing mooring component in the study region. This chapter contains the main results of the 2016 glider study.

### 2.2 Methods

#### 2.2.1 Glider Setup and Sensor Suite

One Slocum G2 Glider (Figure 1), powered by lithium primary batteries, was used for the study. The glider is a self-powered AUV. It undulates up and down the water column, between the surface and 200 m, sampling the ocean. The glider has an endurance of 1–3 months depending on battery type and number of sensors and it can travel for a couple thousand miles on its own power. The glider moves slowly through the water at approximately 0.5 knots. The glider hull is made of composite material holding a partial vacuum inside. The hull can be damaged through scrapes, impacts, drops, and over-pressurization. The glider's scientific sensors are all located in the middle section.





**Figure 1. Slocum G2 Glider.**

The glider was equipped with an extended buoyancy 200 m buoyancy pump and a hybrid thruster; both were designed to deal with freshwater lens penetration when the extreme buoyancy range of a river plume is encountered. The glider's scientific sensor suite included Seabird CTD, WET Labs ECO Puck 3-channel fluorometer which provides measurements for chlorophyll-a, Colored Dissolved Organic Matter (CDOM), optical backscattering (700 nm), Aanderra Dissolved Oxygen optode, Biospherical Photosynthetically Active Radiation (PAR) sensor, and Imagenex 120 kHz acoustic echosounder. All sensors were factory calibrated.

The glider was set to surface every 2–3 hours, calling the dockserver at VIMS to upload a subset of the data for piloting and real-time analysis. The real-time data contained decimated data. The delayed-mode dataset contained full resolution data.

### **2.2.2 Glider Preparation for 2016**

Preparations were made at VIMS to ready the glider for the 2016 deployment. The glider was ballasted by adding salt to a tank filled with York River (Virginia) water until the density equaled that of the expected density of the Mackenzie Trough region during the time of deployment (1,022 kg/m<sup>3</sup>). Internal weight was added to the nose, tail, and mid-sections of the glider so that roll and pitch were each approximately 0°, and the tail floated about an inch above the water's surface when in ballast mode. New O-rings were installed and lubed, and the internal surfaces at hull junctions were examined for scratches that could jeopardize the vacuum integrity.

A test deployment was conducted off Wachapreague, Virginia, on May 20, 2016, for five days, during which a leak developed. The glider was shipped back to TWR for re-examination. The leak was attributed to an improperly sized screw that was used by the manufacturer in the glider's forward section. TWR completed the repair, re-ballasted the glider, and re-tested it down to 200 m depth near the New England shelfbreak on the June 23. The glider performed as required during this test and was shipped directly to Prudhoe Bay on July 1, 2016, in preparation for the field work in the eastern Beaufort Sea.

### **2.2.3 2016 Glider Survey Plan**

MARES 2016 glider deployment focused on a biophysical study of the eastern Beaufort Sea in and around Mackenzie Trough region. The objectives of the glider mission were to:

- Map the spatial distribution of the Mackenzie plume from the US-Canadian border to the head of the Mackenzie Trough

- Characterize the along-shelf and cross-shelf structure of the shelfbreak jet and shelf water masses near the Mackenzie Trough
- Quantify the associated biological response to the physical conditions of the water column

A survey plan was laid out with deployment of the glider north of Kaktovik in US waters, entering the MARES sampling region from the west on its own power. It was anticipated that the glider would perform a cross-shelf transect near the US-Canada border before proceeding to the Mackenzie Trough along the 60 m isobath. Once in the Mackenzie Trough region, the glider would repeat the proposed sampling pattern in the trough two to three times and end with a cross-shelf transect along the proposed mooring sites (Figure 2). The glider would then be recovered by the Canadian Coast Guard Ship (CCGS) *Sir Wilfrid Laurier* after the completion of the mooring deployments (see Section 3). This plan would enable a later glider-mooring cross-shelf comparison, as well as provide additional spatial and temporal context to the moorings.

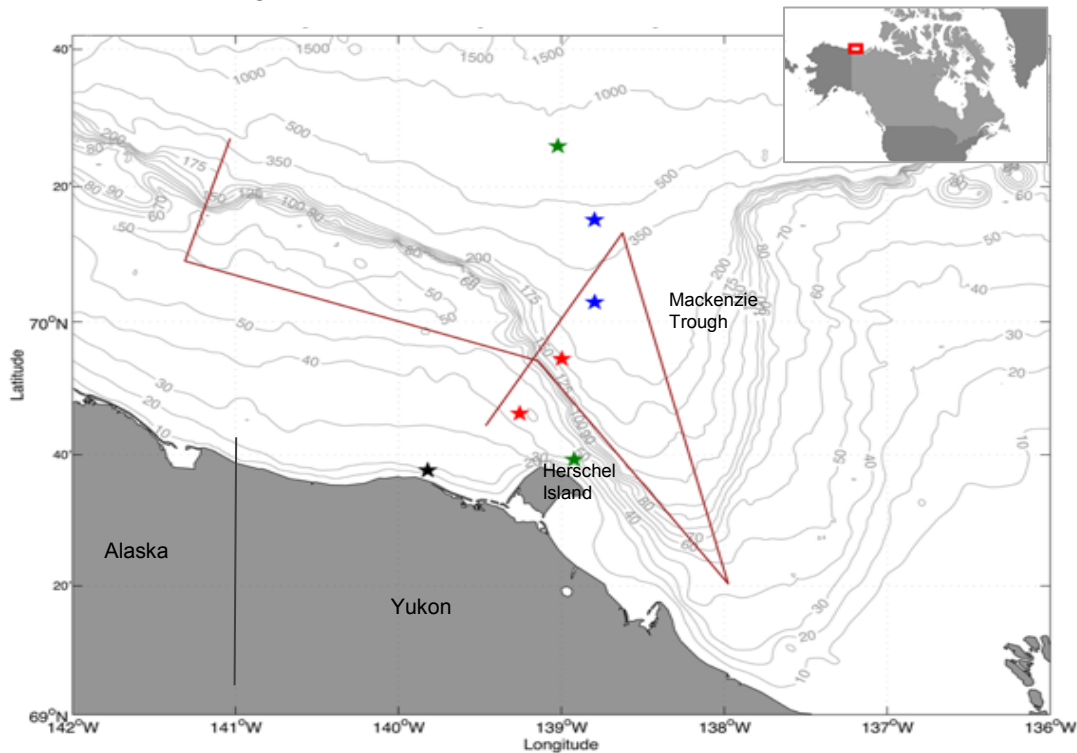


**Figure 2. Planned 2016 glider mission, showing locations of proposed moorings.**

WHOI moorings in red, ASL moorings in blue, University of Alaska Fairbanks (UAF) mooring in black, Canadian moorings in green.

## 2.2.4 Glider Deployment

PI Gong's research technician and graduate student traveled to Prudhoe Bay, AK on August 9, 2016 and picked up the glider on August 10. A functional checkout was performed to ensure all systems and sensors were functioning as expected. This included checking the functionality of the altimeter, Digifin, thruster, nose recovery system, and leak detect. Next, the glider's compass was calibrated to account for the difference in the Earth's magnetic field in Alaska compared to Virginia. A structure was built using ladders and 2" x 4" boards and straps were used to suspend the glider from the boards. The True North Technologies Revolution Test program was used to measure the glider's orientation, pitch, and roll while we rotated the glider 360° in a level, nose up, and nose down orientation and turned on either side. After

calibration, the accuracy was checked against a handheld compass at 30° intervals with the glider level, nose up, and nose down.

When the glider was ready, it was loaded onto a 60 ft coastal research vessel (R/V)—the R/V *Ukpik*. The R/V *Ukpik* arrived on station, 30 nautical miles north of Kaktovik in 200 m of water at the shelfbreak the morning of August 15, and the glider was readied for deployment. The sea state was very calm. Additional on-deck checks were performed to test the glider's Iridium communication and GPS. The glider was placed into the water attached to a buoy, and the roll and pitch were observed to be within acceptable limits. A shallow test dive was completed successfully before removing the buoy. A deeper test dive was also conducted successfully before sending the glider to its first waypoint. The R/V *Ukpik* remained in the area for a short time to ensure the glider was flying well before heading back to port.

### **2.2.5 Piloting**

The glider was piloted by PI Gong at VIMS throughout the mission. The glider performed nominally and successfully completed the planned mission. The glider was set to surface every 2 to 3 hours and upload real-time data while also receiving new mission updates (as needed). The glider experienced several temporary aborts during the mission, mainly due to buoyancy issues as a freshwater lens was encountered. The glider was ballasted for a mean density of 1,022 kg/m<sup>3</sup>. That means with the extended buoyancy pump, the glider should be able to handle  $\pm 5.5$  kg/m<sup>3</sup> density units. We encountered water as fresh as 1,016 kg/m<sup>3</sup> and as dense as 1,027 kg/m<sup>3</sup>, which meant that at times, relying on buoyancy alone wasn't sufficient for bringing the glider back the surface. The hybrid thruster provided the glider with the capability of freshwater lens penetration using an additional 1,000 cc of active buoyancy from the thruster. The thruster was programmed to turn on automatically once upward/downward velocity dropped to less than 0.1 m/s. Except for during two periods near the western wall of the trough when an exceptionally strong current (0.5 m/s or greater) was encountered, the glider was able to make it to all waypoints.

The total mission lasted 52 days for a total distance traveled of approximately 1,100 km.

### **2.2.6 Glider Recovery**

The glider was recovered on October 6, 2016, from the CCGS *Sir Wilfrid Laurier*. The recovery effort was led by the MARES mooring team from WHOI and ASL. PI Gong provided the procedural documentation to the ship's recovery crew. The glider was recovered from a small boat then hoisted onto the larger ship. The sea condition was favorable, and the recovery was uneventful. The glider was stowed onboard using a custom built wooden frame as the CCGS *Sir Wilfred Laurier* did not have a glider cart. The glider remained on board until the CCGS *Sir Wilfrid Laurier* reached its home port at the Institute of Ocean Sciences (IOS) in British Columbia.

### **2.2.7 MARES Glider Data Management and QA/QC**

#### **2.2.7.1 Data Retrieval and Archive**

Once the glider arrived at the IOS in Victoria, Vancouver Island, British Columbia at the end of October, PI Gong downloaded the data and cleaned, inspected, and packed the glider for shipment back to VIMS. The raw data was downloaded from the glider. The original copy is archived at VIMS, and a copy of the raw data was uploaded to the AOOS Workspace.

#### **2.2.7.2 Data Format**

Everything except for the echo sounder data was stored in Dinkum Binary Data (DBD) format. The raw engineering data was stored in SBD (decimated) and DBD (full) files. The raw science data was stored in

TBD (decimated) and EBD (full) files. Real-time data processing used SBD and TBD files while delayed-mode processing used all available data. Raw binary data from the glider was converted to Matlab readable ASCII format using ‘dbd2asc’ and ‘dba2\_glider\_data’ converters provided by TWR.

### **2.2.7.3 CTD, DO, PAR, & Fluorometers**

The glider used a pumped Seabird CTD and its performance was nominal throughout the mission. The CTD, DO, PAR, and ECO Puck all operated in an upcast only mode throughout the mission. The raw data files were converted to Matlab format for analysis. As configured, the glider’s pressure sensor and the science sensors recorded their data at an ‘as fast as possible’ setting; sampling frequencies nominally varied between 0.4 to 1 Hz and provided a vertical resolution between 0.15 to 0.35 meters.

One technical issue encountered during data processing was temporal synchronization of the data time stamp, the pressure sensor values, and the different science sensors’ measurements. For each time stamp, if there is value from any of the sensors, their values are recorded. Otherwise, if a sensor does not report a value, then the value ‘NaN’ is recorded for that sensor at that time stamp. There were times when the pressure sensor values and the science sensors were at different times, which resulted in appearance of a ‘data gap’ when the data was plotted simultaneously against pressure (depth) values and time. This was because the plotting routine required time, pressure, and data values to all be not ‘NaN’ before the data point could be plotted. To address this data synchronization issue and preserve the sampling fidelity of the glider as much as possible, the pressure values were linearly interpolated between data values so that there is guaranteed to be a pressure value for each time stamp. The glider’s flight dynamics are effectively constant over the sampling frequency of the sensors (~0.5 Hz), so the linearly interpolated pressure values are considered representative of the true pressure values. Once the interpolation was completed, the apparent ‘data gap’ issue was resolved. All CTD, DO, PAR, and fluorometer data (both raw and converted) have been archived on a server at VIMS and uploaded to the AOOS Workspace.

### **2.2.7.4 Echo Sounder**

The echo sounder operated in a downcast only mode throughout the mission. It sampled every other cast. Raw echo sounder data was uploaded to AOOS Workspace for later processing. The processing and analysis of glider echo sounder data was not part of this Task Order.

## **2.2.8 Ocean Data and Ocean Model Output Used for Analysis**

### **2.2.8.1 Wind data at Herschel Island**

Wind data at Herschel Island is provided by a Canadian government weather station: [http://climate.weather.gc.ca/climate\\_data/daily\\_data\\_e.html?StationID=1560](http://climate.weather.gc.ca/climate_data/daily_data_e.html?StationID=1560). The station’s location is 69.57 N, 138.91 W at an elevation of 1.2 m with a WMO ID of 71501. Data include temperature, air pressure, dew point, relative humidity, wind direction, wind speed, and wind chill and are available on an hourly basis.

### **2.2.8.2 North American Regional Reanalysis (NARR)**

The North American Regional Reanalysis (NARR) model is produced by the National Centers for Environmental Prediction (NCEP) <https://www.esrl.noaa.gov/psd/data/gridded/data.narr.html>. The NARR model has monthly, daily, and eight-times daily temporal coverage beginning in 1979. Vector wind data at the surface level in the region of deployment was extracted from the model output for different periods of interest. We used daily and monthly output in our analysis.

### **2.2.8.3 Global Hybrid Coordinate Ocean Model**

The US Navy's Global Hybrid Coordinate Model (HYCOM) is used for our analysis of regional scale circulation patterns on event to inter-annual timescales. HYCOM has a coordinate system that is isopycnal in the open, stratified ocean but smoothly reverts to a terrain-following coordinate in shallow coastal regions and to z-level (vertical) coordinates in the mixed layer and/or unstratified seas. The Global HYCOM is a 1/12<sup>th</sup> degree model that assimilates available satellite altimeter observations, satellite, and in situ sea surface temperature as well as in situ vertical temperature and salinity profiles from expendable bathythermograph (XBTs), Argo floats and moored buoys. The model uses the Navy Coupled Ocean Data Assimilation (NCODA) 3D-Var system. Surface information is projected downward into the water column using Improved Synthetic Ocean Profiles (Helber et al. 2013). The Naval Research Lab generates daily nowcast of the 3-D ocean field of temperature, salinity, surface elevation, and horizontal current velocities in near real-time. For this study, we used model output results from HYCOM GOFS 3.0 with 32 vertical layers. In particular, output from expt\_19.1, expt\_90.9, expt\_91.0, expt\_91.1, and expt\_91.2 were used in our analysis of the flow field in and around Mackenzie Trough. For more information, please visit (<https://hycom.org/dataserver>).

### **2.2.8.4 MODIS True Color Ocean Imagery**

True color ocean images from the Moderate Resolution Imaging Spectroradiometer (MODIS) satellite is retrieved using WorldView (<https://earthdata.nasa.gov/labs/worldview/>). It's a web-based tool from NASA's Earth Observing System Data and Information System (EOSDIS) that allows interactive browsing of global satellite imagery from MODIS within hours of data being acquired. High resolution RGB images from WorldView are output in Keyhole Markup Language (KML) format and plots in Google Earth.

## **2.3 Results**

### **2.3.1 Characterization of the Physical Oceanographic Setting**

The physical oceanographic setting can be characterized in three parts: geography of the Mackenzie Trough, Mackenzie River discharge, and winds.

#### **2.3.1.1 Geography of Mackenzie Trough**

The Mackenzie Trough incises the eastern Beaufort shelf (Figure 3). It is situated to the west of the mouth of the Mackenzie River by approximately 80 km. The trough is 120 km long, 65 km wide, 370 m deep at the mouth, and 200 m deep at the center. Shallow and wide continental shelves flank the two sides of the Mackenzie Trough.



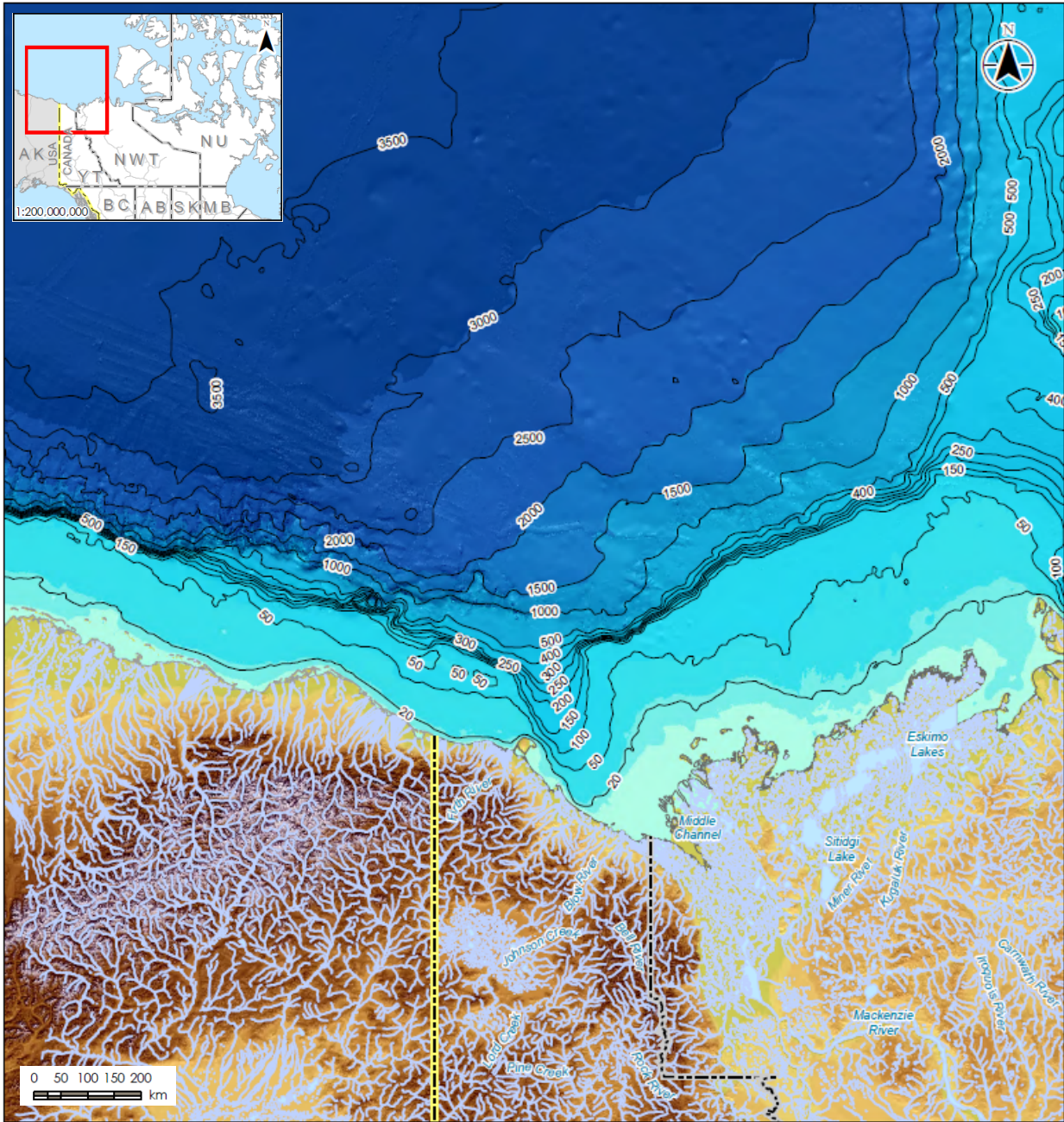


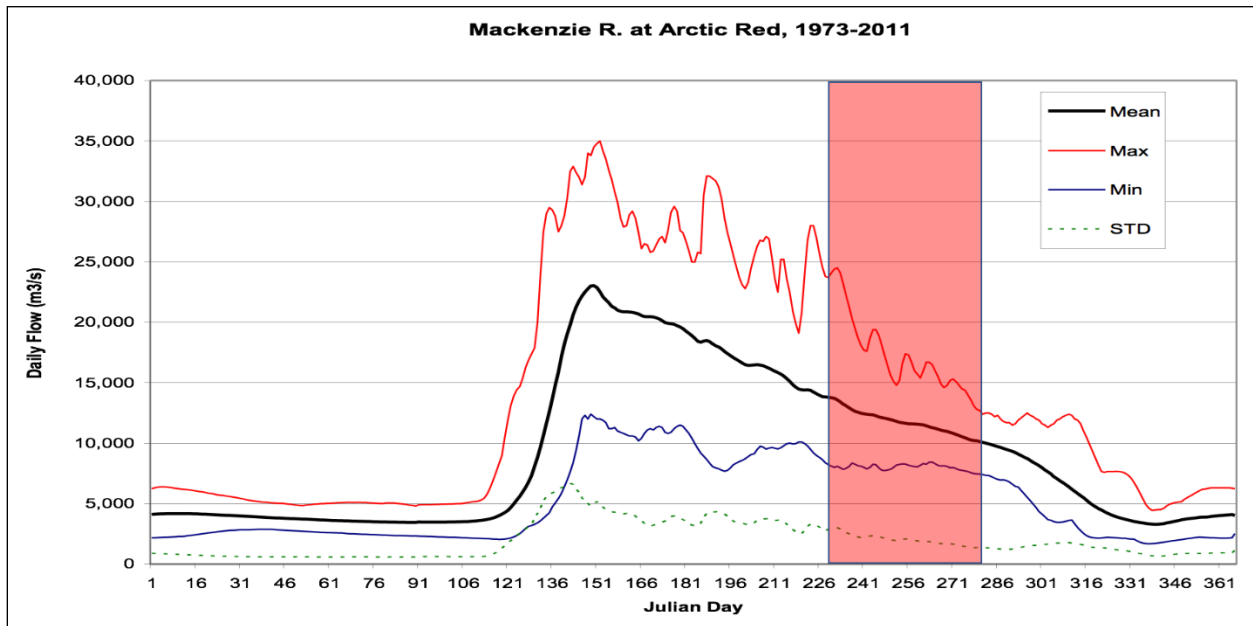
**Figure 3. Map of the Mackenzie Trough. Bathymetry from the National Oceanic and Atmospheric Administration (NOAA) and bathymetry contours from Geological Survey of Canada.**

The shelf to the west is 65 km wide and 50 m deep while the shelf to the east is 150 km wide and 80 m deep. The trough terminates at the continental slope and does not extend into the Beaufort Sea basin. The shelfbreak is located at the 70 m isobath. The 40 m isobath situated mid-shelf delineates the inner shelf and the outer shelf regions. Going shoreward from the shelfbreak, there is a ridge and a valley just shoreward of the 60 m isobath with a peak (45 m deep) to valley (60 m deep) depth range of 15 m. This bathymetric feature extends for 150 km to the west of Mackenzie Trough.



### 2.3.1.2 Mackenzie River Discharge

The Mackenzie River has a highly seasonal discharge pattern. Climatological analysis show that the annual average discharge is  $9,900 \text{ m}^3/\text{s}$ . The seasonal discharge rapidly peaks in spring at Year Day 148 (May 27) with an average maximum of  $22,500 \pm 12,500 \text{ m}^3/\text{s}$  (see Figure 4). The discharge gradually decreases through the summer down to the annual mean discharge by Year Day 286 (October 12). A more rapid drop in the fall lowers the discharge rate to  $4,000 \text{ m}^3/\text{s}$  by Year Day 328 (November 20), which is the wintertime average discharge from late November to late April. The MARES glider study took place from August 15 to October 6 (highlighted in red in Figure 4). During this time, the climatological river discharge was  $14,000 \pm 6,000 \text{ m}^3/\text{s}$  at the beginning of the deployment and  $10,000 \pm 2,500 \text{ m}^3/\text{s}$  by the end of the deployment.



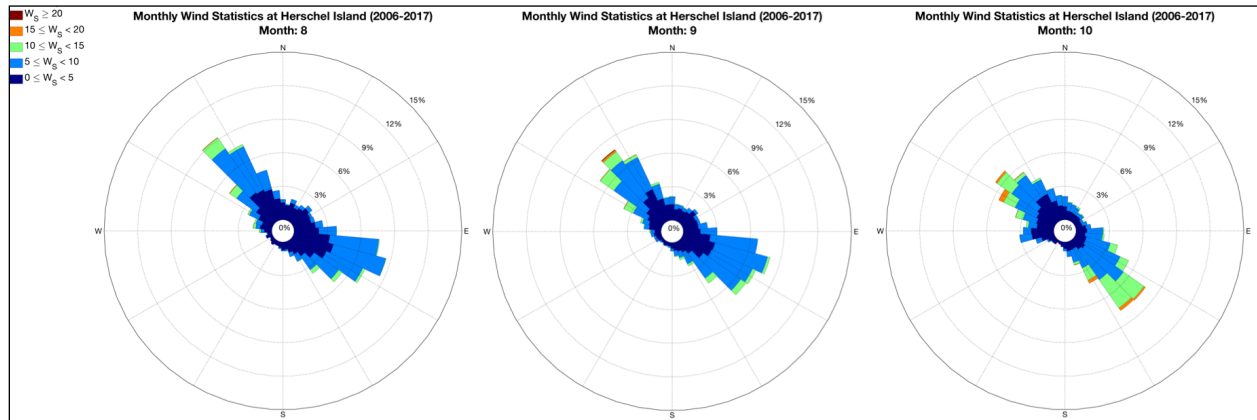
**Figure 4. Climatology plot of Mackenzie River discharge for the period 1973 to 2011.**

Figure adapted from Yang et al. (2015). The red region highlights the period when the MARES glider was deployed.

### 2.3.1.3 Winds

#### 2.3.1.3.1 Climatological Winds

Climatological analysis of winds measured from the Canadian weather station on Herschel Island show that for the months of August, September, and October, the wind directions are predominantly southeasterly (35–45% of total) and northwesterly (25–35% of total) (Figure 5). Wind speed ranged from 0 m/s to 20 m/s. The winds are weakest and more likely to be northwesterly (downwelling favorable) in August, and strongest and more likely to be southeasterly (upwelling favorable) in October.



**Figure 5. Wind rose histograms for Herschel Island (2006–2017) for August, September, and October.**

### **2.3.1.3.2 Winds During the 2016 Field Season**

Winds in the Mackenzie Trough region during the MARES 2016 glider study were highly variable (Figure 6), oscillating between southeasterly (upwelling favorable) and northwesterly (downwelling favorable) on a time scale of 1 to 3 days during the first part of the study (August 15 to September 2, 2016). Wind speeds during this first period ranged from 2–13 m/s. From September 2 to 10, strong northwesterly winds persisted (6–14 m/s), followed by moderate easterly upwelling favorable winds from September 11 to 15 (3–9 m/s). From September 15 to 25, winds were variable (1–7 m/s) except for brief period of westerly downwelling winds from September 18 to 20 (6–10 m/s). From September 15 to 25, winds were variable (1–7 m/s) except for brief period of westerly downwelling winds from September 18 to 20 (6–10 m/s). From September 26 to October 1, winds were predominantly northwesterly (1–12 m/s). Finally, the last period of study, from October 1 to 4, winds were persistent southeasterly upwelling favorable (3–13 m/s). The glider surveyed the Mackenzie Trough three times over the course of the study with each pattern taking approximately 10 days and each transect lasting 2 to 5 days. Throughout the study, given the variable winds, the glider likely experienced different wind-forced circulation even during a single transect.

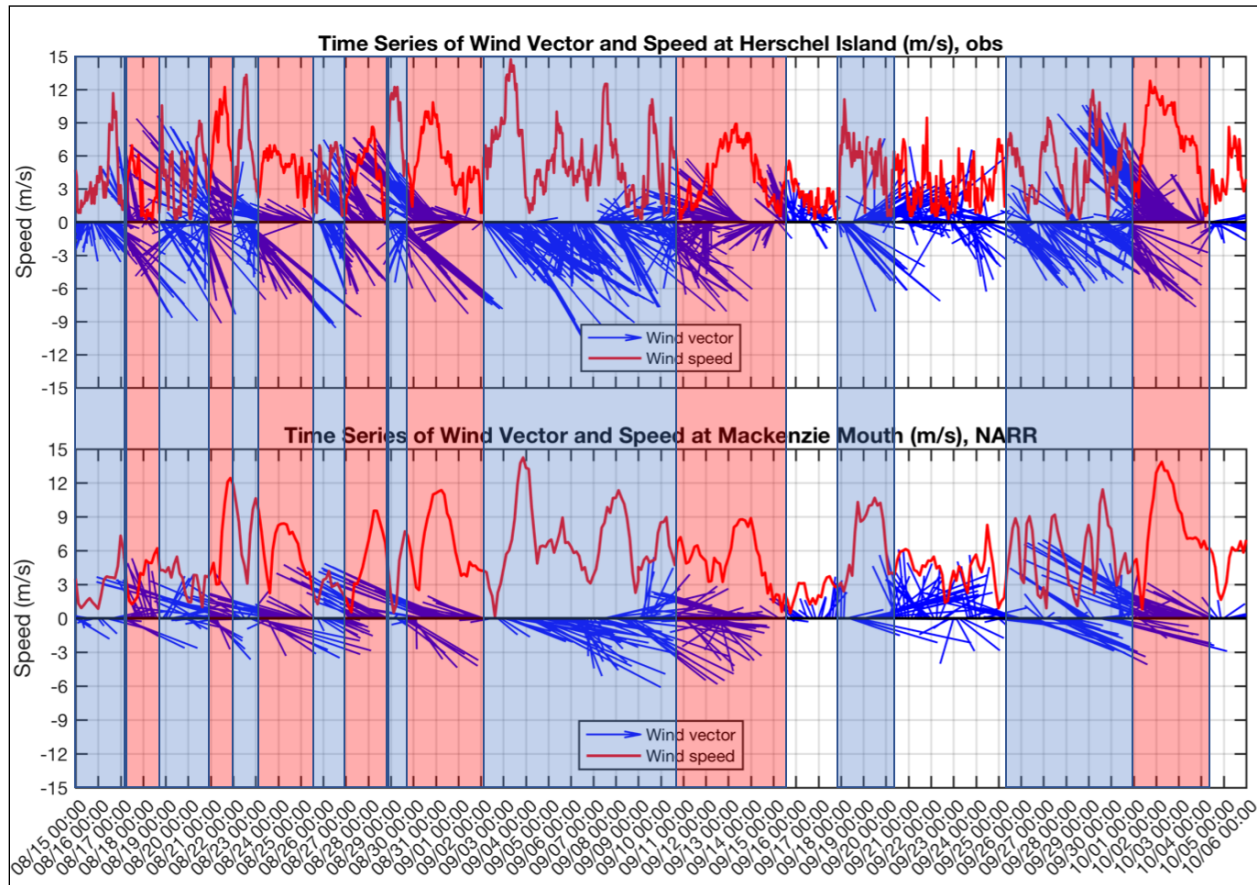


**Figure 6. Plot of wind vectors and speed (2016).**

Top panel shows wind vectors from Herschel Island and the bottom panel shows wind vectors from NARR at the mouth of the Mackenzie Trough. The blue segments represent northeasterly winds and red segments represent southwesterly winds.

### 2.3.2 Hydrography & Water Masses

Mackenzie Plume: During the 2016 MARES deployment, the glider traveled from the Alaska Beaufort shelf to the Mackenzie Trough before completing three repeat pattern surveys (Figure 7).

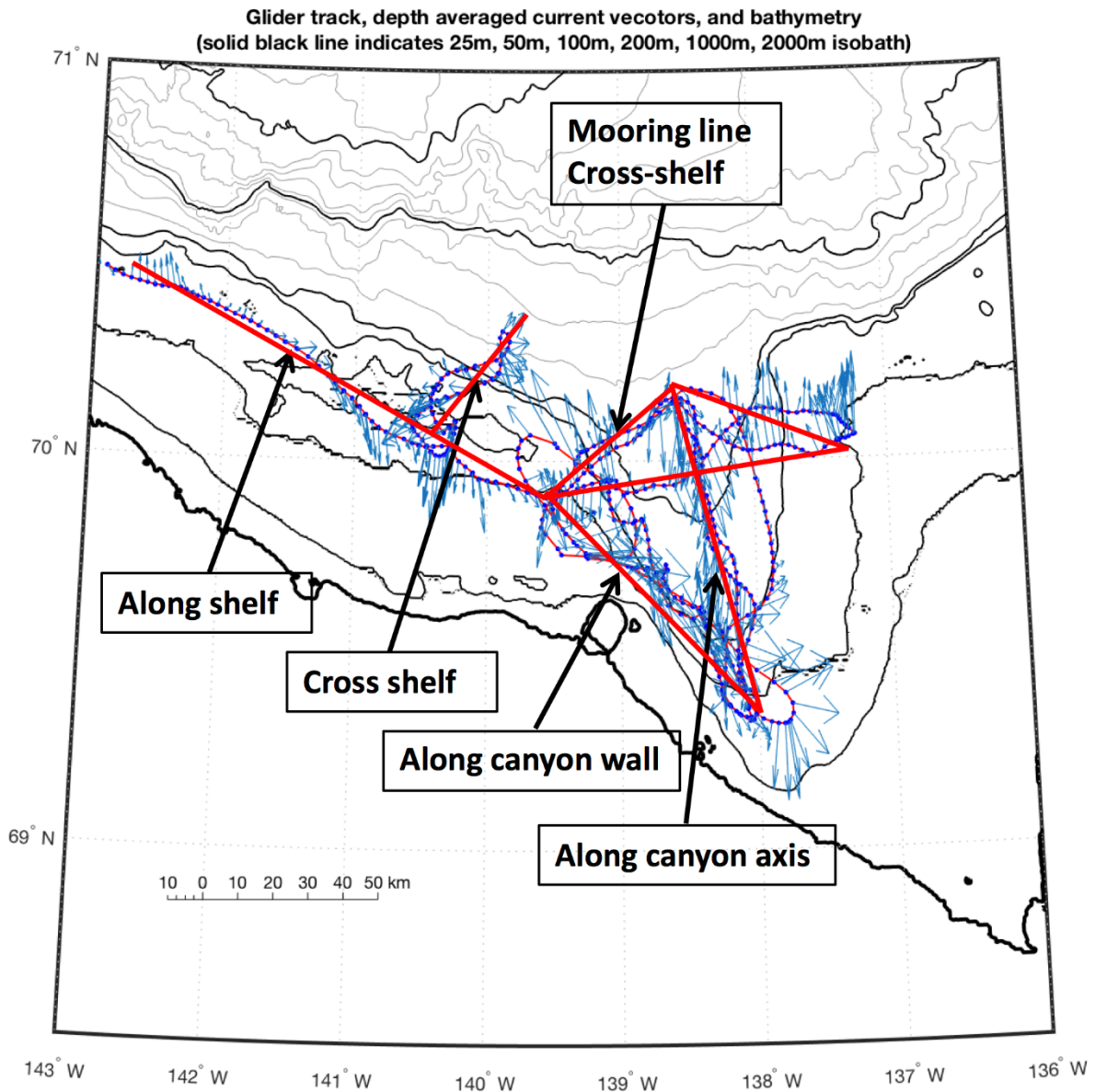


**Figure 7. Map of the Mackenzie Trough region overlaid with glider tracks (purple) and depth-average velocity estimates (blue arrows).**

Red lines indicate idealized transect plans and transect sections.

As the glider progressed from west to east in late August, it began to encounter warm ( $> 4\text{ }^{\circ}\text{C}$ ) and fresh ( $< 27\text{ psu}$ ) riverine water at the surface (Figure 8). The freshest river plume water was found inside Mackenzie Trough with salinity less than 23 psu. The thickness of the Mackenzie River plume varied between 5 m and 15 m.

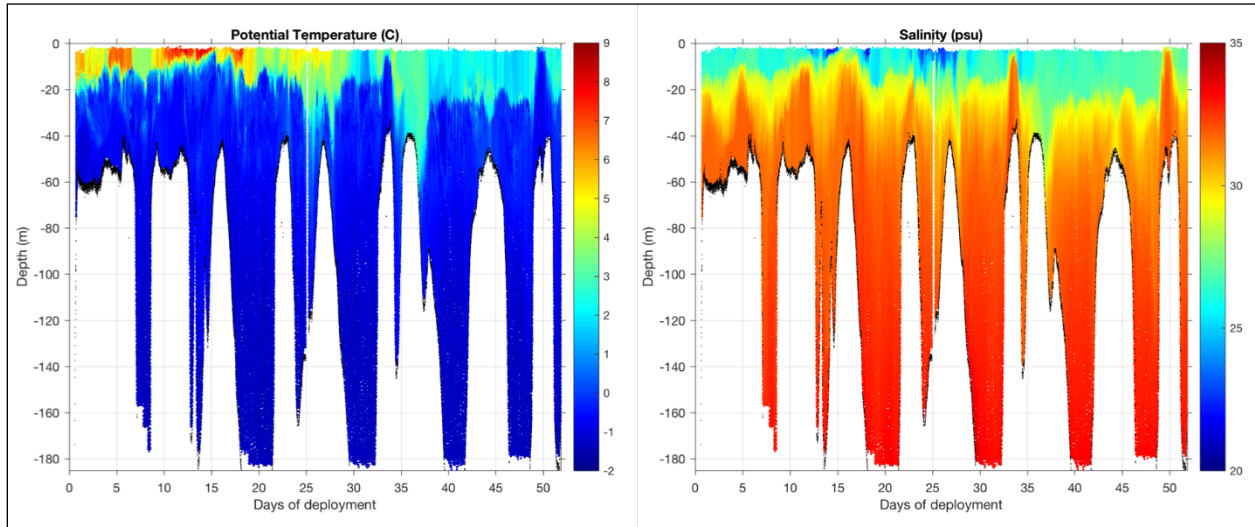


**Figure 8. Plots of potential temperature (left) and salinity (right) versus days of deployment (August 15–October 6, 2016).**

Surface water fresher than salinity of 27 are attributed to Mackenzie River plume.

Surface Mixed Layer: In general, the surface mixed layer had temperatures between 2 °C and 8.5 °C and salinity less than 28 psu. The warmest water was found during the first half of the deployment in and around the Mackenzie plume. The mixed layer temperature cooled rapidly during a couple of mixing events in the second half of September. Except inside the core of the river plume, the mixed layer salinity was relatively uniform with salinity between 26.5 psu and 28 psu. The halocline depth varied between the shallow shelf region and the deeper water offshore from mid-August to mid-September.

Pacific Water: Below the upper mixed layer resides Pacific winter and summer water. Pacific summer water generally had temperatures between -1 °C and 2 °C and salinity between 29 psu and 32 psu at depths between 80 m and 100 m. Pacific winter water had temperatures less than -1 °C and salinity greater than 32 psu and was found at depths between 80 m and 200 m. At two times during the study, one on September 18 and the other on October 3, a large amount of Pacific winter water was upwelled onto the continental shelf to the west of the Mackenzie Trough.

Atlantic Water: The average depth that delineates Pacific winter water and the warmer Atlantic water in the western Arctic is 200 m (Shimada et al. 2005, Steele et al. 2004). The MARES glider detected a hint of Atlantic Water at a depth of 180 m indicated by the saltiest water at temperatures above -1 °C shown in the T/S plot (Figure 9). Atlantic water was only found in the deeper slope and basin region and none was found on the continental shelf or on the flanks of the Trough. The property of the Atlantic water was constant throughout the study.

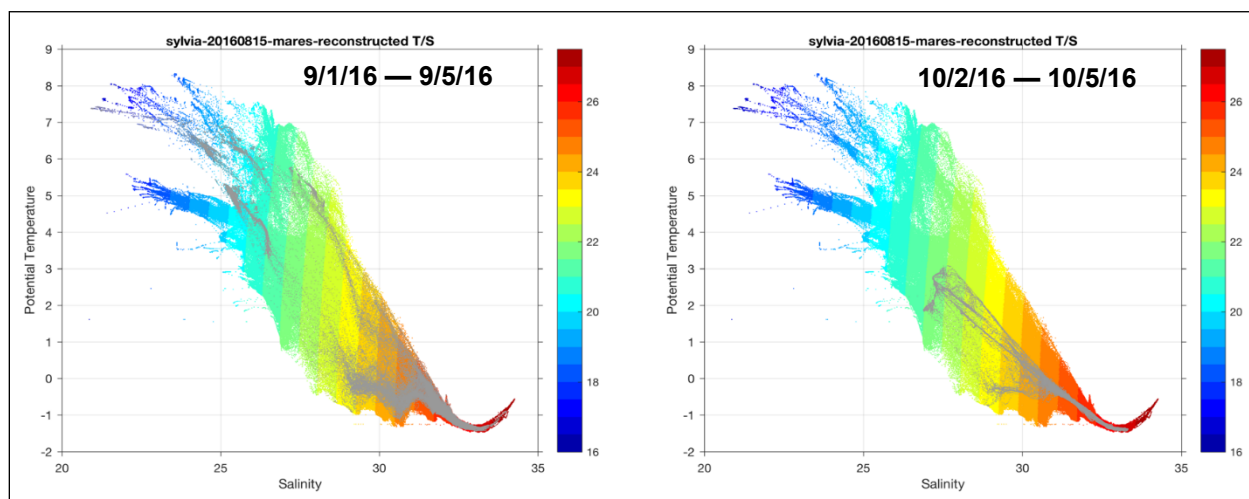


**Figure 9. Temperature-Salinity (T/S) plot for MARES 2016 glider deployment.**

The colors indicate potential density anomaly. The gray dots in each panel represent the T/S for one glider transect overlaid on the T/S for the entire mission. The left panel is for transect in early September, and the right panel is for a transect in early October.

Intra-seasonal evolution of the water masses: The Temperature-Salinity (T/S) diagram for the MARES glider mission is shown in Figure 9. It illustrates the large range of densities encountered by the glider during the study ranging from  $1,016 \text{ kg/m}^3$  in the freshest Mackenzie plume to  $1,027 \text{ kg/m}^3$  at a depth of 190 m offshore. A comparison of the T/S from early September with T/S from early October shows the drastic cooling and salting throughout the upper water column, especially in the surface mixed layer. Below the pycnocline, at depths deeper than 60 m, there was no meaningful intra-seasonal variability.

### 2.3.3 Circulation Based on Glider Observations

The glider encountered different flow conditions. Depth-averaged velocities ranged from 0 cm/s to 60 cm/s and along the walls of the trough was predominantly along-isobath. Cross isobath flow was seen on the shelf to the west and in the center of the Mackenzie Trough. During periods of substantial northwesterly downwelling-favorable winds, the depth-averaged flow was predominantly along-isobath eastward. During periods of substantial southeasterly upwelling-favorable winds, the flow was directed westward. The fastest flow was found on the western wall of the trough offshore of Herschel Island with speeds greater than 50 cm/s in both directions. There is also evidence of a cyclonic eddy on the eastern part of the Mackenzie Trough in late October.

### 2.3.4 Characterization of the Bio-Optical Conditions

#### 2.3.4.1 Chlorophyll-a Fluorescence

Overall, chlorophyll-a concentrations in the Mackenzie Trough region tended to range between 0.2–1  $\mu\text{g/l}$ , with elevated levels observed in the first half of deployment reaching 1.4–2  $\mu\text{g/l}$  (Figure 10). These localized areas of high concentration were identified at the surface and 20 m depth. Less variability was observed from day 30 onward with values 0.7  $\mu\text{g/l}$  or lower. These dense patches may represent late summer blooms in the Mackenzie Trough region during the short ice-free period. There is a clear variation in the depth of the chlorophyll maxima between the shelf and the deeper slope regions. Whereas the chlorophyll maxima are limited to the upper 20 m of the water column on the shelf, the sub-surface chlorophyll maximum is present at a depth range of 40 m and 60 m in deeper water.



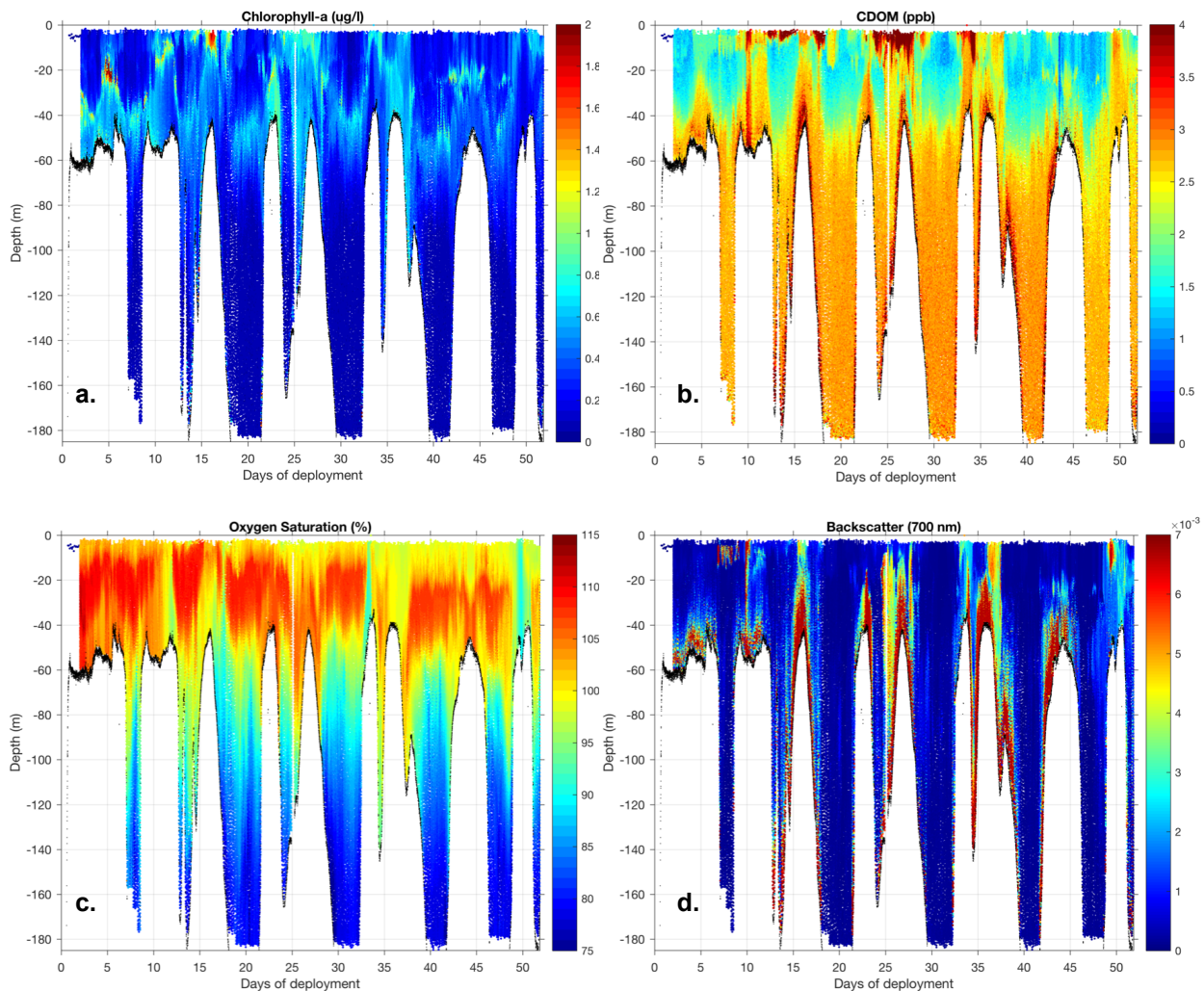


**Figure 10. Plots of: (a) chlorophyll-a fluorescence, (b) CDOM fluorescence, (c) dissolved oxygen saturation, and (d) optical backscattering for the MARES glider study from August 15, 2016, to October 6, 2016.**

### 2.3.4.2 CDOM Fluorescence

Observed CDOM values ranged from 1–4 ppb with the highest concentrations observed at the surface between days 10–35 of deployment (Figure 10). The near-surface high CDOM values are essentially tracers for the Mackenzie River plume. Outside of these localized maxima, values in the upper 40 m of the water column fell between 1–1.5 ppb while areas below 60 m tended to be consistent at approximately 3 ppb. Near-bottom CDOM values were also elevated due to particulate resuspension with values ranging from 2.5 ppb to 3.5 ppb.

### 2.3.4.3 Dissolved Oxygen

Dissolved oxygen saturation decreased with depth with the highest values near the surface for the first half of the deployment and slightly deeper for the second half (Figure 10). Oxygen supersaturation in the upper 60 m of the water column implies primary production and surface mixing are contributing oxygen

to the surface waters. This is corroborated by the variable wind patterns during the first half of the survey period, as well as elevated chlorophyll-a and CDOM.

#### 2.3.4.4 Optical Backscattering

Backscatter was highest near the ocean bottom and in patches near the surface, coinciding closely with areas of observed elevated CDOM and chlorophyll-a levels (Figure 10). Suspension of sediments driven by turbulent mixing near the sea floor as well as the canyon head and shelfbreak areas contribute to the observed high backscattering levels.

#### 2.3.4.5 Photosynthetically Available Radiation (PAR)

We observed day to day variability in the PAR data (Figure 11). On clear days, the euphotic zone extended down to 40 m while on cloudy days, the euphotic zone did not extend past 20 m. PAR data for the upper 5 meters is available during the dives when the glider is surfacing or at the surface; else, the glider normally flies below the upper 4 meters.

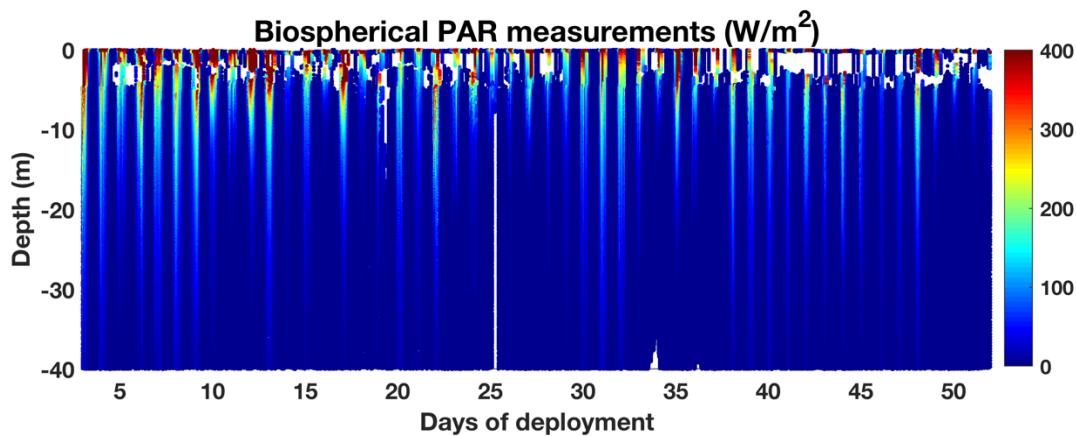
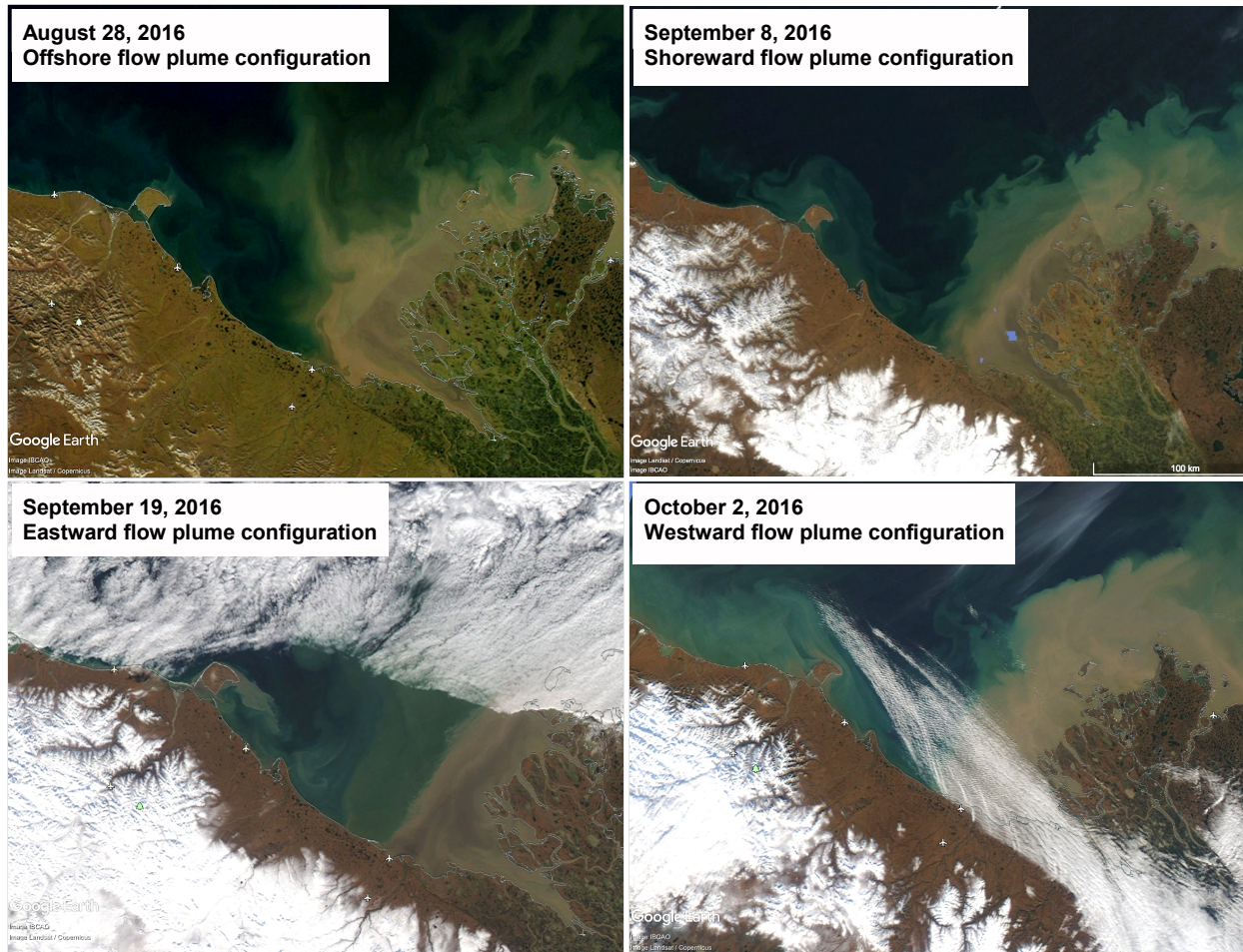


Figure 11. Time series of the photosynthetically available radiation (PAR).

### 2.3.5 Variability of Hydrography and Circulation

#### 2.3.5.1 Mackenzie River Plume

The Mackenzie River plume can be seen in satellite remote sensing images (Figure 12). The plume had varying spatial distributions during the glider mission. The images show the plume in these configurations: offshore, shoreward, eastward, and westward. The area near Herschel Island on the western side of the Mackenzie Trough shows the persistent presence of plume water regardless of the general plume configuration. The highest plume concentration is found at the mouth of the Mackenzie River to the southeast. The plume tends to be wider during easterly (October 2, 2016) and southerly (August 28, 2016) winds and more confined to the coast during westerly (September 19, 2016) and northerly (September 8, 2016) winds. The central (and deeper) parts of the trough have low concentrations of river plume water. Only with westerly winds is a substantial amount of Mackenzie plume water seen on the continental shelf to the west of the trough (October 2, 2016). Cloudy days prevented good satellite coverage for a large part of the field study; therefore, only representative plume conditions during different times of the study are shown.



**Figure 12. Satellite MODIS remote sensing true color images of the Mackenzie Trough region from late August to early October 2016.**

The Mackenzie plume can be seen advected in different directions depending on circulation in the Mackenzie Trough at those times.

### 2.3.5.2 Mixed Layer Depth

The mixed layer depth for the entire glider deployment is shown in Figure 13. The mixed layer was marked as the depth of maximum stratification in the water column. The thermocline shoaled from 15 m in the Alaskan Beaufort Shelf in mid-August to 7 m at the head of the Mackenzie Trough in late August. The average mixed layer depth (MLD) on the shelf was 10–15 m deep, and off the shelfbreak, it was 20–25 m deep.



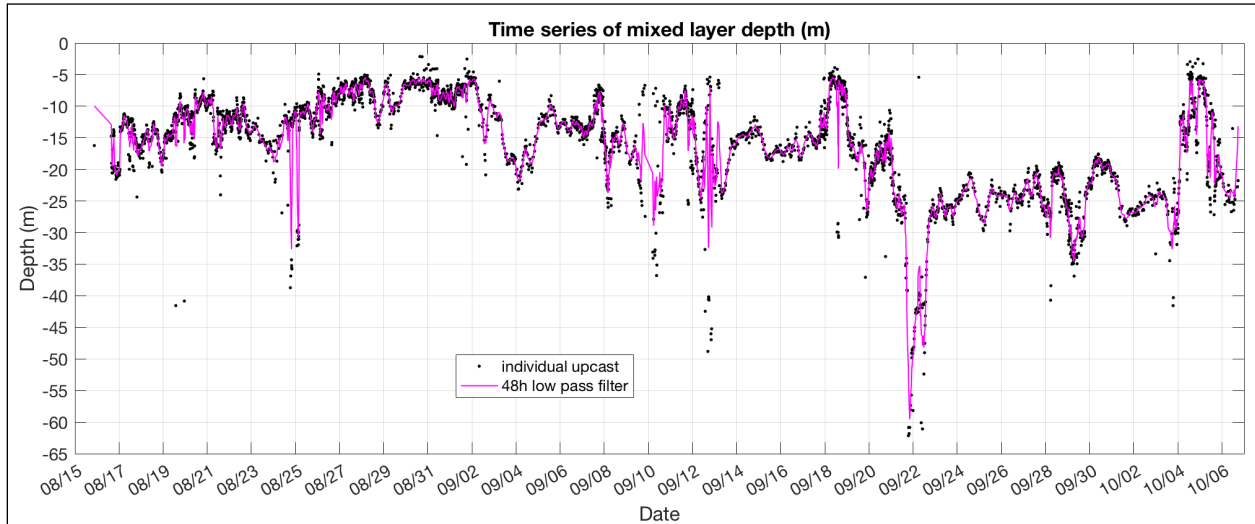


**Figure 13. Mixed layer depth (MLD) during the glider deployment.**

The MLD loosely tracks the thermocline but closely tracks the halocline due to the greater influence of salinity in the Arctic. Inside the Mackenzie Trough, the MLD increased from less than 10 m in early September to 25 m by late September. The MLD held steady at 25 m from late September into early October. On the event timescale, MLD varied in response to wind forcing and shelfbreak boundary current dynamics. The deepening of the MLD tends to be associated with specific surface mixing events. Two substantial MLD deepening events occurred: one in early September when the average MLD dropped from 7 m to 15 m, and another around September 22 when the average MLD deepened further from 15 m to 25 m; in both cases, when the glider was conducting the along-trough-axis survey approximately centered in the Mackenzie Trough. The winds turned from easterly to strongly westerly during the first event, and the winds were westerly downwelling favorable during the second event.

### 2.3.5.3 Sub-Mesoscale Variability

The glider's high spatial resolution allowed it to capture events and processes that take place at the sub-mesoscale (i.e., approximately 0.5 km to 1 km or approximately 2 to 4 hours). A good example of such an event is shown in an along-canyon axis transect from September 11–16, 2016 (Figure 14). During this time, the flow is southwestward. The glider captured what appears to be an internal wave bore-like phenomenon that caused large horizontal temperature and salinity gradient near the head of the trough just below the pycnocline. The bore-like phenomenon encapsulated water with high chlorophyll fluorescence and high optical backscatter. There were several such high frequency variabilities in the glider's hydrographic and bio-optical data. Future detailed inspections of each event will be required to understand the drivers and significance of these events.

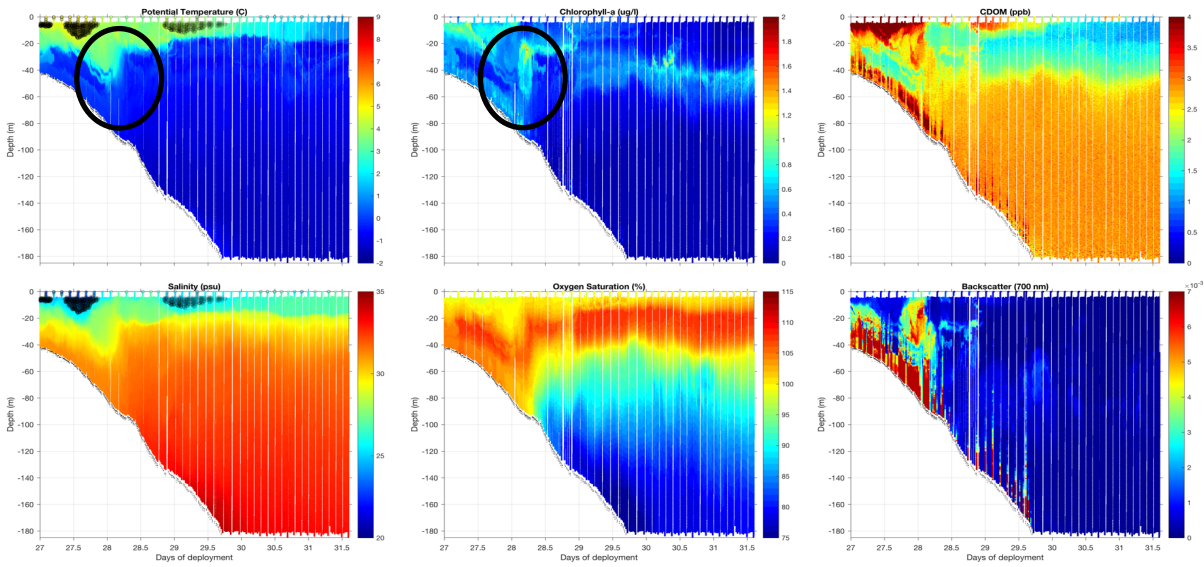


**Figure 14. Sub-mesoscale variability in the along-canyon axis transect from Sept.11–16, 2016.** The black circle identifies the internal wave bore-like phenomenon.

#### 2.3.5.4 Heat and Salt Transport

The heat and salt flux for each MARES glider section was calculated. Two representative along-canyon axis sections are shown in Figure 15. The first was during a westward flow period and the second was during an eastward flow period. Although the directions were opposite of each other, the magnitude of the net heat and salt transport for each glider transect were comparable. The net heat transport was on the order of 2 TW to 2.3 TW and the salt transport was on the order 0.03 Sv.

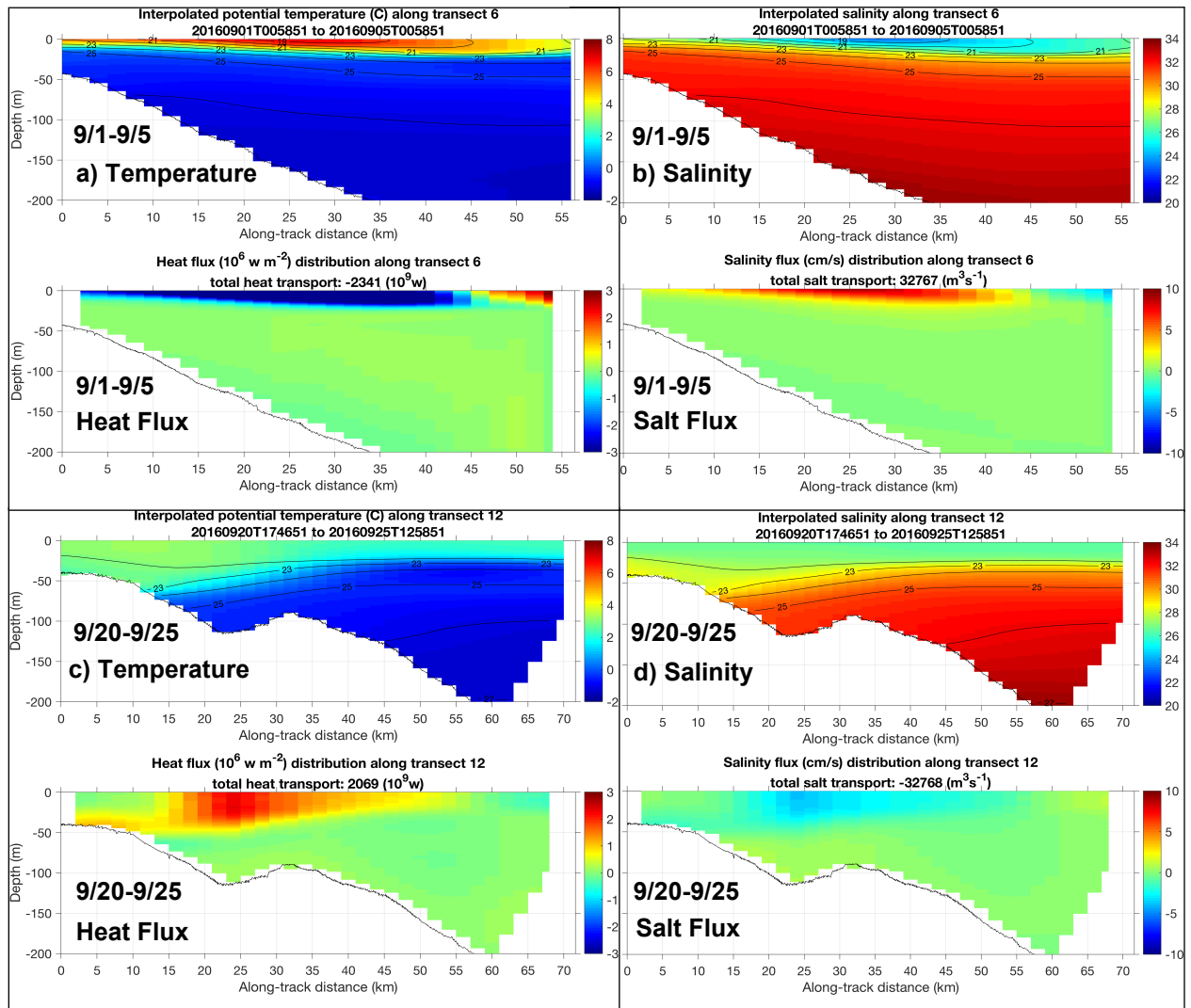


**Figure 15. Plot of temperature and salinity as well as heat and salt fluxes for two along-canyon axis glider transects.**

(a) Temperature and heat flux for transect on 9/1/16. (b) Salinity and salt flux for same transect as (a). (c) Temperature and heat flux for transect on 9/20/16 to 9/25/16. (d) Salinity and salt flux for same transect as (c).

## 2.3.6 Wind-Driven Circulation

### 2.3.6.1 Event-Scale Winds

The NARR wind fields corresponding to the four Mackenzie plume conditions are shown in Figure 16.

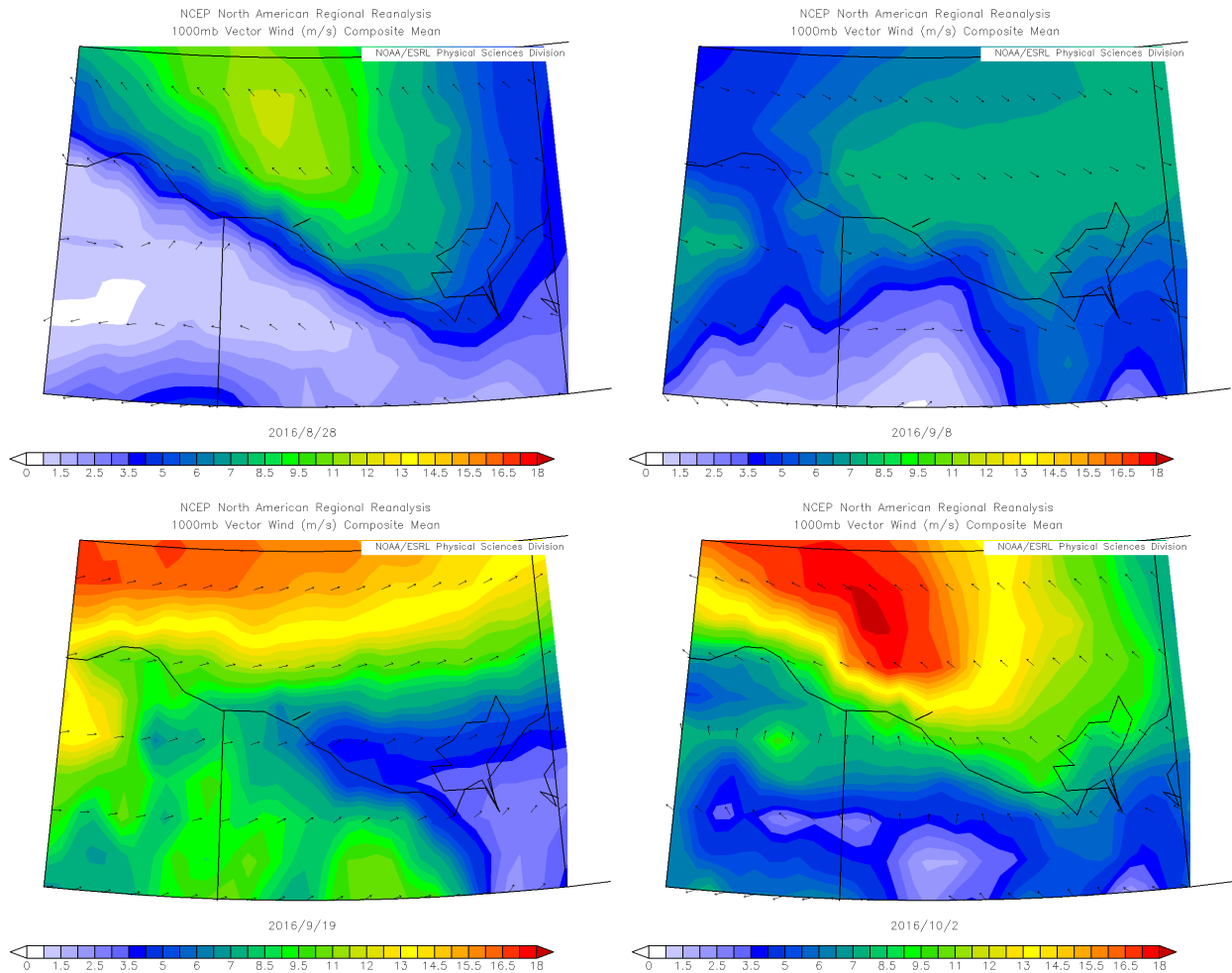


**Figure 16. NARR daily composite of surface vector winds for the Mackenzie Trough region.** The color indicates wind speed (0–18 m/s). The four time periods correspond to the four satellite images shown in Figure 12. For each time period, the winds are blowing from a different direction.

The plume (Figure 16, August 28, 2016) was observed to be heading almost straight offshore during a period of oscillating winds but predominantly southeasterly (upwelling favorable) with the daily average wind speed of 10 m/s near the trough. The glider detected a thin layer of river water (~5 m thick) on the western side of the trough, which is consistent with what the satellite image show. Conversely, during a period of northwesterly winds (Figure 16, September 8, 2016) with wind speeds of 6–7 m/s, the plume was advected shoreward while at the same time cooled and deepened the surface mixed layer. While the plume water was seen on two sides of the trough, very little plume water was found in the central portion of the trough. The eastward flow configuration of the plume (Figure 16, September 19, 2016) was seen during a period of strong westerly winds with wind speeds of 10–12 m/s. This wind produced a narrower plume that is advected to the east. A patch of plume is clearly seen just southeast of Herschel Island. During this period of westerly winds, the mixed layer substantially deepened once again. The westward flow configuration of the plume (Figure 16, October 2, 2016) had strong northeast winds of 10–13 m/s. Although the river plume water was clearly seen in the satellite RGB data, the glider data was inconclusive during this time.

### 2.3.6.2 Two Circulation Regimes in the Mackenzie Trough

Looking closely at the glider depth-averaged velocities, we found that the circulation in the region can be classified into two general flow regimes: eastward flow and westward flow. Figure 17 shows examples of each flow regime with glider tracks (blue) and estimates of the depth-averaged velocities (red arrows) overlaid on sea surface height (colormap) and HYCOM daily depth-averaged currents (black arrows). By visual inspection, we see that the glider's depth-averaged velocity estimates are largely consistent with depth-averaged velocities from HYCOM, especially during eastward flow regimes. HYCOM can also capture westward flow regimes but the modeled velocities tend to be weaker than the measured velocities. In terms of the flow on the continental shelves, we see that eastward along-shelf transport is correlated with sea level setup at the coast, while the sea level appears basically flat in the model during westward flow regimes. This basic data-model comparison gives us some confidence in using HYCOM to characterize the flow field in a larger spatial and temporal context.

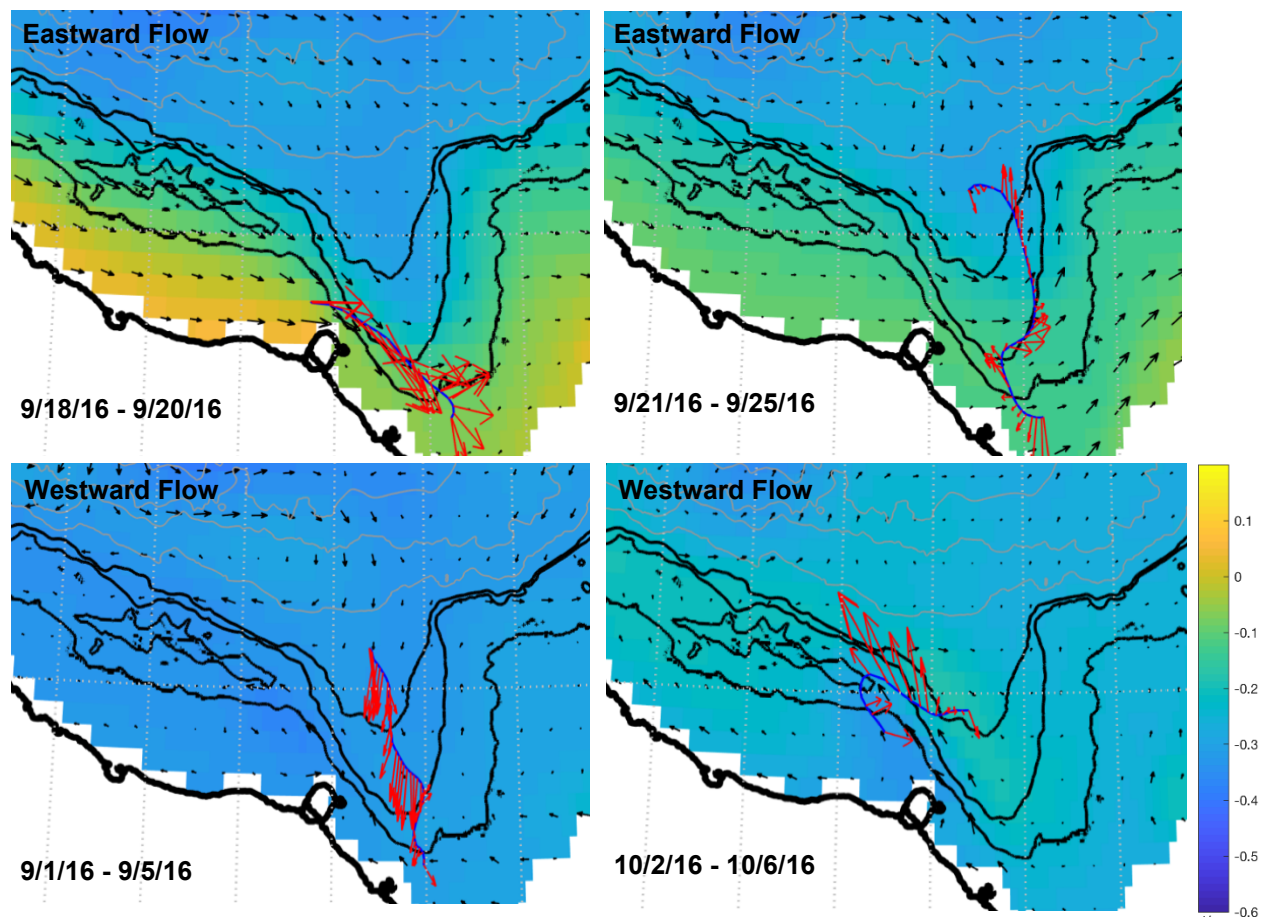


Figure 17. Glider path (blue) and glider estimated depth-averaged velocities (red arrows) overlaid on top of HYCOM sea surface height field and depth-averaged currents (upper 200 m of the water column).

### 2.3.6.3 Hydrographic Response to Eastward and Westward Transport

The water column responses for the two circulation regimes outlined in the previous section are sharply different, especially during periods of strong along-shelf transport (Figure 18). Eastward flow is associated with westerly winds and high sea level setup at the coast. Although the winds during September 21–25 were variable, it followed a period of strong westerly winds that likely setup the



observed downwelling response. The pycnocline at a depth of 30 m was depressed near the head of the trough to a depth of 60 m. Only surface shelf water with salinity greater than 27 psu was seen at the head of the Mackenzie Trough. Mackenzie River water was not observed after a period of eastward flow driven by downwelling, as expected. Westward flow is associated with strong easterly winds and low or flat sea level setup at the coast. Strong easterly upwelling-favorable winds occurred during the October 2–5 transect. This wind condition led to the upwelling of cold ( $< 0\text{ }^{\circ}\text{C}$ ) and salty ( $> 31\text{ psu}$ ) Pacific water onto the continental shelf to the west of Mackenzie Trough. The upwelling set up a very sharp density front across the shelfbreak. The glider measured depth-averaged velocity at the density front was over 50 cm/s. There is a hint of fresh shelf water landward of the upwelled Pacific water on the shelf. The glider did not go far enough landward to capture the coastal plume that was presumably on the shelf.

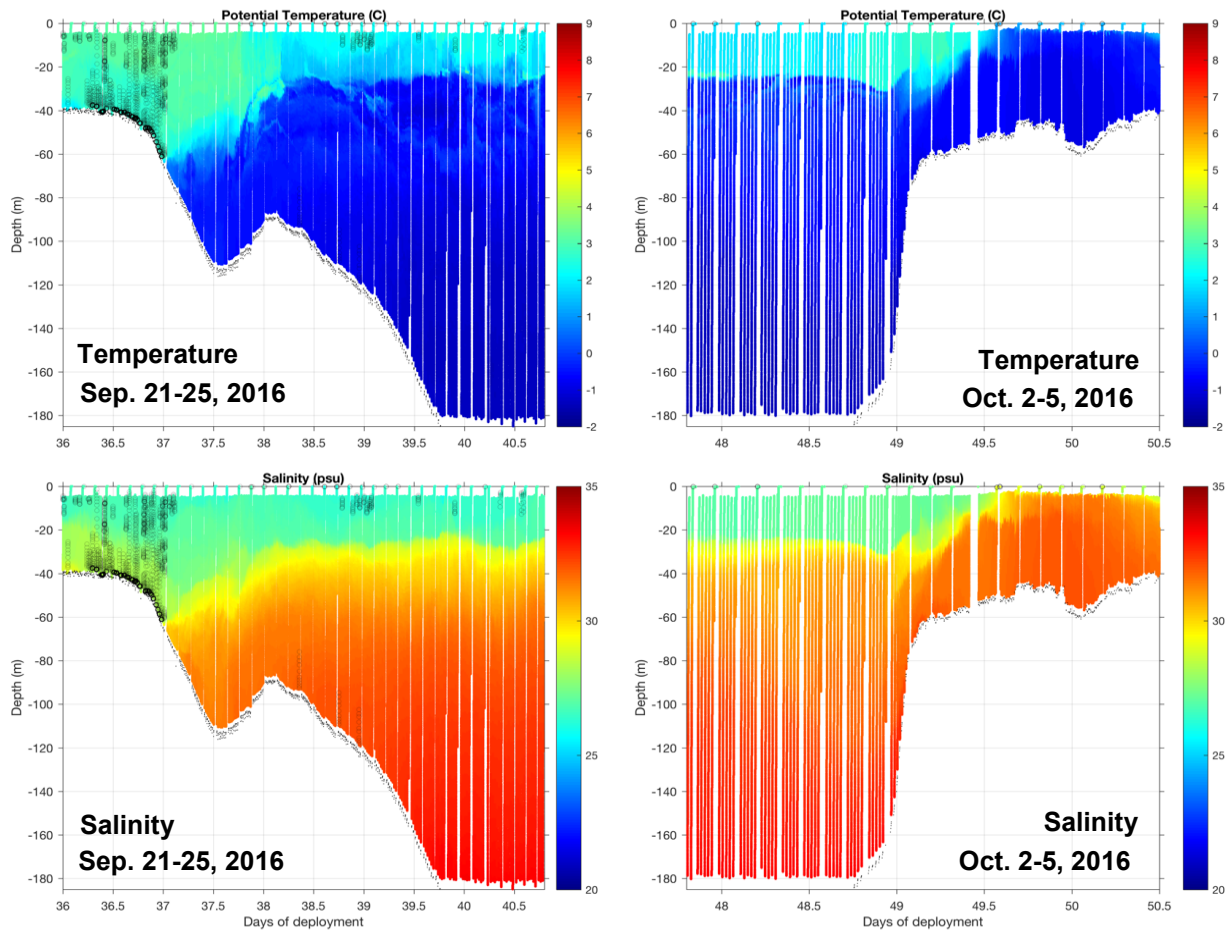


**Figure 18. Cross-shelf glider sections of temperature and salinity showing the hydrographic responses during strong eastward flow (left panel) and strong westward flow (right panel) conditions.**

#### 2.3.6.4 Inter-Annual Variability of Wind and Circulation

Extending the analysis of event-scale circulation patterns in the eastern Beaufort Sea, we proceeded to analyze the seasonal scale wind forcing and the circulation pattern for the entire Beaufort and Chukchi Sea for open water season in the summer. We focused on the peak open water month of September. Monthly composites of surface winds from NARR show that there is considerable year to year variability in terms of the wind pattern, direction, and strength. For example, during September of 2011 (Figure 19,

left column), the average wind in the Chukchi and Beaufort shelves was strongly easterly with wind speed more than 5 m/s. The monthly averaged HYCOM depth-averaged current for the same period shows that flow along the Beaufort shelfbreak, slope, and the Mackenzie Trough regions are all directed westward. In contrast, the average winds in September 2016 were moderately westerly with wind speeds of 3–4 m/s (Figure 19, right column). During this period, the HYCOM flow showed a well-developed Alaskan Coastal Current at Barrow Canyon. An eastward flowing coastal current stretches from the Chukchi shelf to Mackenzie Trough and into Amundsen Gulf. If we assume an advection speed of 0.1 m/s for Mackenzie plume water then, depending on the average winds over the course of a month, the plume water could end up in either the Canadian Arctic Archipelago or in the Beaufort Gyre. The two scenarios have very different implications for how Mackenzie River water impacts the western Arctic Ocean.

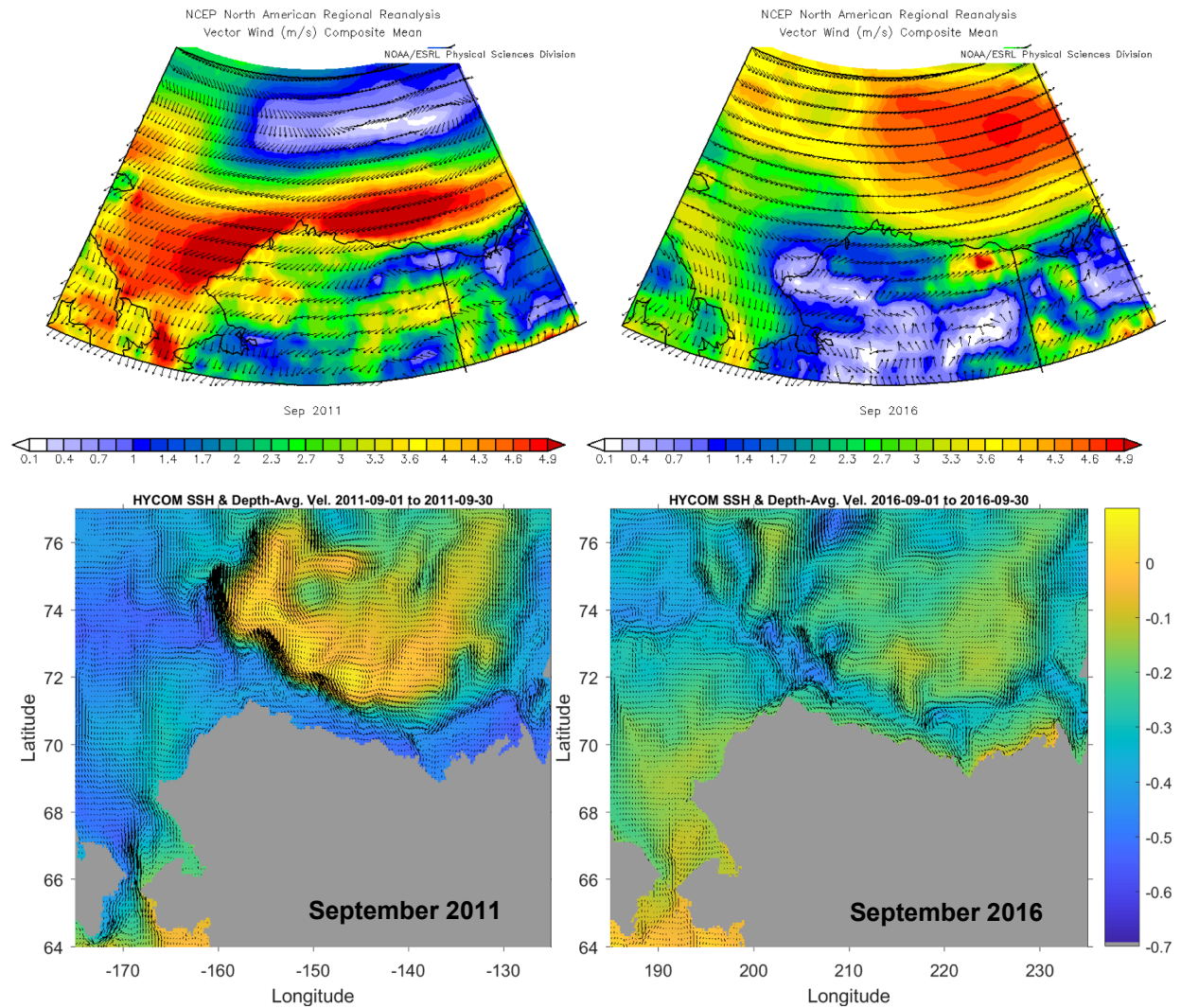


**Figure 19. Top panels: NARR monthly mean surface winds for September 2011 (left) and September 2016 (right). Bottom panels: HYCOM depth-averaged currents and sea surface heights for September 2011 (left) and September 2016 (right).**

One other notable difference between 2016 and 2011 was the strength of the Beaufort Gyre. If we use the sea surface height field as a proxy for the gyre strength, then the anticyclonic circulation around the gyre is much stronger in 2011. This is likely a direct result of the large-scale wind field as the winds in

September 2011 strengthened the anticyclonic gyre circulation, while the winds in September 2016 were in the opposite direction of the gyre circulation.

The climatological monthly average wind fields for the Chukchi and Beaufort Seas during the high discharge open water season are shown in Figure 20. In general, the climatological winds for each month are almost always easterly. On an annual cycle, the wind is weakest in August, which is also when we expect the eastward coastal transport to be strongest, and strongest in November. For September, the average winds over most of Chukchi and Beaufort shelves are weakly easterly (2–3 m/s). Although this is in an upwelling-favorable direction, the strength may not be enough to reverse the direction of the eastward flowing coastal current. To address the question of climatological circulation for the summer months, a more in-depth analysis of long-term HYCOM reanalysis would be needed.

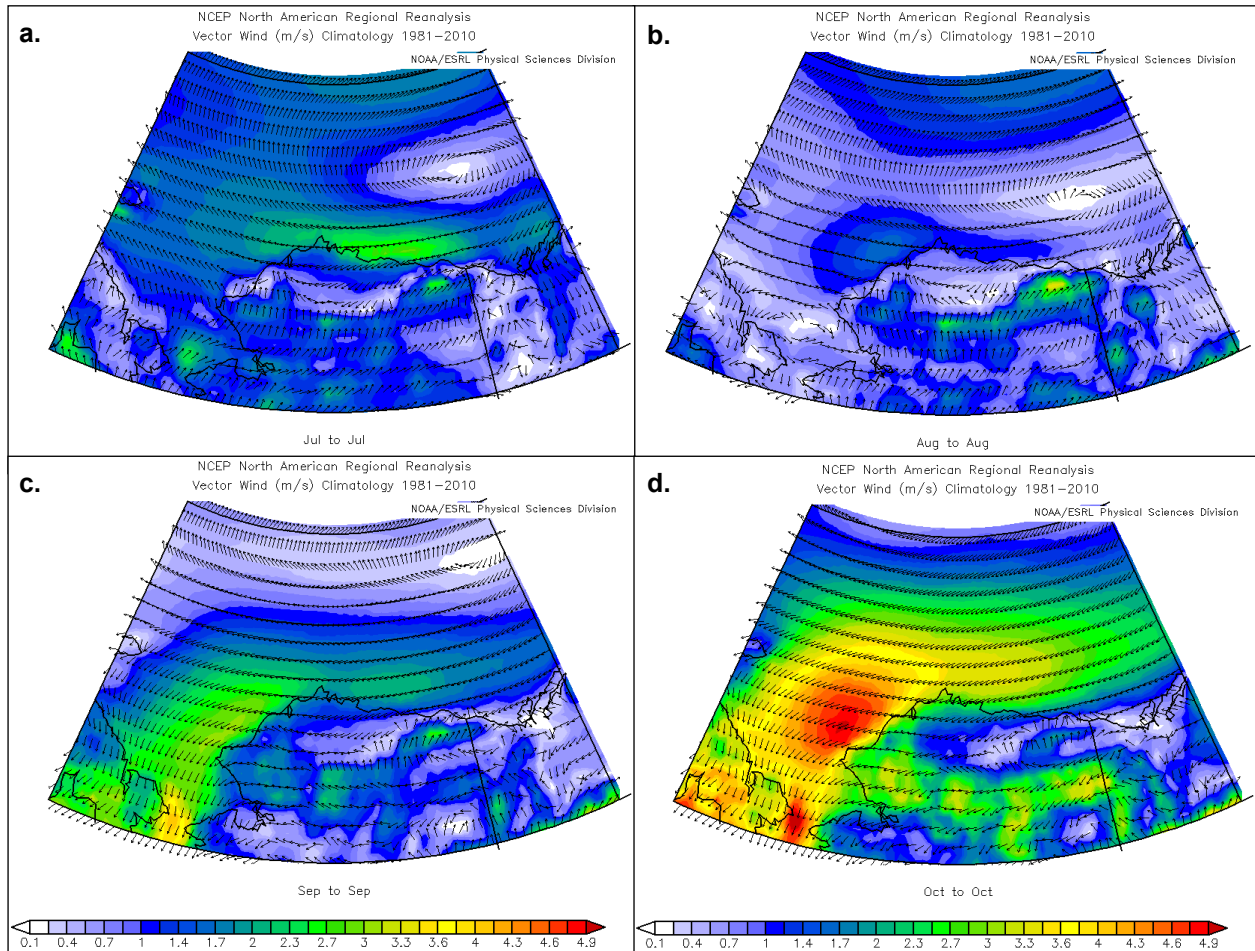


Figure 20. Climatological NARR winds for (a) July, (b) August, (c) September, and (d) October.

### 2.3.6.5 Multi-Year Variability of Winds and Circulation in the Western Arctic

On the inter-annual and multi-year timescales, we found a long-term variability of the seasonal winds in the western Arctic. For example, in the most recent years from 2012 to 2017, the winds in the Chukchi and Beaufort shelves, averaged for the entire summer, are weakly easterly with an average speed of 2 m/s. On the other hand, during the period from 2005 to 2011, the average summertime winds are much stronger easterlies with speeds up to 5 m/s. If we compare with the period from 2000 to 2004, the average summertime winds are nearly zero, averaging around 1 m/s.



Based on these observations, we think that during the years when the average summertime winds are strongly easterly (i.e., 2005–2011), most of the Mackenzie River water would end up being advected westward and eventually end up in the Beaufort Gyre, adding to the gyre’s freshwater supply and potentially being trapped in the Arctic for 4–14 years (Figure 21; Bauch et al. 1995, Chen et al. 2008, Ekwurzel et al. 2001). On the other hand, during weak wind years, most of the Mackenzie River water would flow eastward into the Canadian Arctic Archipelago and exit the Arctic much faster, likely in the order of just a couple of years (Fichot et al. 2013).

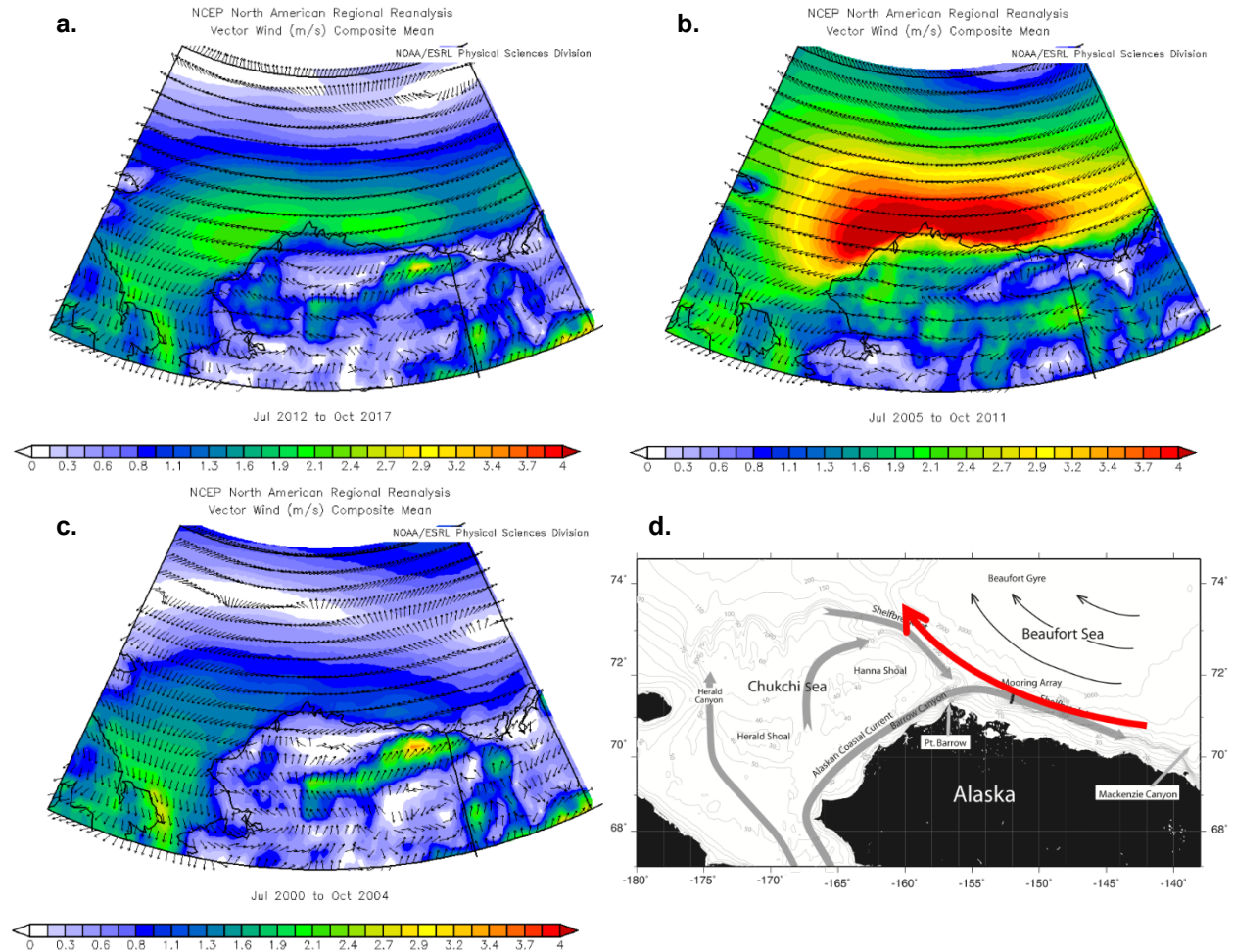


**Figure 21. Average NARR surface summer (July–October) winds for (a) 2012–2017, (b) 2005–2011, (c) 2000–2004. (d) An illustration of the major currents in the Chukchi and Beaufort Seas (adopted from Schulze et al. 2013).**

The red arrow indicates the likely direction of the shelfbreak boundary current during times of strong easterly winds.

## 2.4 Discussion

The hypotheses tested during the AUV glider component included:

- The Mackenzie River plume strongly affects the stratification and bio-optical properties of the surface mixed layer on both Canadian and US continental shelves. This is discussed in sections 2.3.2, 2.3.3, and 2.3.4.
- River-shelf-basin exchange is strongly affected by seasonal heating and cooling, wind-driven advection, and interaction with shelfbreak frontal currents. This is discussed in sections 2.3.5 and 2.3.6.
- In the absence of strong wind forcing, buoyancy-driven shelf flow and the shelfbreak jet advects fresh Mackenzie River water eastward toward the Amundsen Gulf. Under moderate to strong easterly winds, however, the Mackenzie River plume is advected westward toward the Alaskan Beaufort Sea. This is discussed in section 2.3.6.
- The Mackenzie River plume and wind forcing vary on time scale of 1 to 2 weeks driven by regional weather and variability of shelf and shelfbreak circulation. This is discussed in section 2.3.6.

#### **2.4.1 Connection Between Beaufort Shelf and Beaufort Gyre**

It is worth highlighting the ephemeral nature of the coastal and shelfbreak circulation in the Beaufort Sea. Although the anticyclonic Beaufort Gyre is a persistent feature, which may strengthen or weaken over the course of multiple years, the shelfbreak jet and the coastal current can change strength and direction on event time scales of days to weeks. Under strong easterly winds, the shelf current, shelfbreak jet, and the Beaufort Gyre all flow in the same direction. Based on the HYCOM model output, it is not clear whether the gyre circulation and the shelfbreak boundary current merge as one or whether they maintain their separate identities.

During one part of the MARES glider deployment (October 2–5, 2016), the strong westward current at the shelfbreak, formed directly as a result of shelfbreak upwelling, had its own well-defined structure with peak velocity right at the shelfbreak. However, at other times, the shelfbreak jet was not well defined, just a westward transport across the entire glider cross-shelfbreak transect (September 5–7, 11–16). Although we cannot definitively address this issue with the current dataset, we hypothesize that, depending on the forcing condition, the Beaufort shelfbreak jet is a separate flow feature at times, or it can be part of the Beaufort Gyre pressed southward against the continental slope at other times. The difference depends on local zonal wind shear and the magnitude of shelfbreak upwelling.

#### **2.4.2 Multi-Year Variability of Zonal Winds in the Beaufort Sea**

There is multi-year variability to the summertime wind pattern in the Chukchi and Beaufort Sea. This can be seen when considering the wind data observed during the glider deployment and the other time periods discussed above into a multi-year and even multi-decade context (Figure 22). Overall, the data show that the summertime zonally averaged wind speed for the Chukchi-Beaufort shelf, and slope region for all years from 1948–2004 and 2012–2017 reached a maximum speed of approximately 10 m/s (average wind speed of 4 m/s) and have been predominantly easterly winds. This pattern held true except for the period from 2005 to 2011 when the average easterly zonal wind speed was  $10 \pm 5$  m/s. This is a substantial departure from the climatological mean and would likely have driven an anomalous westward flow along the Chukchi and Beaufort shelves and shelfbreak during those years.

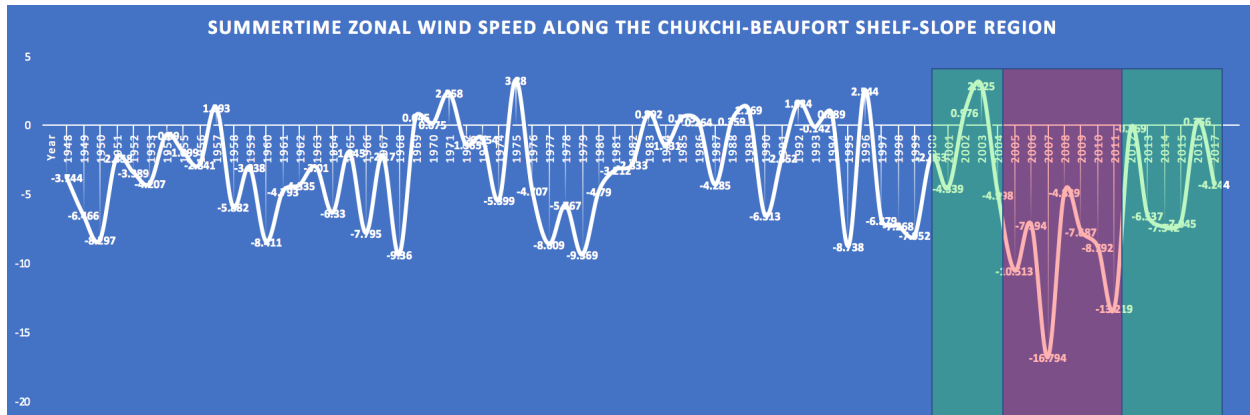


**Figure 22. Summertime zonally averaged wind speed for the Chukchi-Beaufort shelf and slope region (1948 to 2017 NCEP reanalysis).**  
The alternating green, pink, green regions highlights the three periods considered in our temporal variability analysis.

### 2.4.3 Fate of the Mackenzie Plume

In the context of considering the fate of freshwater discharging into the Arctic from the Mackenzie River, strong and persistent westward transport could lead to advection of Mackenzie River water onto the Alaskan Beaufort Shelf and eventual entrainment into the Beaufort Gyre. The nominal residence time of water in the western Arctic is 4–14 years (Bauch et al. 1995, Chen et al. 2008, Ekwurzel et al. 2001). On the other hand, there is substantial transport of freshwater from the western Arctic into the Atlantic Ocean through the Canadian Arctic Archipelago, if a persistent westerly wind supports eastward along-shelf transport. In that case it is possible for Mackenzie River water to flow directly into and through the Canadian Arctic Archipelago along the Canadian Beaufort shelf, where it may stay for a couple of years before exiting the Arctic into the North Atlantic (Fichot et al. 2013).

## 2.5 Conclusions

The glider component of the MARES project provided physical, biological, and chemical observations acquired from a moving platform and allowed for the collection of fine scale information on the Mackenzie River plume. The glider study complemented the ongoing mooring component in the study region and found that:

- Wind appears to be the main driver of shelfbreak and Mackenzie Trough circulation.
- Multi-year variability of summertime winds affects the structure of the Beaufort Gyre, shelfbreak boundary current, and downstream fate of Mackenzie River water.
- The shelfbreak jet and the coastal current can change strength and direction on event time scales of days to weeks.
- In years when the average summertime winds are strongly easterly (i.e., 2005–2011), most of the Mackenzie River water flows westward and eventually ends up in the Beaufort Gyre, adding to the gyre’s freshwater supply and potentially being trapped in the Arctic for up to 14 years.
- During weak wind years, most of the Mackenzie River water is downwelled, flows eastward into the Canadian Arctic Archipelago, and exits the Arctic much faster (a couple of years).
- The summertime Chukchi and Beaufort shelfbreak jet cannot be assumed to be steady on the inter-annual timescale. The timeframe of 2005–2011 appears to be an exceptional period with stronger easterly winds (upwelling conditions with plume going westward) than any period before or since.

## **2.6 Limitations of the MARES Glider Survey**

The MARES glider deployment collected unprecedented high resolution physical, bio-optical, and bio-acoustic data in the Mackenzie Trough region during the summer open water season in 2016. The study was enabled by new advancement in glider technology, such as large displacement buoyancy pumps, hybrid thrusters, and new bio-optical and bio-acoustic sensors. At the same time, the glider program was one part of a larger study involving ship-based sampling and moorings.

Because of the large size of the Mackenzie Trough and the importance of mesoscale processes, it is impossible for a single glider to conduct a synoptic survey of the entire region. Each complete survey of the trough took 10–15 days, during which the circulation pattern could have changed several times (as we have found in this study). To overcome this sampling issue in our interpretation of the data, we divided the glider survey into quasi-synoptic individual transects, each 2–5 days long. We were further guided by the insight that the circulation is largely wind-driven. By using a combination of reanalysis wind modelling, data assimilative ocean modelling, and satellite remote sensing to complement the glider observations, we were able to reconstruct the major events and circulation regimes encountered during the MARES 2016 summer field season. To capture important event drivers at the appropriate temporal scales and thus enable true synoptic sampling using autonomous platforms, we recommend that a minimum of three underwater gliders be deployed simultaneously.

## **2.7 Future Research**

### **2.7.1.1 Synthesis With MARES Moorings**

The MARES moorings were deployed in fall of 2016 and were scheduled be re-deployed in October 2017. An obvious synthesis effort between the glider and mooring data will be needed when the mooring data have been retrieved and processed. The mooring array, deployed across the western wall of the Mackenzie Trough, should be able to capture the temporal variability of the shelf and shelfbreak circulation and hydrography in detail. These data should shine light on the issue of how the circulation might respond to changes in wind forcing and may determine the threshold wind velocity which can reverse the direction of the eastward flowing coastal and shelfbreak current.

### **2.7.1.2 Detailed Analysis of Bio-optical Data**

There is a substantial amount of bio-optical and bio-acoustic data from the glider that remain to be analyzed in detail. The relationships between water masses, stratification, light, primary production, and dissolved oxygen have yet to be explored. As one example, preliminary analyses have shown evidence of biological heating at depth below the mixed layer. Two examples of this phenomenon are shown in the profile plots in Figure 23 where at depths of 20–25 m and 30–35 m, sub-surface chlorophyll maxima at the bottom of the pycnocline spatially correspond to positive temperature anomalies of nearly 1 °C. A detailed quantitative analysis of this phenomenon has yet to be completed.

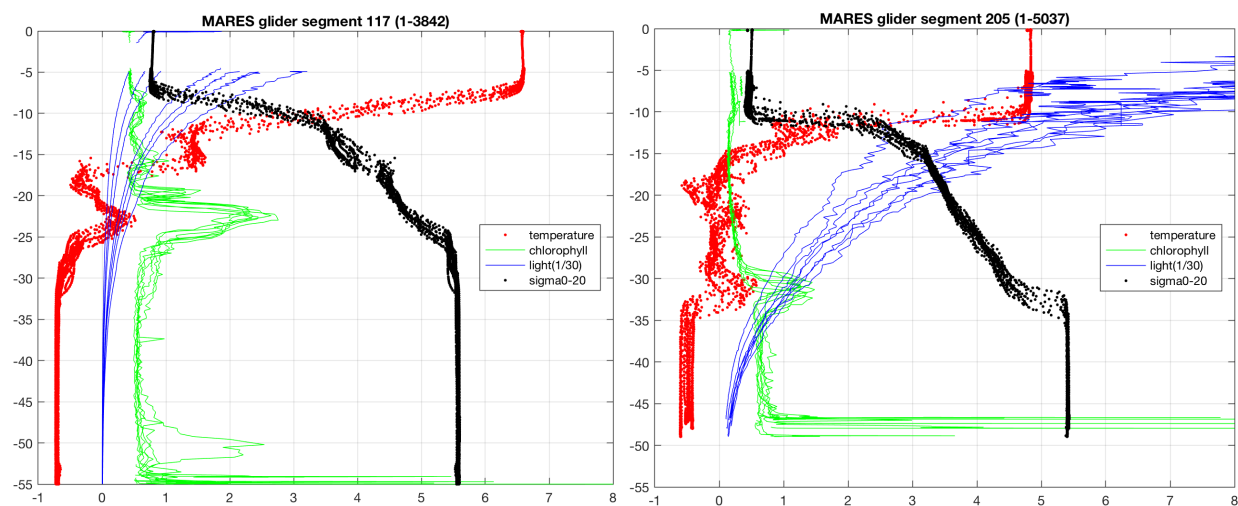


**Figure 23. Profile plot of glider temperature (red), chlorophyll-a (green), light (blue), and density (black) measurements for two glider transects during MARES 2016.**

Both transects were on the Beaufort shelf to the west of Mackenzie Trough in the first half of the deployment.

### 2.7.1.3 Data Assimilative Modeling and Model-data Comparison

Though not part of the currently funded MARES study, validation and assimilation for future process-oriented high resolution numerical modeling studies would help resolve the detailed circulation and dynamics inside the Mackenzie Trough. A recent idealized modeling study (Machuca and Allen 2018) has shown interesting coastal trapped waves, which affect the dynamics of canyon upwelling and downwelling inside the Mackenzie Trough. A comparison analysis of the glider data with the model could help us better understand the sub-mesoscale variabilities observed with the glider.

Furthermore, upgrades to the Global HYCOM model with the addition of more vertical layers targeting the shallow continental shelf environment (GOFS 3.1 with 41 layers vs. GOFS 3.0 with 32 layers), as well as a detailed comparison of the HYCOM output with the glider data with hydrography in addition to velocity, would be highly useful. When the longer term HYCOM reanalysis product is available and validated, we could use the model to make regional scale heat and salt budget calculations.

Finally, changes in ice conditions and longer open water seasons and fetch have likely been affecting these wind-driven dynamics and possibly been accentuating the difference between these two regimes and their subsequent effects on circulation and plume entrainment. Given the implications for oil spill trajectories and potential ecological impacts of spills, it would be beneficial to couple our findings with regional models that include ice cover and wind forcing factors.

### 2.7.1.4 Lagrangian Analysis of the Mackenzie Plume

Finally, using virtual Lagrangian tools such as tracers and drifters, we could conduct long-term release experiments with validated models to better determine the downstream fate of Mackenzie River plume on a range of space and time scales.



### 3 Mooring Array

#### 3.1 Introduction

As part of MARES, a mooring array was deployed October 5th and 6th, 2016 across the shelf-slope of the Canadian Beaufort Sea (Figure 24). In addition to the four MARES moorings, an inshore mooring was deployed for the UAF, and an offshore mooring was deployed the previous month by DFO Canada. Hence, the composite MARES/UAF/DFO array consists of six moorings spanning from the inner shelf (14 m depth) to the mid-continental slope (750 m depth) This unique group of mooring provide a yearlong time series of the biophysical and chemical characteristics along the shelf and on to the continental slope, including under-ice periods, and able to capture the influence of the Mackenzie River plume in this region.

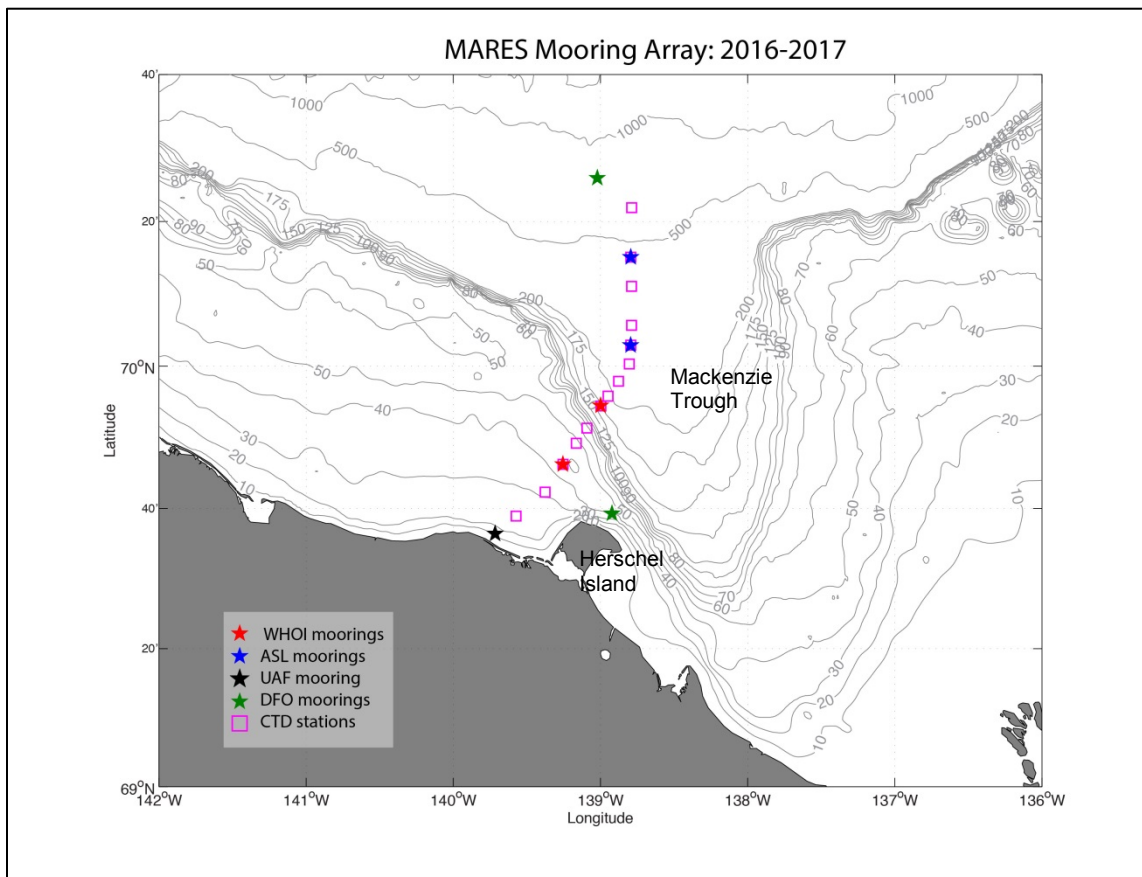


**Figure 24. Locations of the moorings comprising the composite MARES/UAF/DFO array (see the legend). Also shown are the locations of the CTD stations occupied during the deployment cruise. The bathymetry is from the International Bathymetric Chart of the Arctic Ocean (IBCAO) version 3.**

#### 3.2 Methods

##### 3.2.1 Field Methods and Equipment

The CCGS *Sir Wilfrid Laurier* was loaded on June 19, 2016 in Victoria, B.C., Canada, with all the necessary mooring equipment. On September 20, 2016, the ASL mooring technician boarded the ship in

Cambridge Bay, enabling him to locate, prepare, and program most of the ASL and WHOI mooring instrumentation prior to the beginning of the MARES segment of the cruise. This included performing the compass spins of the Acoustic Doppler Current Profilers (ADCPs). All of the other ASL and WHOI equipment checked out properly. The rest of the MARES team embarked the ship at Herschel Island via helicopter on October 3, and science operations began the morning of October 4.

First, the ship collected bathymetric data at the inshore end of the line to determine the location of the UAF inner-shelf mooring. Following this, the conductivity-temperature-depth (CTD)/water sample section was carried out, consisting of 14 stations along the mooring line (Figure 24), five of which included water sampling. The CTD section included water samples for inorganic nutrients, dissolved inorganic carbon (DIC), and carbon characterization of suspended sediments. During this time, the last of the mooring instrumentation was prepped, and the assembly of the mooring components started.

On October 5, 2016, the two ASL moorings (M4 and M3) were deployed along with the offshore WHOI mooring (M2). On October 6, 2016, the MARES glider was successfully recovered (see Section 2), and the WHOI mid-shelf mooring (M1) and UAF inner-shelf tripod were deployed (Figure 24; Table 1). Except during the deployment of the M3 and M4 moorings, when the sea state was marginal with 10–15 knot winds, the weather throughout the MARES segment of the cruise was ideal: light winds, calm seas, and good visibility. For the ASL and WHOI tall moorings, an acoustic survey was done after the deployments to precisely determine their locations (the tripods were lowered to the seafloor, hence no survey was required).

The instrumentation on each mooring is listed in Table 2 and shown schematically in the vertical plane in Figure 25–Figure 27. For the most part, the point temperature/salinity/pressure instruments (MicroCat T/S/P) record data every 15 minutes, the WHOI ADCPs sample hourly, the ASL Long Ranger ADCPs sample every 5 minutes, and the ASL's Quartermasters sample every 2 minutes. The moored profiler collects a vertical trace every 4 hours. This configuration enabled us to construct vertical sections of hydrographic properties and velocity numerous times per day. Both the zooplankton/fish recorders and point chemical sensors sample every hour, and the upward-looking sonars record ice drafts every few minutes. Finally, the passive acoustic marine mammal recorder samples 20 minutes out of every hour.

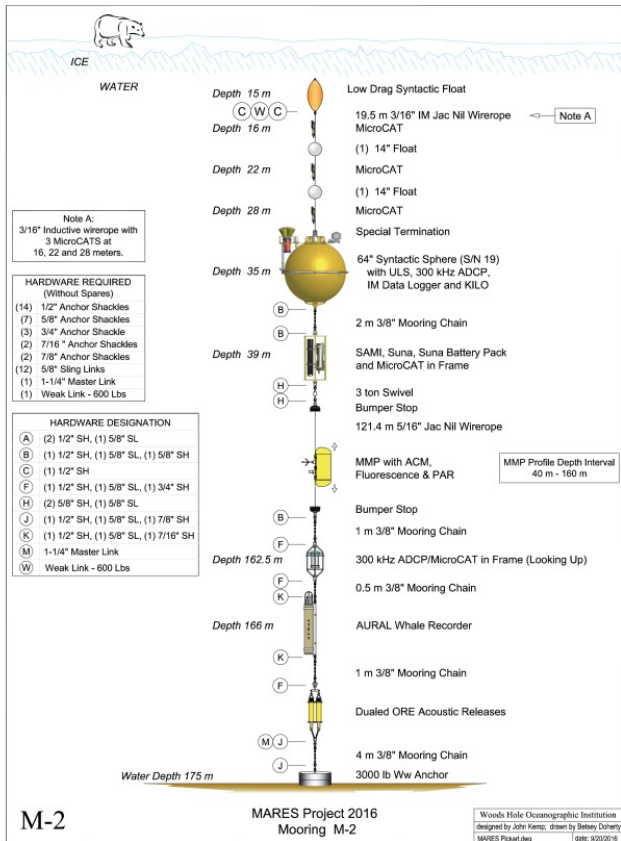
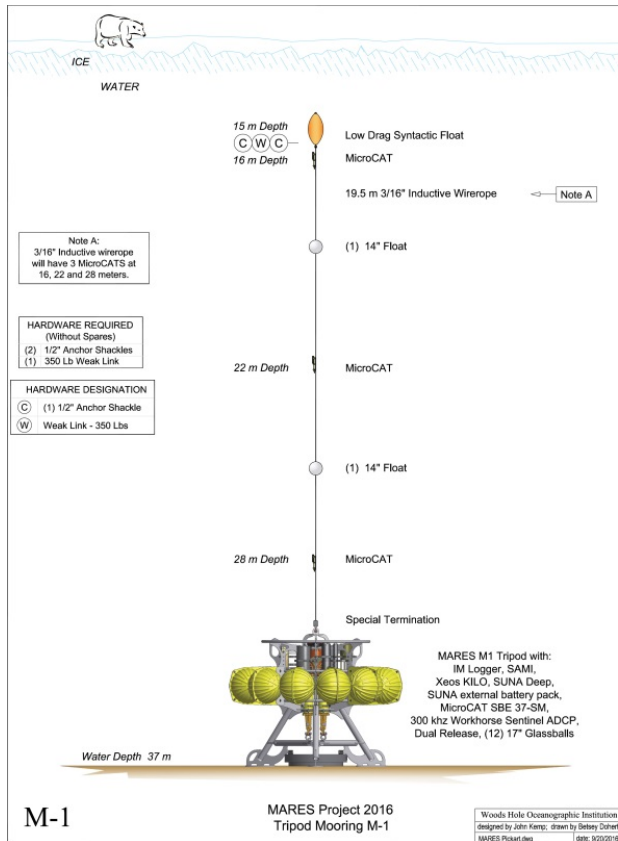
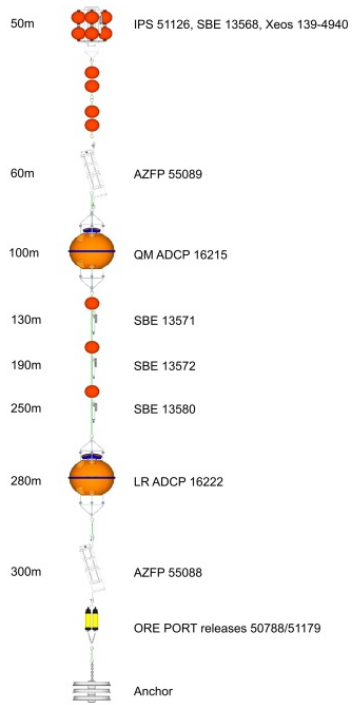


Figure 25. WHOI moorings M1 and M2.

### M3 mooring (300m depth)



### M4 mooring (440m depth)

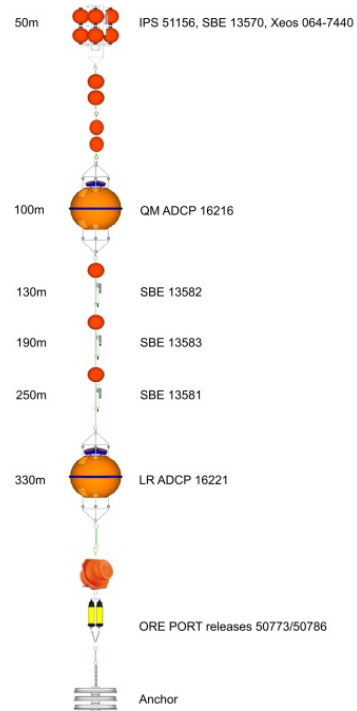
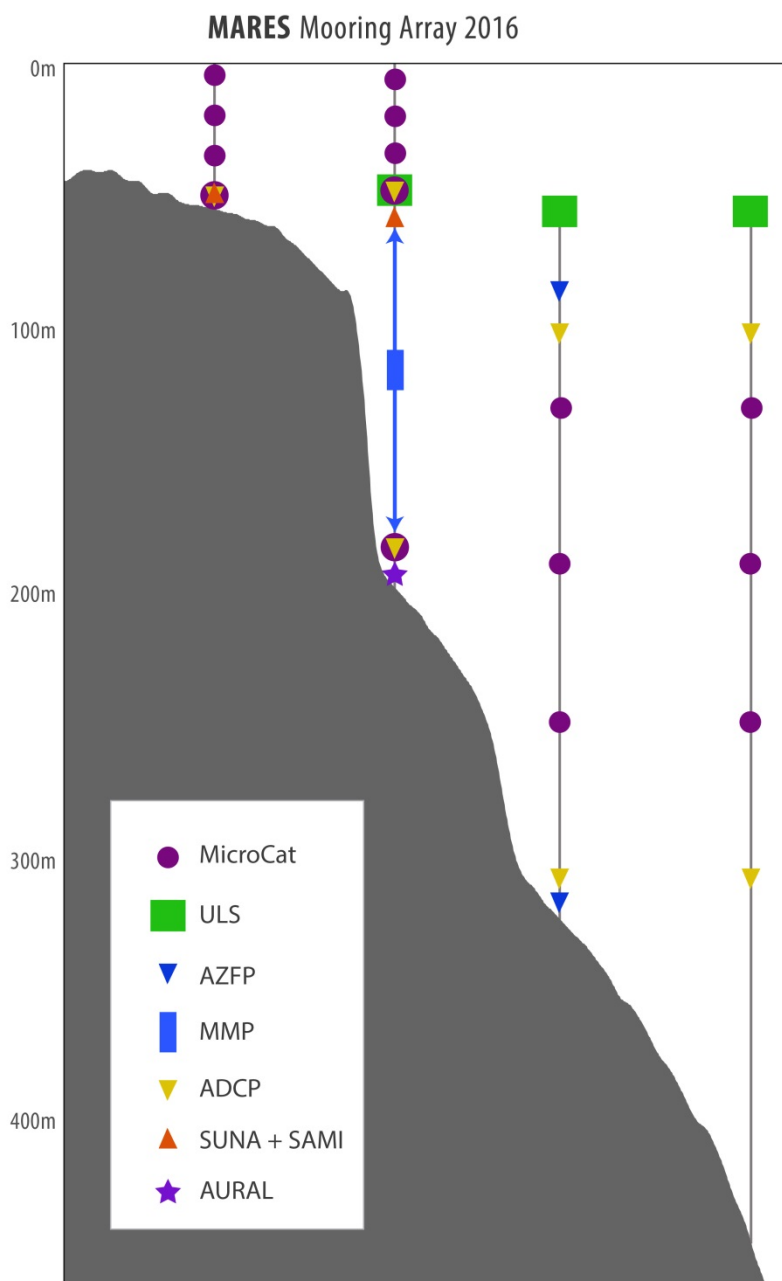


Figure 26. Mooring M3 and M4 (ASL).



**Figure 27. Instrumentation on the UAF, WHOI, and ASL moorings.**

**Table 1. UAF, WHOI, and ASL moorings deployed on the CCGS *Sir Wilfrid Laurier* cruise.**

Name	Latitude	Longitude	Bottom depth (m)	Date	Position method
UAF	69 36.426	139 42.925	14	10/06/2016	Anchor splash
M1 (WHOI)	69 46.235	139 15.286	40	10/06/2016	Anchor splash
M2 (WHOI)	69 54.475	138 59.925	175	10/05/2016	Surveyed position
M3 (ASL-300)	70 2.909	138 47.691	300	10/05/2016	Surveyed position
M4 (ASL-440)	70 15.101	138 47.626	440	10/05/2016	Surveyed position

**Table 2. List of the instrumentation contained on the WHOI and ASL moorings.**

Mooring	Deploy depth (m)	Instrument
M1	16	MicroCat T/S/P
	22	MicroCat T/S/P
	28	MicroCat T/S/P
	39	MIR logger
	39	SUNA nitrate
	39	SAMI pCO2 sensor
	39	SAMI battery
	39	Upward-facing 300 kHz ADCP
M2	20	MicroCat T/S/P
	26	MicroCat T/S/P
	31	MicroCat T/S/P
	35	Upward Looking Sonar (ULS)
	35	Upward-facing 300 kHz ADCP
	35	MIR data logger
	39	SAMI pCO2 sensor
	39	SUNA nitrate sensor
	39	SUNA Battery
	39	MicroCat T/S/P
	-	MMP T/S/P/O2 + fluorescence, PAR, turbidity
	162.5	Upward-facing 300 kHz ADCP
	162.5	MicroCat T/S/P
	166	AURAL whale recorder
M3	50	IPS 5 Ice Profiling Sonar
	50	SBE Temperature Sensor
	60	Acoustic Zooplankton Fish Profiler (AZFP)
	100	Upward-facing 150 kHz ADCP-QM
	130	SBE
	190	SBE
	250	SBE
	280	Upward-facing 75 kHz ADCP-LR
	300	Acoustic Zooplankton Fish Profiler (AZFP)
	302	ORE PORT
	39	MicroCat T/S/P
M4	50	IPS 5 Ice Profiling Sonar
	50	SBE
	100	Upward-facing 150 kHz ADCP-QM
	130	SBE
	190	SBE

Mooring	Deploy depth (m)	Instrument
	250	SBE
	330	Upward-facing 75 kHz ADCP-LR
	428	ORE PORT

### 3.3 Results and Conclusions

The 2016 mooring deployment program was successful in deploying the four MARES moorings and the UAF mooring and collecting data via CTD casts and water samples. All mooring sensors were tested and deemed functional. The moorings remained in place until a recovery and redeploy cruise undertaken in the fall of 2017.

The CTD data was successfully collected at 14 stations along the mooring line, and potential temperature and salinity profiles were calculated (Figure 28, Figure 29). The thermocline and halocline were shallower than 50 m at all the stations, but comparatively shallower over the shelf. The layer of fresher and warmer surface waters were indicative of a freshwater input, probably from the Mackenzie River, given the samples were taken during the ice-free season long after ice melt.

At five of the CTD stations, water sampling was also completed (Figure 28). Measurements of temperature, salinity, DIC, nutrients, and total alkalinity were collected at varying depths at the M1, M2, M3, and M4 mooring locations, as well as at a midpoint along the line (Figure 30).

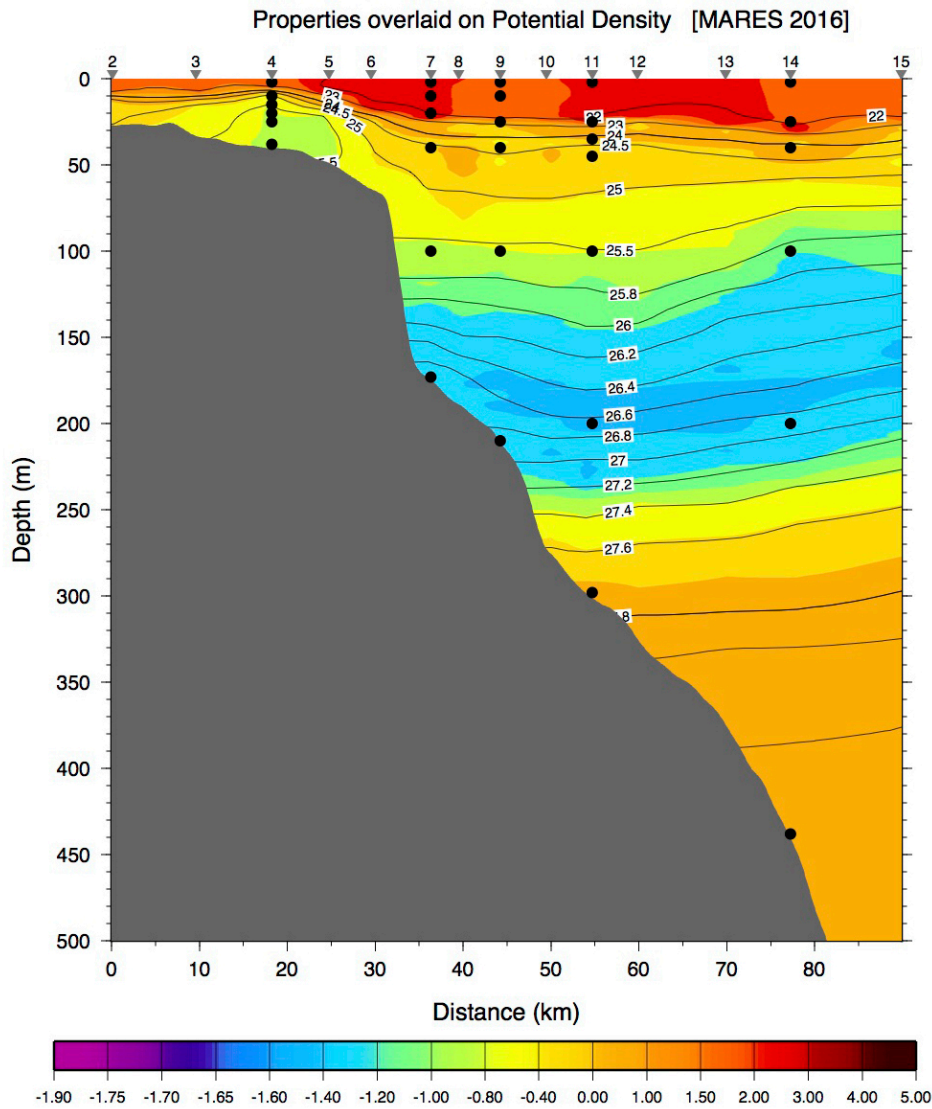


**Figure 28. Vertical section of potential temperature ( $^{\circ}\text{C}$ , color), as estimated from the CTD casts, overlain by potential density ( $\text{kg}/\text{m}^3$ , contours), occupied during the deployment cruise.** The black circles denote water sample locations. The CTD station numbers are listed at the top. The bottom topography is from the *CCGS Sir Wilfrid Laurier's* echosounder.



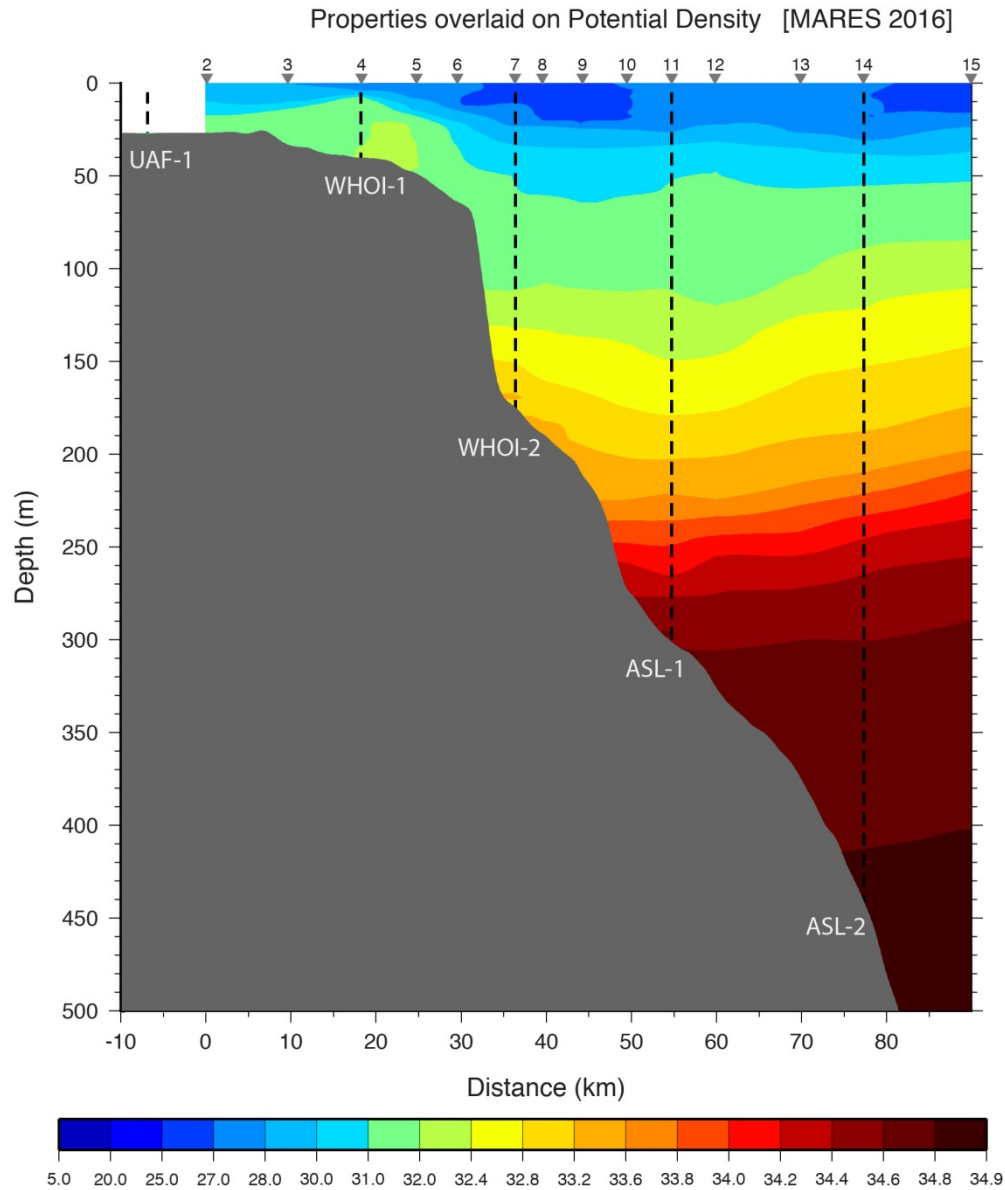


**Figure 29. Vertical section of potential salinity, as estimated from the CTD casts, and locations of the UAF, WHOI, and ASL moorings.**  
 The CTD station numbers are listed at the top. The bottom topography is from the *CCGS Sir Wilfrid Laurier's* echosounder.

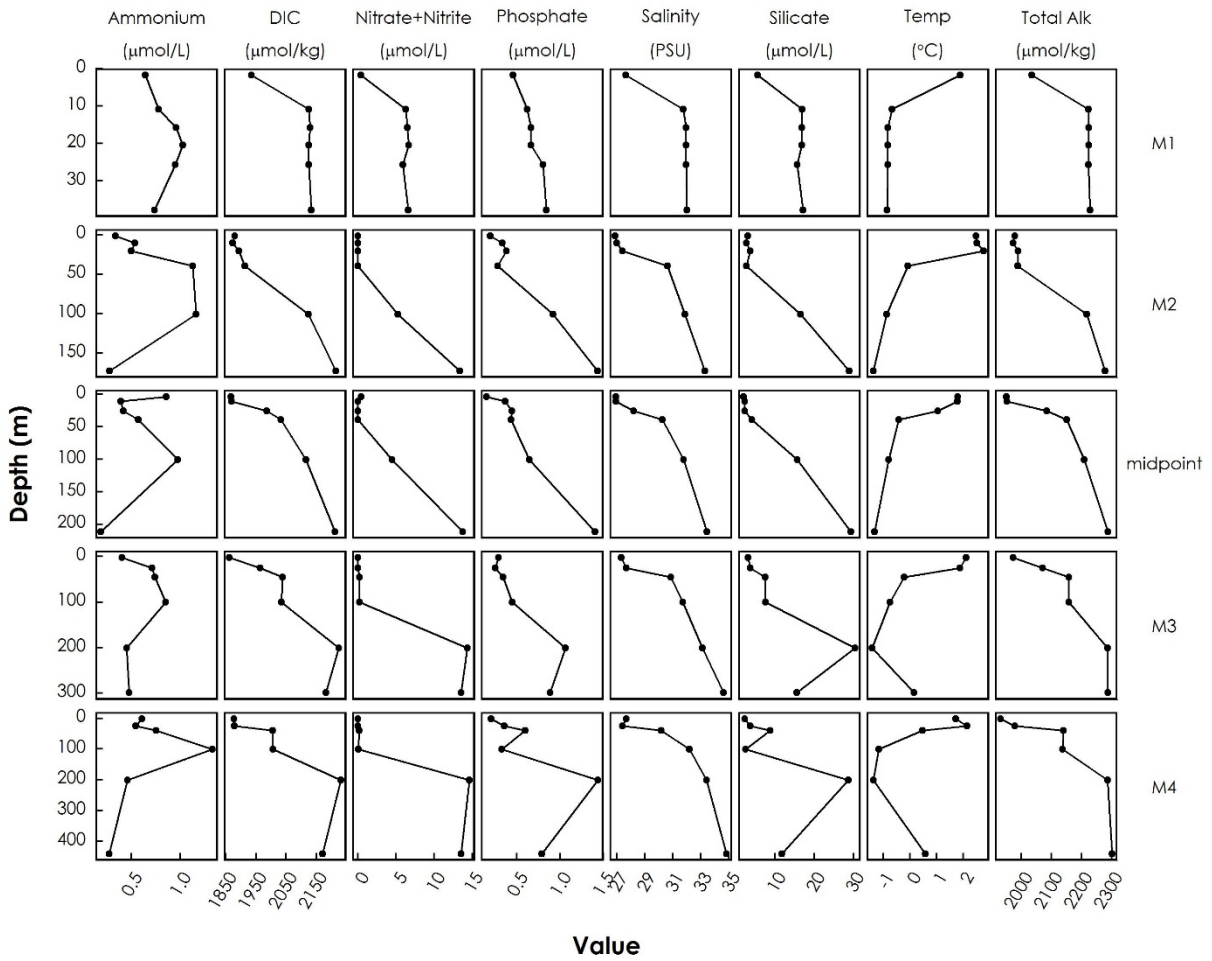


**Figure 30. Profiles of water data collected at the mooring locations and at the midpoint along the MARES mooring line in October 2016 (note different y-axis scales for each row of data).**

## 4 Linking Organic Carbon Sources with Meiofauna Abundance and Diversity

### 4.1 Introduction

Linking organic carbon sources with meiofauna abundance and diversity across the coastal shelf of the Mackenzie Delta involved sediment sampling, isotope and fatty acid analysis, and taxonomic identification. The Mackenzie continental shelf spans the northern part of the Canadian Arctic Ocean between the Amundsen Gulf on the east and the Mackenzie Trough to the west (Rachold et al. 2004). Ice typically begins to form on the shelf in mid-October and the delta, and nearshore areas stay ice covered until the spring break up in mid-May (O'Brien et al. 2006). Across the Mackenzie shelf and in the adjacent Beaufort Sea, the Mackenzie River dominates the supply of particulate organic carbon (POC) to the sediments with inputs of 2.1 Mt/yr, making it the largest sediment load from river input in the Arctic Ocean (Macdonald et al. 1998). About 70% of the freshwater discharges occur between May and September with the spring freshet, with 90% of the particulate flux occurring in June, July, and August (Yunker et al. 1995). Autochthonous primary production in the delta and nearby shelf is estimated to add at least an additional 3.3 Mt/yr of POC (Macdonald et al. 1998). Carbon preservation estimates in the region are limited but suggest that up to 97% of new production may be recycled and never reach the underlying sediments, while 60% of the POC from the terrestrial dominated Mackenzie River outflow, reaches sediments to be retained (Yunker et al. 1995, 2005). Sediments in the northern Beaufort Sea have been found to be dominated by a mixture of refractory marine and terrigenous carbon (Magen et al. 2010). A detailed comparison of carbon sources across the eastern Beaufort shelf using multiple methods found terrestrial carbon accounted for 11% to 44% of sedimentary organic matter, indicating that land-derived organic matter can play a substantial role in carbon dynamics in this region (Belicka and Harvey 2009). On the Beaufort shelf, eddies also play an important role in moving these sources of particulate organics, mixing old and newer materials. Data from stations at the eddy influenced shelf edge were found to be dominated by biogenic organic matter (O'Brien et al. 2013).

The goal of this study component was to understand the linkages between the flux of multiple sources of organic matter reaching bottom sediments, its recycling by the benthic community, and the impact on the community it supports. To accomplish this, four stations transecting the Mackenzie shelf and located directly below the four MARES moorings (see Section 3) were sampled for water column particles and sediments via box core during the mooring deployments (Figure 24). An additional station, located midway between the moorings, was sampled for water column particles only. Sediment sampling started at the 40 m isobath and ended at the approximate 440 m isobath. Sediments were analyzed for organic carbon and grain size as well as a suite of organic biomarkers combined with identification of benthic meiofaunal community structure. The analysis of amino acids, POC, and fatty acid and sterol biomarkers were performed and compared to meiobenthic diversity and abundance.

### 4.2 Methods

#### 4.2.1 Sampling Locations

Field sampling was performed on the CCGS *Sir Wilfrid Laurier* in the Fall (October) of 2016 as part of the MARES mooring deployment cruise. Station locations are shown in Figure 24 and Table 3.

**Table 3. Sampling locations for water and sediment collections.**

Station	Latitude	Longitude	Date sampled	Sample type
M1 (CTD station 4)	69 46.24 N	139 15.56 W	Oct 04 2016	Water/ Sediments
M2 (CTD station 7)	69 54.43 N	138 59.81 W	Oct 04 2016	Water/ Sediments
Midpoint (CTD station 9)	69 57.90 N	138 52.62 W	Oct 05 2016	Water only
M3 (CTD station 11)	70 02.92 N	138 47.62 W	Oct 05 2016	Water/ Sediments
M4 (CTD station 14)	70 15.09 N	138 47.65 W	Oct 05 2016	Water/ Sediments

#### 4.2.2 Water Column Particles

Particles were collected using Niskin bottle samplers attached to a rosette and deployed with a Seabird CTD to collect water column profile data on the downcast (Table 4). Water samples were taken at two depths: near the bottom at approximately 1 m above the sediment surface, as well as at the fluorescence-maximum of each station. The particle fraction was obtained by filtration through pre-combusted (400 °C) Whatman glass fiber filter (GF/F, nominal pore size 0.7µm) and immediately frozen to -20 °C until analysis. Samples were also collected for nutrient analysis, shown in Section 3.

**Table 4. Water column sample collection and depths (m) at each station.**

Sample collected	M1 (CTD station 4)	M2 (CTD station 7)	Midpoint (CTD station 9)	M3 (CTD station 11)	M4 (CTD station 14)
POC	37.7	172.5	-	299.3	439.6
POC	37.7	172.5	-	299.3	439.6
POC	37.7	172.5	-	299.3	439.6
DIC and Nutrients	37.7	172.5	211.9	299.3	439.6
DIC and Nutrients	25.6	101.1	100.9	201.1	201.2
POC	10.8	20.6	-	35.6	40.4
POC	10.8	20.6	-	35.6	40.4
POC	10.8	20.6	-	35.6	40.4
DIC and Nutrients	20.4	39.8	39.2	100.2	100.8
DIC and Nutrients	15.8	20.6	25.3	45.6	40.4
DIC and Nutrients	10.8	10.7	10.7	25.5	25.6
DIC and Nutrients	1.7	1.7	3.8	3	1.6

#### 4.2.3 Sediments

Surface sediment (0–10 cm) samples were collected (Table 5) using a 0.25 m<sup>2</sup> stainless steel box core (KC–Denmark). Upon retrieval, the undisturbed interface water and outer 2 cm of the core were removed and the rest of box core sliced into 1 cm horizontal increments to 10 cm using a slicing table. The 1 cm slices were homogenized, and separate samples were taken for meiofaunal abundance and organic matter characterization. Samplers were sliced in a closed van and otherwise protected from stack smoke, grease drips from winches and wire, and other potential contamination during preparation. Contamination blanks

for deck and laboratory processing of samples were collected in parallel with samples to be analyzed for biology and chemistry. Sediments for organic analysis were stored in pre-cleaned plastic I-Chem jars with Teflon-lined screw-cap lids and immediately frozen. Prior to grain size and organic analysis, sediments at each depth increment were homogenized and lyophilized, and samples for organic analysis were then taken from freeze dried sediments only. Meiofaunal counts were performed from whole sediment samples preserved in 5% formalin.

**Table 5. Locations of sediment collections for organic and meiofaunal analysis**

Site	Latitude			Longitude			Bottom depth (m)	Date	Comment
M4	70	15.1011	N	138	47.6262	W	440	5-Oct-16	
M3	70	02.9093	N	138	47.6911	W	300	5-Oct-16	
M2	69	54.4778	N	138	59.9251	W	175	5-Oct-16	
M1	69	46.1113	N	139	15.1418	W	40	6-Oct-16	
UAF	69	36.4259	N	139	42.9254	W	14	6-Oct-16	No sample, gravel at seabed

#### 4.2.4 Total Organic Carbon

Total organic carbon and particulate nitrogen was determined in lyophilized and homogenized sediments using standard combustion methods (Zimmerman et al. 1997) after removal of carbonates by treatment with 1 M HCl and evaporation to dryness.

#### 4.2.5 Grain Size

Particles size distributions of the sediment from the four stations along the transect (Figure 24) were determined from lyophilized sediments, which were homogenized and subsampled. Following removal of organic materials with aqueous hypochlorite (5%), particles distributions were determined using standard methods with a Malvern sediment grain size instrument (Sperazza et al. 2004).

#### 4.2.6 Meiofaunal Abundance and Diversity

Samples in 1 cm intervals through the first 5 cm of the sediment column were preserved using 5% formaldehyde and then analyzed for meiofaunal diversity and abundance. Upon receiving samples in the laboratory, they were transferred from formalin to ethanol and processed on a 45µm mesh screen to remove sediment but retain organisms. Once samples were in ethanol they were stained using Rose Bengal, a vital dye that stains protein to facilitate sorting of organisms from the sediment. Samples were sorted to major taxonomic group and then identified to the lowest practical taxonomic level following a two-day staining process. It was not feasible to obtain biomass by weighing meiofaunal organisms, because the organisms were sparse and the potential for loss of organisms during the weighing process was high. Additionally, this program specified retaining specimens for future studies and comparison. As a result, wet weight and dry weight biomass for major taxonomic groups were calculated based on measurements obtained in previously published literature.

#### 4.2.7 Organic Biomarkers

##### 4.2.7.1 Amino Acids

For amino acids, both particulate organic matter (POM) and sediments were hydrolyzed at 110 °C for 16 hours in 6 N HCl. After hydrolysis, sediments and particle samples were decanted, leaving the

supernatant for analysis. Samples hydrolyzed for amino acids were then dried under ultrapure liquid nitrogen and rinsed three times with nanopure water. Samples were subsequently spiked with the set of deuterated internal standards representative of each functional group present in amino acids. The analysis was performed using liquid chromatography-mass spectrometry (LC-MS) with no derivatization step; instead, ion pairing mobile phases and retention time-based mass selection were used. For analysis, an Agilent 1290 Infinity LC was used in connection to a bonded silica C18 Dionex Acclaim Polar advantage Rapid Separation Liquid Chromatography (RSLC) column (2.2  $\mu\text{m}$ , 120 A x 150 mm) for chromatographic separation and paired with a Thermo Scientific Orbitrap XL mass spectrometer. A guard column was added in line having the same column as the analytical column but with a 5 $\mu\text{m}$  particle size. The gradient used for mobile phase A included the ion pairing reagent (0.4% of phase) HFBA, formic acid (0.02% of phase) and LC-MS grade water. Mobile phase B included formic acid (0.1% of phase) in acetonitrile. The gradient program, modified from Piraud et al. (2005) utilized 100% mobile phase A from 0 to 1 minutes, 85% A from 1–6 minutes, 85% to 75% between 6 to 9 minutes, and 75% mobile phase A from 9–15 minutes; from 15–16 minutes the gradient was set to an isocratic state of 100% mobile phase A. All amino acids were observed over a 16-minute window, followed by a 15-minute isocratic recondition of the column with a 100% mobile phase A.

The LC was integrated with a Thermo Scientific Orbitrap XL via an ESI interface for structural analysis. Data was acquired and processed in Xcalibur software (Thermo Scientific, Rockford, IL) at a scan range of 50–300 m/z using positive ion mode using a scan. The collision energy was kept constant through the entire run at 35 V with collision-induced dissociation (CID) activation in the primary scan and a scan cycle (resolution) of 30,000. The ESI source parameters included a capillary temperature of 275 °C, spray voltage of 3.5 V, and capillary voltage of 2.5 V. All ESI source parameters were tuned and maximized before sample runs.

#### **4.2.7.2 Calibration and Standards**

Amino acid concentrations were calibrated using an internal standard/external standard paired set to provide coverage over the major functional groups of amino acids being determined. Each amino acid used an individual calibration curve that was normalized to one of the five chosen internal standards based on the functional groups. Most amino acids were calibrated from a commercial set of 30 known amino acids (Phenomenex) plus internal standards which include L-Aspartic-2,3,3-d<sub>3</sub> acid, L-cystine-2,2',3,3,3',3'-d<sub>6</sub>, DL-Lysine-4,4,5,5-d<sub>4</sub>, L-Leucine-5,5,5-d<sub>3</sub>, L-Phenylalanine ring-D<sub>5</sub>. The final sample concentrations were determined based on the ratio of amino acid peak area to the internal standard peak area. In total, 45 amino acids were calibrated and identified with mass values based on retention times and published literature mass spectrums for each amino acid.

#### **4.2.8 Lipid Markers**

##### **4.2.8.1 Extraction**

Surface sediment increments (0–1 cm) were thoroughly homogenized prior to chemical analysis. Lyophilized sediment was transferred to Green Chem glass vessels with Teflon screw-cap lids and two internal standards added prior to extraction (N-nonadecanoic acid and 5 $\alpha$ -cholestane) for calculation of recoveries and concentrations of polar and neutral products respectively. Sediments were extracted with a ratio of 1:1 hexane: acetone (35 ml) at 80 °C for 30 minutes and stirred on the high setting using a MARS microwave assisted extraction system (CEM Corp., Matthews, NC) operating at 1,200 W (refinement of EPA Method 3546). After extraction, vessels were cooled to room temperature before being opened. The supernatant was initially filtered through pre-cleaned and combusted glass wool and then combined with 2–4 ml hexane: acetone (1:1) rinses of the extraction vessel containing the sample. Sediment extracts were concentrated to 3 ml using rotary evaporation and then further hydrolyzed in 0.5 NaOH to partition

neutral and polar products (e.g., Belicka et al. 2009). Labware (glass or Teflon) used in the extraction process was washed in Alconox, soaked in RBS-35 detergent and then 15% HCl each for 24 hr, and rinsed three times with reverse osmosis (RO) or ultraviolet (UV) Nanopure water after each washing step. Glassware was dried and then combusted at 450 °C for 4 hours to remove any possibility of remaining organics. A procedural blank was prepared and analyzed in parallel with each round of samples extracted.

#### **4.2.8.2 Structural Characterization**

Neutral and polar lipid markers were analyzed by capillary gas chromatography (GC) with an Agilent 6890 system coupled to an Agilent 5973 Network Mass Selective (MS) Detector operated in electron ionization mode following previously described procedures for structural analysis of lipids (e.g., Belicka et al. 2009). The GC-MS system was equipped with a J&W Scientific DB-5MS fused silica column (30 m, 0.25 mm id, 0.25 film thickness) and operated in full scan mode with acquisition over 100–600 amu. Samples were injected in splitless mode at an initial oven temperature of 50 °C and an injector temperature of 250 °C with helium as the carrier gas. The oven temperature was ramped at 15 °C/min to 120 °C and then 3.5 °C/min to 300 °C before holding at 300 °C for 10 minutes. Calibration and tuning of the mass spectrometer was carried out after each set of 10 samples using perfluorotributylamine (PFTBA) as the calibrant. For each round of 12 samples, one procedural blank was prepared to monitor potential contamination resulting from glassware, solvents, and processing procedures.

### **4.3 Results**

#### **4.3.1 Water Structure Across the Shelf**

Water samples collected from the four Mackenzie shelf station locations displayed a fresh and warm near-surface layer with increased salinity at depth (near-bottom) (Figure 31–Figure 34). The halocline varied with each station but occurred in the first 50 db (50 m) of the water column. This suggested that surface waters receive a substantial input of fresher water associated with river runoff as there was no ice during the time samples were collected.

Sub-surface chlorophyll maxima were observed at all stations in the top 35 m, but the fluorescence levels at Mooring M3 and M4 were nearly twice those as compared to stations M1 and M2. Fluorescence was closely related to the thermocline, and decreasing rapidly after the halocline.

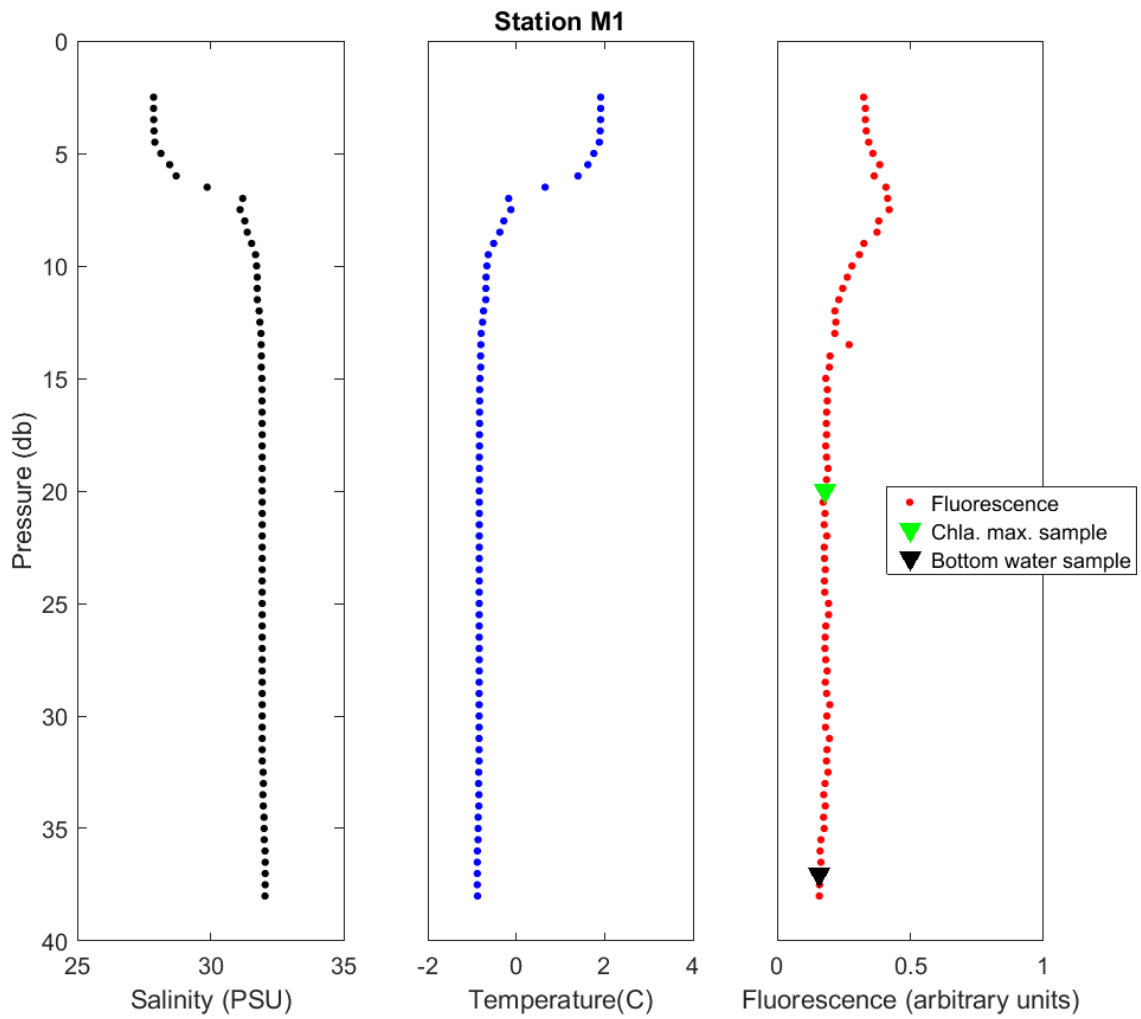


**Figure 31. Physical parameters of station M1 at the time of sampling.**

Salinity, temperature, and fluorescence are reported through the water column. Sampling depths for POM at the chlorophyll maximum and bottom of water column are reported by the green and black triangles respectively.



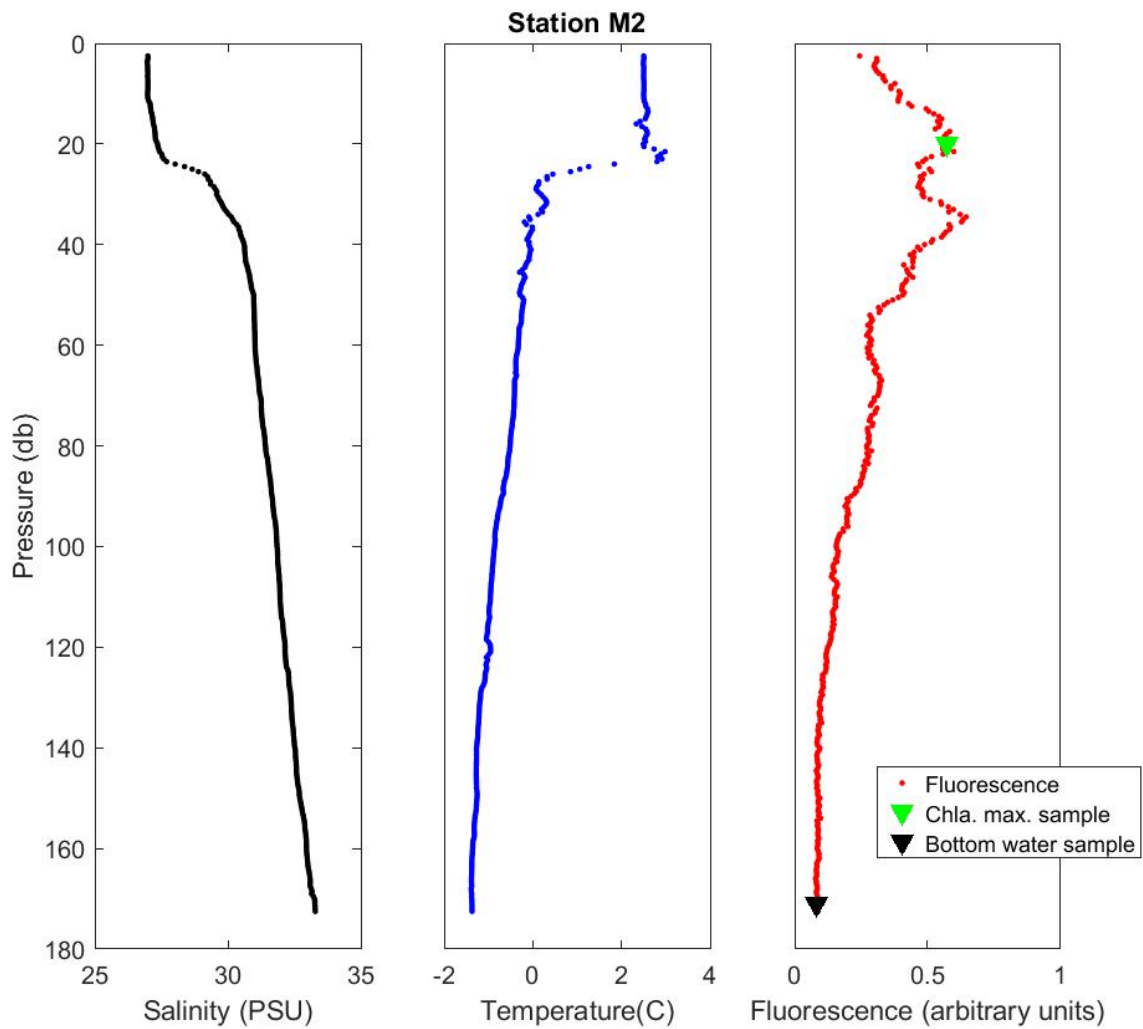


**Figure 32. Physical parameters of station M2 at the time of sampling.**

Salinity, temperature, and fluorescence are reported through the water column. Sampling depths for POM at the chlorophyll maximum and bottom of water column are reported by the green and black triangles respectively.

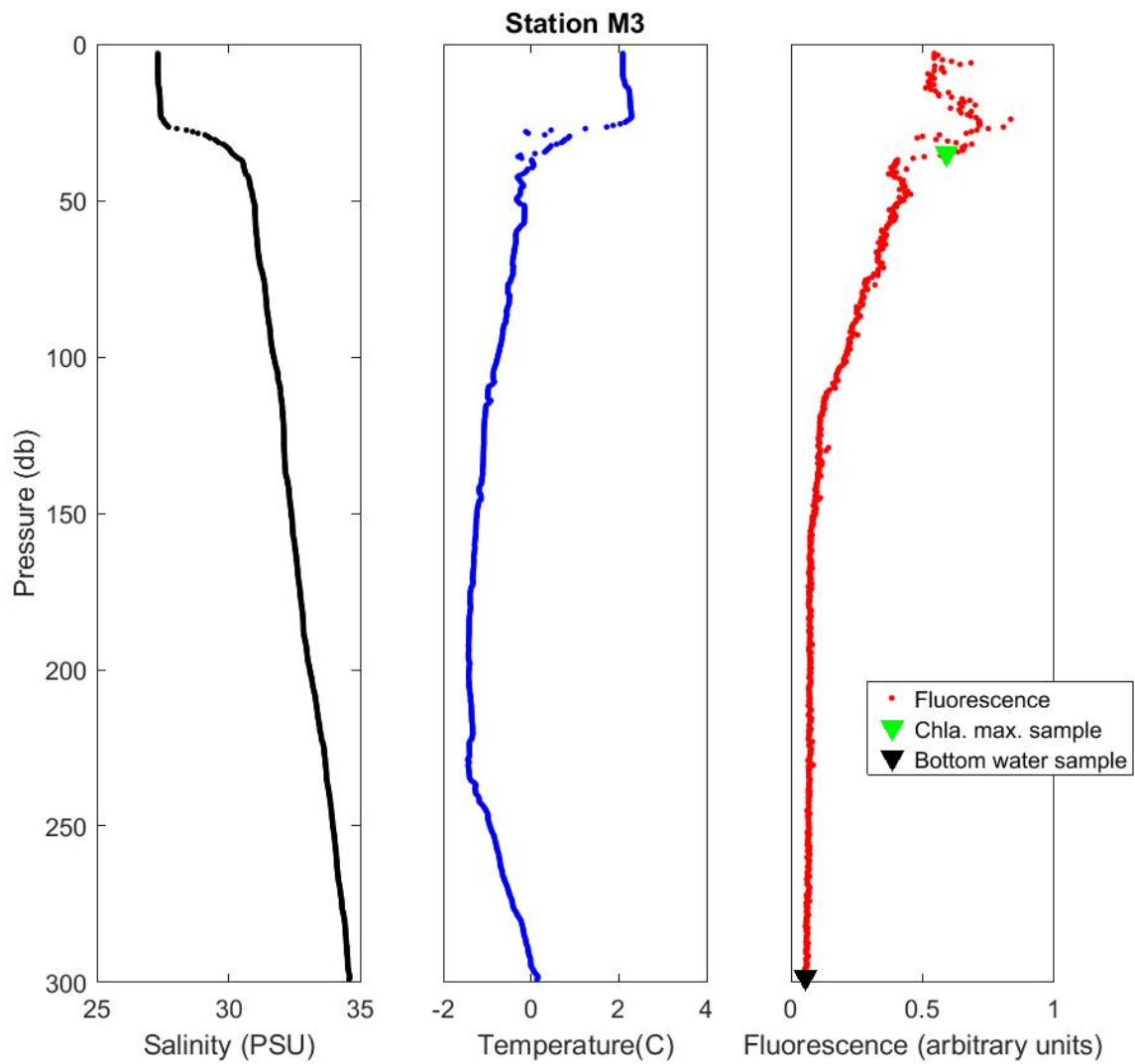


**Figure 33. Physical parameters of station M3 at the time of sampling.**

Salinity, temperature, and fluorescence are reported through the water column. Sampling depths for POM at the chlorophyll maximum and bottom of water column are reported by the green and black triangles respectively.

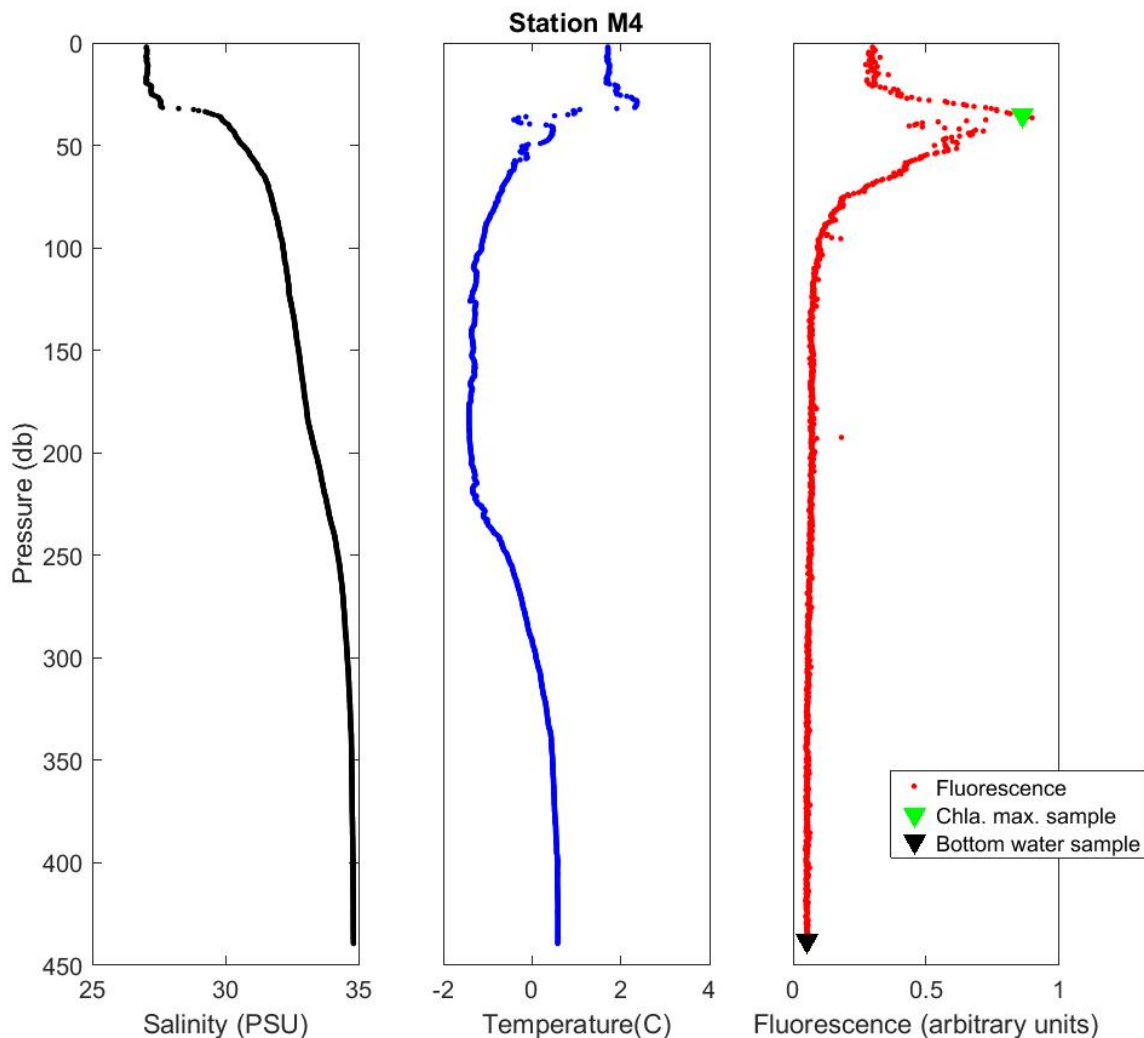


**Figure 34. Physical parameters of station M4 at the time of sampling.**

Salinity, temperature, and fluorescence are reported through the water column. Sampling depths for POM at the chlorophyll maximum and bottom of water column are reported by the green and black triangles respectively.

#### 4.3.2 Total Carbon and Grain Size

Sediments collected along the cross-shelf transect were consistent in both organic carbon content (Table 6) and grain size (Figure 35). Levels of surface sediment organic carbon were below 2% of the dry weight at the four stations, with station M2 having the highest value at 1.6%. In the water column, POC values at fluorescence maximum varied with station. M4 (deepest location) had the lowest value of POC at 0.036 mg/L, while the highest values in the water column were seen at station M2 (mid-shelf) with 0.062 mg/L, and at the bottom at M4 with 0.077 mg/L (Table 6). Station M3 also had high POC results when compared to station M4, with nearly 50% more POC (0.058 mg/L) at the fluorescence maxima.

**Table 6. Organic carbon content of all samples from the water column and surface sediments.**

Sample Type	Depth	M1	M2	M3	M4
Water column POC (mg/L)	10 m	0.046	-	-	-
	20 m	-	0.062	-	-
	35 m	-	-	0.053	0.036
	Bottom	0.058	0.058	0.050	0.077
Surface sediments organic carbon (% carbon dry weight)	0-1 cm	1.1%	1.6%	1.4%	1.3%

Grain size was overall uniform along the cross-shelf transect (Figure 35). Mineral fractions peaked between 3–5  $\mu\text{m}$  in the clay size range for surface sediments. Station M4 was also examined at horizon to 5 cm and had consistent mineral fractions, highlighting the extensive mixing that materials must undergo prior to sediment deposition.

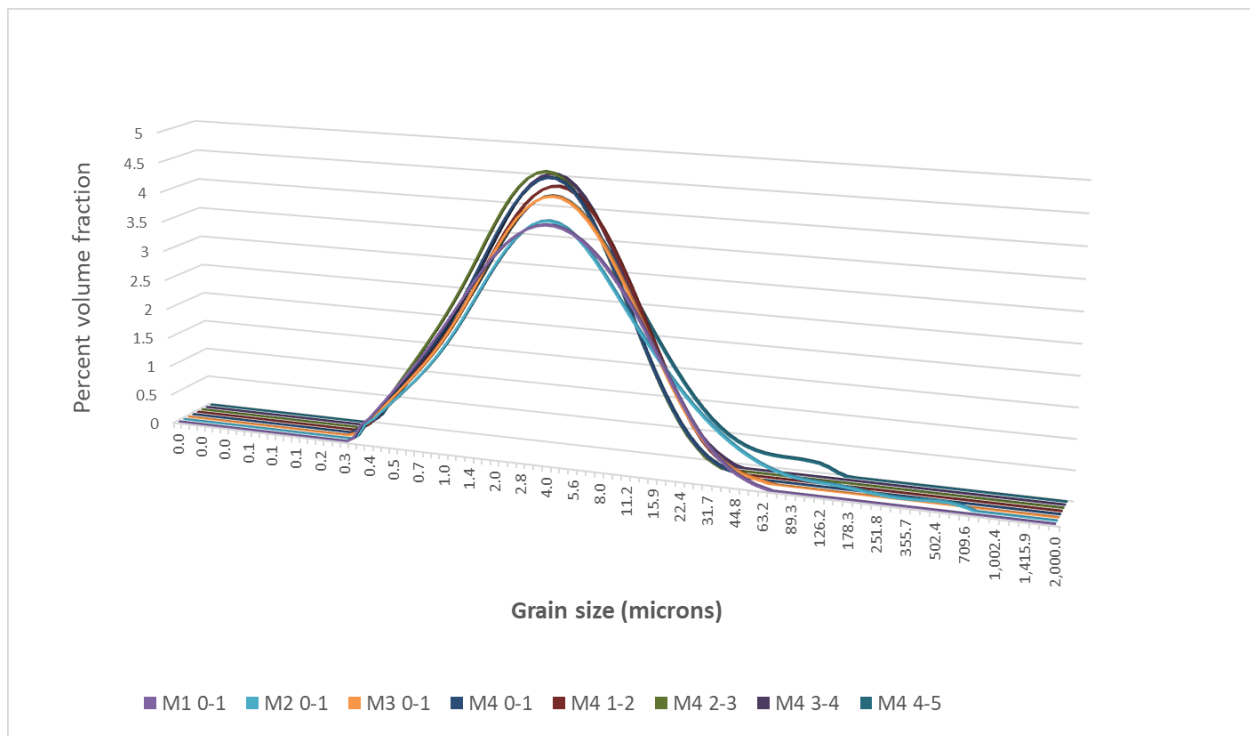


**Figure 35. Grain size across the four shelf stations of the Mackenzie shelf transect.**

Overall sediments at surface and at depth showed a uniform grain size distribution suggesting little sorting prior to transport and deposition.

### 4.3.3 Organic Markers

Samples of POM and sediments along the Mackenzie shelf basin yielded variable concentrations of hydrolysable amino acids. Surface sediments at station M1 have the lowest levels of THAA  $\mu\text{g}/\text{OC}$  across the four stations, while station M2 has the highest (Figure 36). In the water column at chlorophyll maximum, amino acids concentrations increased from inshore to offshore, with station M4 clearly showing the highest levels (Figure 36). The range of amino acids contributing to the total organic carbon

present ranged from 0.02% amino acids (bottom water POM station M2) to a maximum of 3.5% in particles at the M4 fluorescence maximum depth.

Amino acid composition varied across stations (Figure 37). M4 had more hydroxyproline than station M1, while M1 had tyrosine and M4 did not. Glutamic acid and lysine were consistently the most abundant amino acids in the sediments at the four stations but had its highest contribution at M2. Glycine was observed everywhere in the sediments but absent in the water column. In the particulate matter, glutamic acid and gamma aminobutyric acid (GABA) were the most abundant amino acids. GABA showed highest levels furthest from shore (M4) (Figure 38).

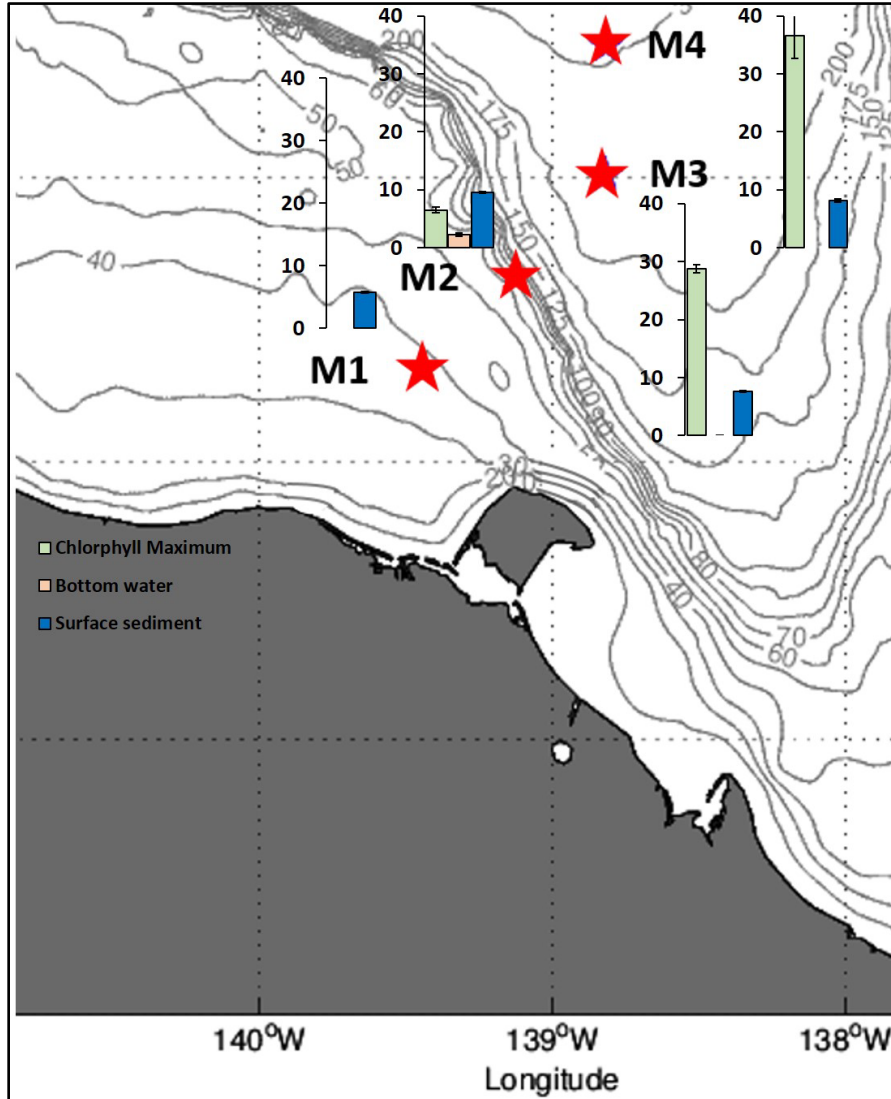


**Figure 36. Measure of total hydrolysable amino acids (THAA) normalized to organic carbon microgram in particles and sediments across the Mackenzie shelf.** Samples depths for the chlorophyll maximum and bottom particles (POM) are shown in Figure 31. Measure of THAA in surface sediment were defined as the 0–1 cm horizon.

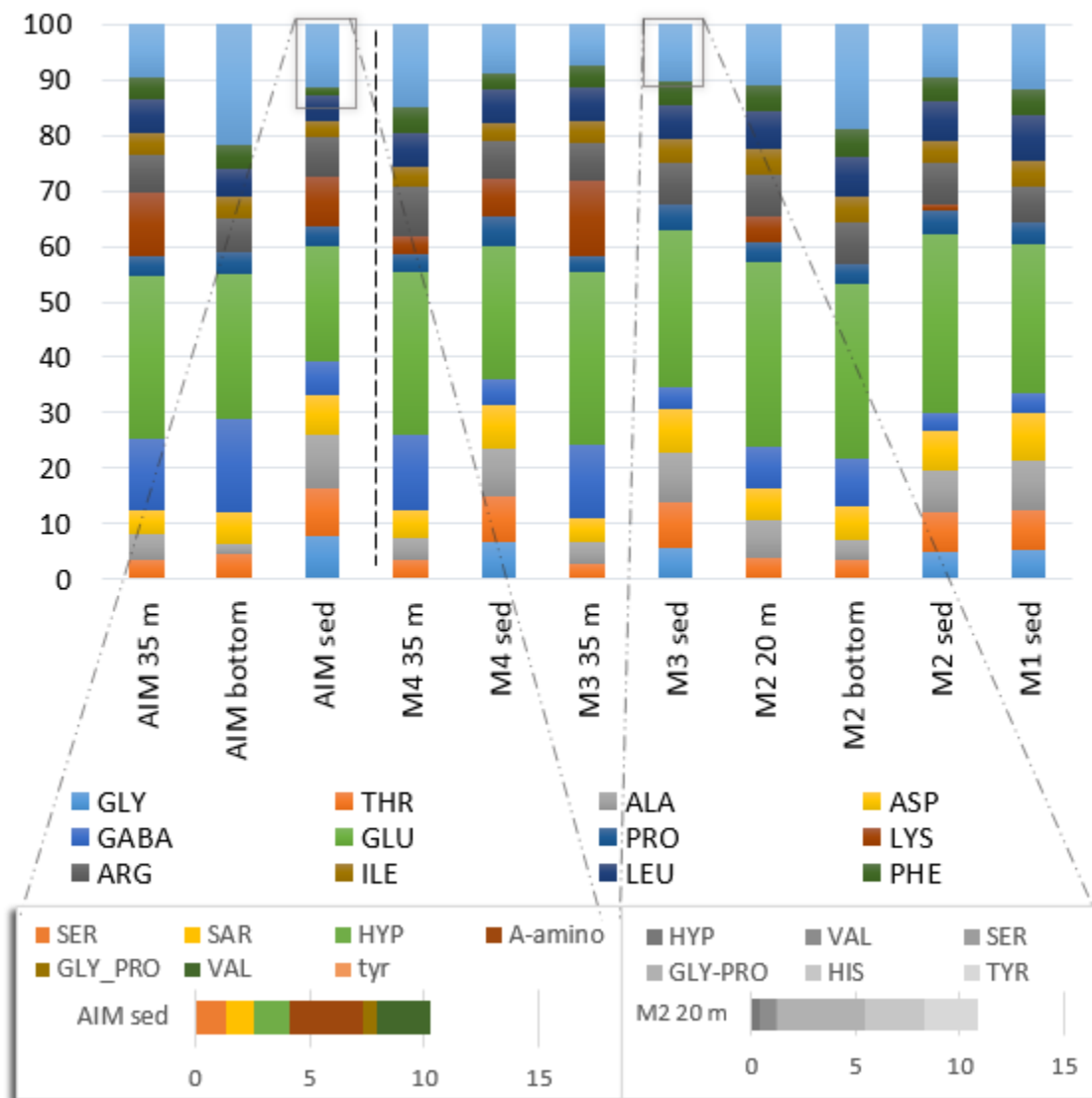


**Figure 37. Distribution of individual amino acids in each sample represented in a unit of relative abundance, percent of each amino acid that contributes toward the total sum of all amino acids in that sample.**

Samples gathered at the AIM site, which was not part of this study, are shown to the left with a black dashed line, as a representative pelagic site (AIM site is located at 75 05.79 N, 168 03.54 W). Those labeled 'sed' represent surface sediment samples from the first 1 cm of the sediment. Those marked with a depth represent the sampled chlorophyll maximum POM. Those marked with bottom were sampled in the water column right above the surface of the sediments. Amino acids not displayed in the top most abundant 12 amino acids were summed together in the category of 'sum of others.' The inserted plots on the bottom represent an example of what amino acids were seen in small abundances in both sediment samples, AIM sediments and water column POM (M2 20 m), which are representative of the sum of others category.

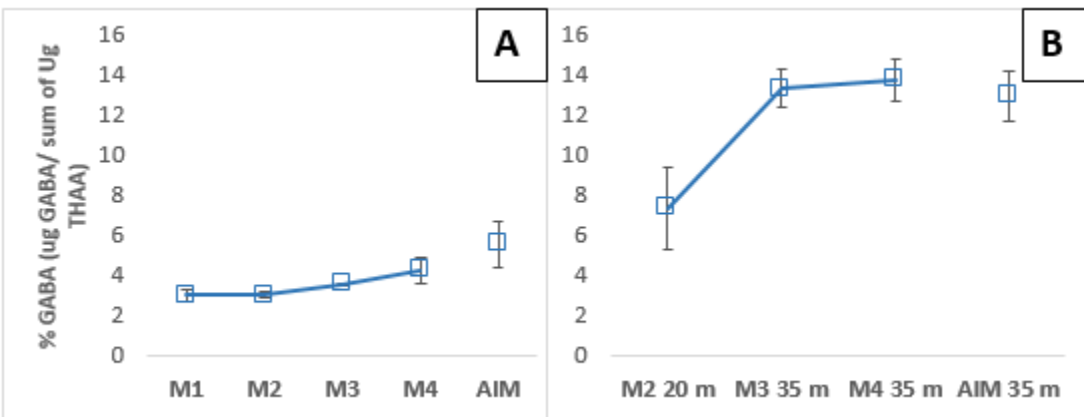


**Figure 38. A) The % GABA as fraction of total amino acids in surface sediments across the MARES transect plus the AIM pelagic site for comparison. B) The % GABA as fraction of amino acids in POM collected at the fluorescence maximum at available water column sites.** Error bars in this plot represent the standard deviation of analytical replicates.

#### 4.3.4 Fatty Acids and Sterol Biomarkers

Fatty acids detected were grouped depending on their structure and are presented in Figure 39. Phytol, a side chain of chlorophyll and sterols, showed an increase in marine related biomarkers in the sediment at mid-shelf stations. Sterols linked to terrestrial sources, were highest at station M1 as expected. The sum of fatty acids was highest at station M2 and M3 at 2 mg/g dry weight as compared to half that quantity seen at station M1. Polyunsaturated fatty acids were higher at stations M2 and M4, while long-chain fatty acids, typically representative of higher plants, were highest at station M1. In the sterols, dinosterol was observed in significant amounts across the four samples but was highest at station M4. Brassicasterol, a diatom specific sterol (Volkmann 1986), was absent at M1 but seen at stations M2 through M4 (Figure 39). Several sterols more specific to higher plants, including 24-ethylcholestan-3b-ol, decreased further offshore, while increases in marine diatom related markers such as brassicasterol, 24-methylcholest-7-22-en-3β-ol and polyunsaturated fatty acids (PUFAs) occurred at mid-shelf and offshore stations.



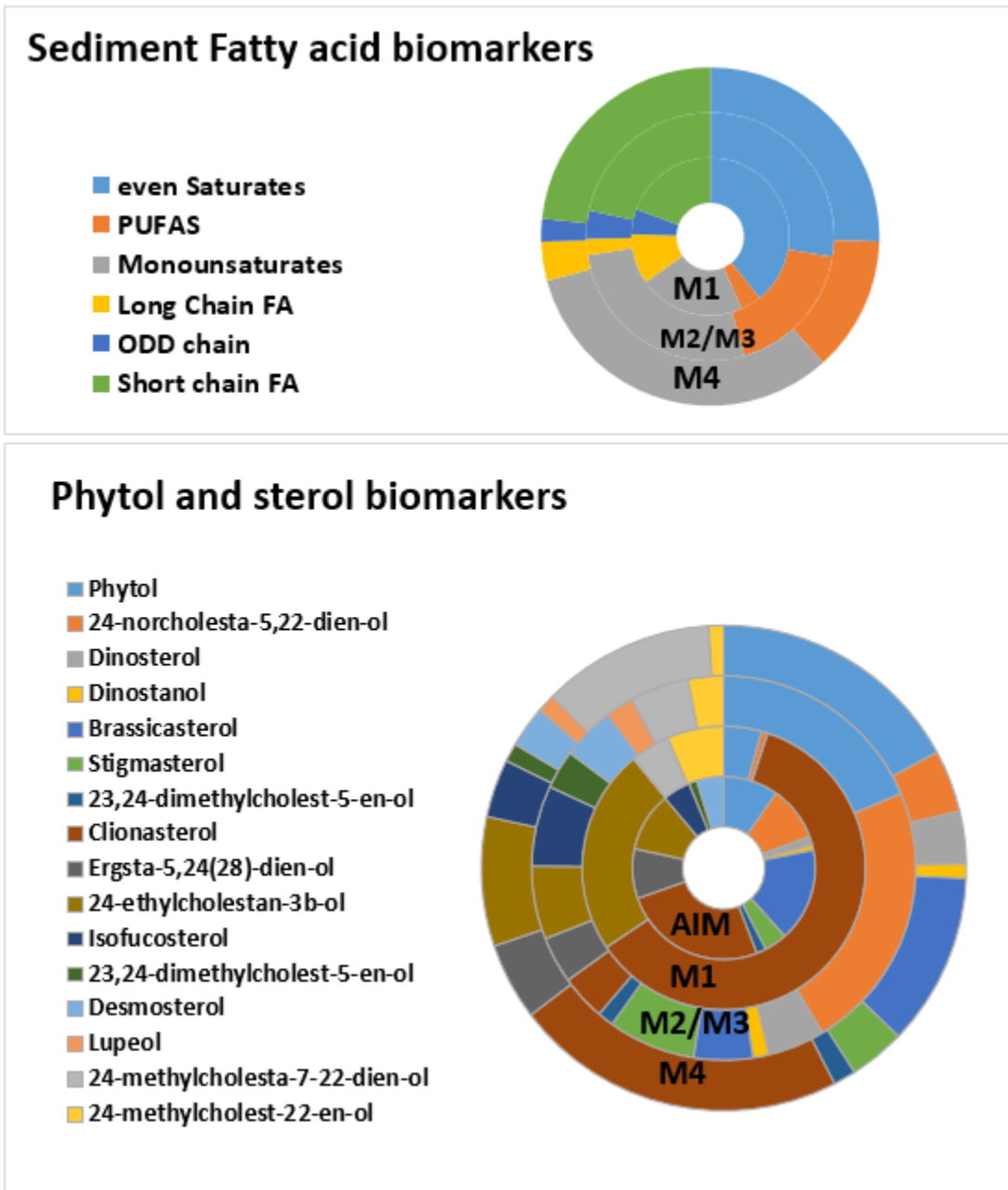


**Figure 39. The distribution and abundance of major sterol markers plus phytol across the Mackenzie shelf transect.**

Fatty acid and sterol biomarkers show increases in marine related markers from M1 to the M4 stations. Diagnostic markers of higher plants, including long-chain fatty acids, 24-ethylcholestan-3β-ol, and isofucosterol, decrease further offshore. In contrast, increases are seen in broader measures of phytoplankton as phytol plus specific marine algal markers, including brassicasterol and 24-methylcholest-7-22-en-3β-ol, at mid-shelf and offshore stations.

#### 4.3.5 Meiofaunal Community

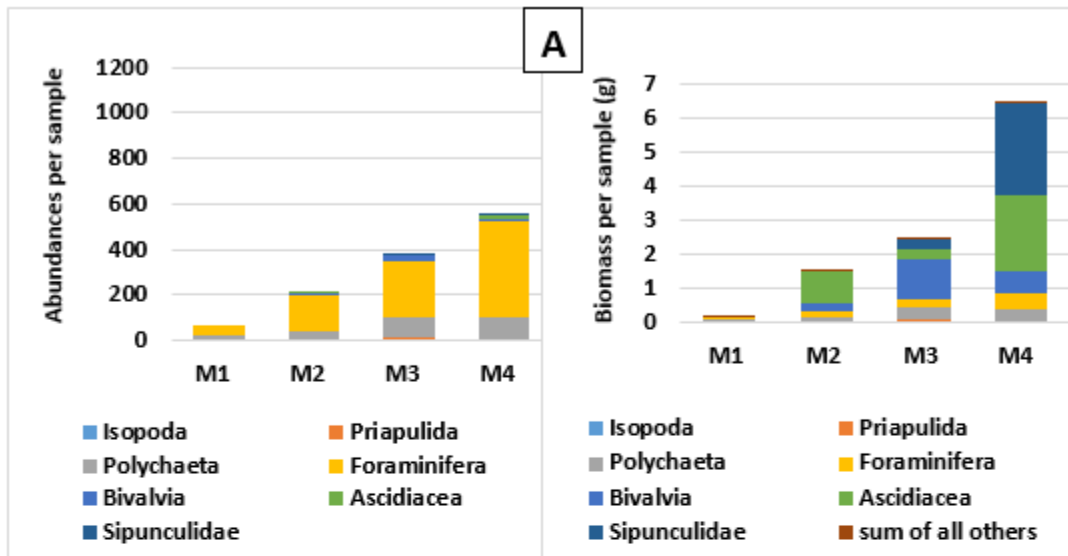
Abundances of surface deposit feeders dominated the meiofaunal population across the four stations. Abundances were highest and most diverse at the mid-shelf stations (M2 and M3). Wet weight biomass calculated for the meiofaunal organisms was highest at station M4, while calculated dry weight biomass

was greatest at M3 (Table 7). Foraminifera was the most abundant taxa, with increasing abundance toward greater depth. Harpacticoid copepods and diatoms were the second most abundant taxa with their maximum abundances occurring at the mid-shelf stations (Figure 40). The major taxonomic groups that were most abundant did not account for greatest calculated biomass; Sipunculida and Bivalvia outweighed copepods and diatoms, while small Foraminifera provided significant contribution to the biomass calculation (wet and dry weight). Abundances of non-protist, non-algal related organisms were low, however there were 23 Families of Polychaeta and 19 Families of Crustacea identified from the samples (Appendix B).

**Table 7. Calculated wet and dry weight biomass (grams) based on literature values for major meiofaunal taxonomic groups identified from MARES cross-shelf transect.**

Taxonomic Group	M1 Abundance	M1 Wet Biomass	M1 Dry Biomass	M2 Abundance	M2 Wet Biomass	M2 Dry Biomass	M3 Abundance	M3 Wet Biomass	M3 Dry Biomass	M4 Abundance	M4 Wet Biomass	M4 Dry Biomass
Polychaeta	47	0.1753	0.0088	67	0.2499	0.0126	144	0.5371	0.0271	122	0.4550	0.0230
Oligochaeta	1	0.0001	<0.0001	0	0.0000	0.0000	0	0.0000	0.0000	0	0.0000	0.0000
Acari	0	0.0000	0.0000	0	0.0000	0.0000	0	0.0000	0.0000	3	0.0012	0.0001
Ostracoda	0	0.0000	0.0000	0	0.0000	0.0000	10	0.0004	0.0002	3	0.0001	0.0001
Tanaiacea	6	0.0005	<0.0001	7	0.0006	<0.0001	4	0.0003	<0.0001	3	0.0003	<0.0001
Amphipoda	6	0.0020	<0.0001	2	0.0007	<0.0001	3	0.0010	<0.0001	0	0.0000	0.0000
Isopoda	3	0.0222	0.0011	0	0.0000	0.0000	5	0.0370	0.0018	2	0.0148	0.0007
Cumacea	0	0.0000	0.0000	0	0.0000	0.0000	5	0.0010	0.0001	2	0.0004	<0.0001
Copepoda	15	0.0001	<0.0001	165	0.0011	0.0003	254	0.0017	0.0004	101	0.0007	0.0002
Anthozoa	0	0.0000	0.0000	0	0.0000	0.0000	1	0.1172	1.6759	0	0.0000	0.0000
Foraminifera	251	0.2742	0.0041	493	0.5386	0.0080	651	0.7112	0.0106	946	1.0335	0.0154
Kinorhyncha	0	0.0000	0.0000	12	<0.0001	<0.0001	61	0.0001	0.0001	14	<0.0001	<0.0001
Bivalvia	0	0.0000	0.0000	4	0.2324	<0.0001	27	1.5686	0.0001	20	1.1619	0.0001
Nematoda	10	0.0002	<0.0001	50	0.0008	<0.0001	334	0.0056	0.0001	276	0.0046	0.0001
Nemertea	9	0.0036	0.0002	7	0.0028	0.0001	6	0.0024	0.0001	4	0.0016	0.0001
Priapulida	0	0.0000	0.0000	0	0.0000	0.0000	11	0.0634	0.0065	3	0.0173	0.0018
Sipunculidae	0	0.0000	0.0000	0	0.0000	0.0000	1	0.3038	0.0174	10	3.0383	0.1736
Diatoms	0	0.0000	0.0000	259	0.0000	0.0000	365	0.0000	0.0000	80	0.0000	0.0000
Asciacea	0	0.0000	0.0000	7	0.9124	0.1472	2	0.2607	0.0420	17	2.2158	0.3574
Platyhelminthes	0	0.0000	0.0000	1	0.0254	0.0012	0	0.0000	0.0000	0	0.0000	0.0000
<b>Total</b>	<b>348</b>	<b>0.478</b>	<b>0.0144</b>	<b>1,074</b>	<b>1.965</b>	<b>0.1696</b>	<b>1,884</b>	<b>3.612</b>	<b>1.7826</b>	<b>1,606</b>	<b>7.946</b>	<b>0.5726</b>

### Major meiofaunal phyla (as biomass) and corresponding abundances



### Seven most abundant meiofauna phyla and biomass

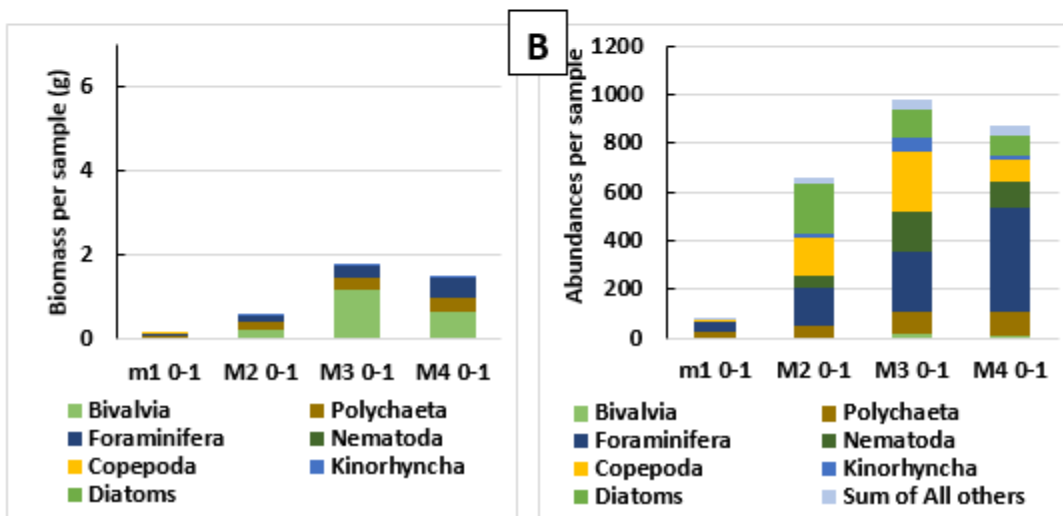


**Figure 40: Meiofaunal abundances and biomass that represent the majority of the benthic community in the meio size range.**

Overall trends across the shelf show larger communities at the mid-shelf stations with corresponding increase in diversity at these mid-shelf stations (M2 and M3). (A) shows the top seven benthic communities, which make up the majority of the biomass but very little of the overall abundances. (B) represents the seven most abundant benthic meiofauna which make up a smaller portion of the biomass than those benthic animals that are larger and contribute more to the total biomass.

## 4.4 Discussion

Past studies have used various suites of organic carbon signatures (i.e., long-chain n-alkanes, fatty acids and alcohols, triterpenoids) to quantify the input and movement of terrestrial carbon to the Arctic Ocean (e.g., Belicka et al. 2004, Boucsein and Stein 2000, Goñi et al. 2005 Schubert and Calvert 2001, Stein et

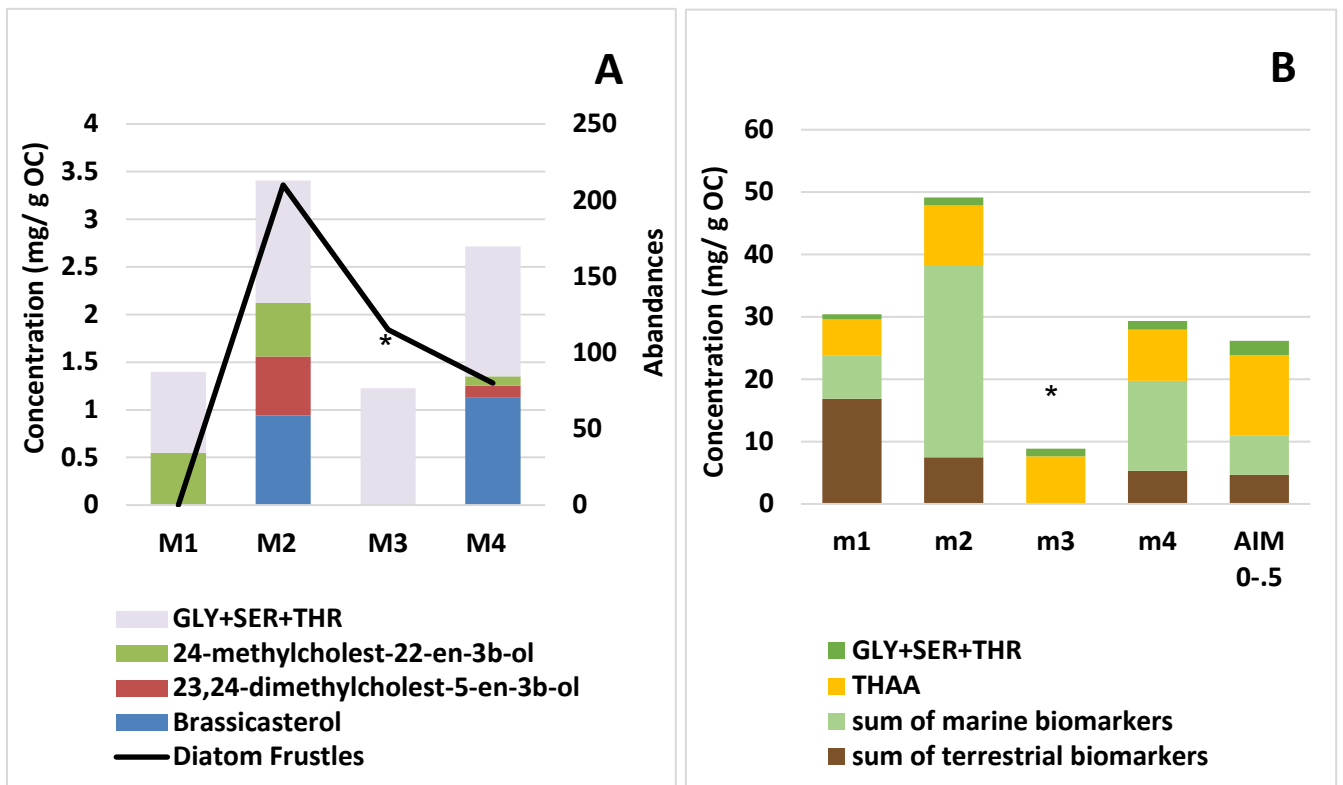
al. 1994, Taylor and Harvey 2011). Although these studies show that terrestrial carbon is both ubiquitous and varied in contribution, information on the response of the benthic community is limited. Although this limited set of stations provides only a snapshot of the organic sources and meiobenthic diversity across the Mackenzie shelf, it suggests that benthic abundance reflects marine inputs to sediments.

Previous work along the Mackenzie shelf has shown that sinking fluxes are generally highest early in the summer (June, July, and August) and generally similar each year during the fall (Pedersen et al. 2010). On the eastern Beaufort Sea shelf, Mackenzie River melt water and an increase in solar and nutrient fluxes can lead to highest sinking fluxes of carbon in the summer (O'Brien et al. 2006). Although there are no previous carbon sediment measurements in the vicinity of our mooring locations, the low carbon values we measured in the sediments at stations M3 and M4 agree well with previous estimates of carbon flux measured on the Mackenzie shelf below the euphotic zone in fall (Pedersen et al. 2010). Station M2, a mid-shelf station, was the highest in organic carbon in the sediments and showed the greatest fluorescence maximum of the water column. This suggests these mid-shelf stations receive a substantial organic input from marine sources rather than river deposition. The lack of grain size differences across shelf stations (Figure 35) suggests that grain size has little impact on the community structure. Work by T. Richerol et al. (2008) concluded that the first 1 cm of sediments are heavily bioturbated at M3 and M4, suggesting that the material deposited across the Mackenzie Delta shelf includes a mixture of terrestrial deposition, labile marine production, and in situ benthic activity.

The range of amino acids contributing to the total organic carbon (TOC) present in surface sediment was considered low for coastal shelf values. Station M1 has the lowest value in the sediments at only 1.1% THAA, with an increase of THAA in the sediments at station M2 and moving further offshore at stations M3 and M4. In the water column, the highest THAA contributions occur at the fluorescence maximum of station M4 (3.5%). This increase in THAA in the sediments and POC could suggest an offshore production of material not related to terrestrial inputs. Total amino acids per unit carbon suggested that mid-shelf stations receive the highest deposition of labile organic matter to the sediments and the highest water column production furthest offshore at station M4. Past studies of amino acids in marine organic matter showed that relative abundances of GABA present in a sample (% GABA) can be used to represent the level of degradation of organic material (e.g., Keil et al. 1998). Across the MARES sites examined, the GABA fraction in surface sediments, as well as POM at the fluorescence maximum, increased from inshore to offshore and consistently indicated the presence of degraded organic matter as an important component. Keil et al. (1998) determined that sediment samples low in organic carbon are often higher in non-protein amino acids like GABA, which are produced in situ rather than sourced from depositing POM. Increases in GABA in POM may also suggest more mixed sources of amino acids further offshore. The increased concentration seen in GABA offshore is balanced by the decrease seen in glutamic acid, which acts as the primary substrate to be decarboxylated to GABA. Other amino acids of interest included glycine, serine, and threonine, which are well preserved in diatom frustules. In the four cross-shelf stations, glycine, serine, and threonine contribute to a larger fraction to the sediment amino acids than those found in the water column POM.

Overall results for fatty acid and sterol biomarkers as a fraction of organic carbon showed increases in algal related markers across the shelf, while long-chain fatty acids and sterols with higher plant origins decreased from M1 through M4. The presence of other marine related biomarkers, including the long-chain fatty acids sourced from higher plant matter, were elevated closer to shore at stations M1 and M2 (Figure 39). M1 is unique to the sampled transect with more than 50% of the measured organic matter apparently derived from terrestrial carbon. In contrast, station M2 and M3 appeared to have organic carbon largely derived from the water column, based on the presence of labile and diagnostic polyunsaturated fatty acids taxonomically specific sterol and diatom frustules present in samples (Figure

41). These sources of organic carbon appear predominantly from water column production as opposed to particulate transport from the Mackenzie Delta and may include ice algal sources (Gradinger 2009).



\* All other biomarkers data unavailable at this station

Note: Diatom frustules and meiofaunal data not available at the AIM site.

**Figure 41. Lipid and amino acid biomarkers of marine origin (panel A) versus summed organic markers both of terrestrial and marine organic matter (panel B).**

Marine biomarkers suggest an increase in marine materials at mid-shelf stations, while the terrestrial biomarkers are highest at station M1 (panel B). The sum of all amino acids (THAA) is also highest mid-shelf, suggesting an availability of labial material at these stations. Of the amino acids measured, glycine, serine, and threonine are enriched sediments due to their association with diatoms. Diatom levels as biomarkers match well with the increase in meiofaunal size class of diatom frustules in the sediments. The AIM site, a pelagic site comparable to that seen at station M4, is higher in labile amino acids representative of recent organic inputs.

Benthic meiofauna showed highest diversity and abundances at mid-shelf stations. Station M3 has the highest overall abundances and diversity in contrast to organic carbon in the sediments, which was greatest at station M2. Most of the benthic meiofauna identified were surface deposit feeders, who graze on available sources of organic matter near the sediment-water interface (Rhoades and Germano 1982). The mismatch in organic carbon and benthic abundance and diversity can be explained by the fact that the multitude of surface deposit feeders at M3 are quickly taking advantage of available carbon and grazing it down more aggressively when compared to station M2. Station M1 had the lowest abundance, diversity, and organic carbon, which is thought to be a result of ice scouring and coarse sediment texture (mostly gravel and rocks). Station M4 had the second greatest abundance among the four stations sampled for meiofauna, with the greatest calculated wet weight biomass but lower dry weight biomass than station M3. This is related to the presence of larger benthic fauna identified further from shore. To support a community with larger organisms such as Sipuncula and Bivalvia, a larger source of fresh organic matter must reach the sediments from the water column or by other depositional processes.

Results from the meiofauna population combined with information gathered from amino acids, carbon, and lipid biomarkers strongly suggested that the highest carbon fluxes and available (labile) organics in the sediments occur at mid-shelf stations, and that these are fueled by marine sources. Although we anticipated that inner-shelf stations would show highest carbon because of the large flux of POC associated with the Mackenzie River freshet, it may be that both summer zonal winds (see Section 2) and winter ice conditions interfered with this process, at least in 2016. In this area of the Beaufort Sea, the wintertime ice front extends from surface to the bottom in the nearshore, and if landfast ice persisted, it might have blocked the interaction of the Mackenzie River water (laden with particulates) with the coastal sea water early in the season (Carmack and Macdonald 2002; Macdonald et al. 2004). At the edge of this ice pack further away from shore but over the shelf, the annual sea-ice melt leads to ice edge blooms. Spring phytoplankton blooms in the Arctic, which may occur at a time when there are minimal to no additions of Mackenzie River POC, generally lead to large fluxes of marine carbon to the seafloor. Carbon fluxes in the water column subsequently increase as the condition become more favorable for phytoplankton production after the Mackenzie River runoff can flow over these mid-shelf areas. If such conditions coincided with zonal winds that favored easterly versus westerly transport of the plume during a significant amount of time in the spring and summer of 2016, it might explain why our observed results at the mid-shelf stations showed the highest amounts of carbon, diatom markers, diatom frustules, and benthic surface deposit communities, and why these originated predominantly from marine instead of from terrestrial sources.

#### **4.5 Summary**

The broad shelf off the Mackenzie Delta includes multiple sources of organic matter derived from both inflow and in situ production. Organic carbon, total THAA, and detrital grazers were highest at the mid-shelf stations (M2, M3) despite a uniform grain size across the four stations sampled across the Beaufort Sea shelf. Water column THAA are greater than that observed in the sediments analyzed, but the water column was lower in diatom related amino acids and higher non-protein amino acids than the sediment surface sampled. Lipid and fatty acid biomarkers also reflect that algal inputs to mid-shelf sediments are enhanced compared to terrestrial material, with major portions appearing as diatoms. The organic analysis completed as part of this MARES program agrees with benthic meiofaunal data measured with mid-shelf stations, which were highest in overall abundance. Although some taxa such as foraminifera increase further from shore, most of the measured parameters indicate that in situ marine production in the sediments and water column primary production are more important to carbon cycling and fluxes than previously reported. The data also suggest that inputs from Mackenzie River freshet may not be the dominant source responsible for supporting marine benthic communities with labile organic carbon food sources. Subsequent benthic samples will be needed to estimate a regional carbon budget, determine residence times under different environmental conditions, and bound the measurements reported here.

#### **4.6 Future Research**

While this study provided an initial snapshot of the Mackenzie delta system and its physical setting, the limited sampling for other parameters of the system did not allow temporal trends to be determined. Future work should take advantage of the well informed physical setting to follow the production and fate of carbon across the land-ocean boundary to allow development of regional carbon budgets and long-term estimates of carbon sequestration.



## 5 Conclusions

The components of MARES aimed to:

1. Start the collection of physical, biological, and chemical observations in the Eastern Beaufort Sea from moored platforms
2. Describe and analyze physical, biological, and chemical observations acquired from a moving platform
3. Gather water and sediment samples at the mooring locations simultaneously with the mooring deployment operation to estimate the carbon budgets and describe carbon cycling processes

The successful deployment of this unique array of moorings is providing us with a yearlong time series of the biophysical and chemical characteristics across the eastern Beaufort Sea shelf and continental slope, allowing us to capture regional ecosystem drivers in this region, including the influence of the Mackenzie River plume.

The successful deployment of the Slocum G2 Glider and the subsequent high-resolution data collected provided insights into the flow of the Mackenzie plume, identifying four different plume flow regimes, as well as the temporal and spatial scales at which key processes are occurring. These flow regimes, largely influenced by wind forcing, have significant impacts on the final destination of the plume waters, their retention within Arctic waters, and their influence on biological communities, with implications for potential anthropogenic impacts such as those that may be predicted by regional oil trajectory models.

Sediment samples provided a snapshot of the organic sources and meiobenthic diversity across the Mackenzie shelf and suggested that benthic abundance reflects marine inputs to sediments (water column production) rather than river deposition. Benthic meiofauna patterns, however, may vary across years depending on zonal winds causing opposing directional transport of Mackenzie plume material.

## 6 References

- Bauch D, Schlosser P, Fairbanks RG. 1995. Freshwater balance and the sources of deep and bottom waters in the Arctic Ocean inferred from the distribution of H<sub>2</sub>18O. *Progress in Oceanography*. 35(1):53–80.
- Belicka LL, Macdonald RW, Yunker MB, Harvey HR. 2004. The role of depositional regime on carbon transport and preservation in Arctic Ocean sediments. *Mar Chem*. 86:65–88.
- Belicka LL, Harvey HR. 2009. The sequestration of terrestrial organic carbon in Arctic Ocean sediments: a comparison of methods and implications for regional carbon budgets. *Geochim Cosmochim Acta*. 73:6231–6248.
- Belicka LL, Macdonald RW, Harvey HR. 2009. Trace element and molecular markers of organic carbon dynamics along a shelf–basin continuum in sediments of the western Arctic Ocean. *Mar Chem*. 115:72–85.
- Boucsein B, Stein R. 2000. Particulate organic matter in surface sediments of the Laptev Sea (Arctic Ocean): Application of maceral analysis as organic-carbon-source indicator. *Mar Geol*. 162(2):573–586.
- Carmack E, MacDonald R. 2002. Oceanography of the Canadian Shelf of the Beaufort Sea: A Setting for Marine Life. *Arctic*. 55:29–45.
- Chen M, Xing N, Huang Y, Qiu Y. 2008. The mean residence time of river water in the Canada Basin. *Chinese Science Bulletin*. 53(5):777–783.
- Ekurzel B, Schlosser P, Mortlock RA, Fairbanks RG, Swift JH. 2001. River runoff, sea ice meltwater, and Pacific water distribution and mean residence times in the Arctic Ocean. *Journal of Geophysical Research: Oceans*. 106(C5):9075–9092.
- Fichot CG, Kaiser K, Hooker SB, Amon RMW, Babin M, Bélanger S, Walker SA, Benner R. 2013. Pan-Arctic distributions of continental runoff in the Arctic Ocean. *Scientific Reports*. 3:1053; DOI:10.1038/srep01053 (2013).
- Goñi MA, Yunker MB, Macdonald RW, Eglinton TI. 2005. The supply and preservation of ancient and modern components of organic carbon in the Canadian Beaufort Shelf of the Arctic Ocean *Mar Chem*. 93(1):53–73.
- Gradinger R. 2009. Sea ice algae: major contributors to primary production and algal biomass in the Chukchi and Beaufort Sea during May/June 2002. *Deep-Sea Res II*. 56:1201–1212.
- Helber RW, Townsend TL, Barron CN, Dastugue JM. 2013. Validation test report for the improved synthetic ocean profile (ISOP) system, part I: Synthetic profile methods and algorithm. NRLMR/7320-13-9364.
- Keil RG, Tsamakis E, Giddings JC, Hedges J. 1998. Biochemical distributions (amino acids, neutral sugars, and lignin phenols) among size-classes of modern marine sediments from the Washington coast. *Geochimica et Cosmochimica Acta*. 62(8):1347–1364.

- Macdonald RW, Solomon SM, Cranston RE, Welch HE, Yunker MB, Gobeil C. 1998. A sediment and organic carbon budget for the Canadian Beaufort Shelf. *Mar Geol.* 144:255–273.
- Machuca IA, Allen SE. 2018. Effects of a dynamic wide submarine canyon on coastal currents during an upwelling event. 2018 Ocean Sciences Meeting, Portland, Oregon.
- Magen C, Chaillou G, Crowe SA, Mucci A, Sundby B, Gao A, Makabe R, Sasaki H. 2010. Origin and fate of particulate organic matter in the southern Beaufort Sea – Amundsen Gulf region, Canadian Arctic. *Est Coast Shelf Sci.* 86:31–41.
- O'Brien MC, Macdonald RW, Melling H, Iseki K. 2006. Particle fluxes and geochemistry on the Canadian Beaufort Shelf: Implications for sediment transport and deposition. *Cont Shelf Res.* 26(1):41–81.
- O'Brien MC, Melling H, Pedersen TF, Macdonald, R.W. 2013. The role of eddies on particle flux in the Canada Basin of the Arctic Ocean. *Deep Sea Res. Part I: Oceanogr Res Pap.* 71:1–20.
- Pedersen J-T, Michel C, Gosselin M. 2010. Sinking export of particulate organic material from the euphotic zone in the eastern Beaufort Sea. *Mar Ecol Prog Ser.* 410:55–70.
- Piraud M, Vianey-Saban C, Petritis K, Elfakir C, Steghens J, Bouchu D. 2005a. Ion-pairing reversed-phase liquid chromatography/electrospray ionization mass spectrometric analysis of 76 underivatized amino acids of biological interest: a new tool for the diagnosis of inherited disorders of amino acid metabolism. *Rapid Commun Mass Spec.* 19:1587–1602.
- Rachold V, Eicken H, Gordeev VV, Grigoriev MN, Hubberten H-W, Lisitzin AP, Shevchenko VP, Schirrmeister L. 2004. Modern Terrigenous organic carbon input to the Arctic Ocean. In *The Organic Carbon Cycle in the Arctic Ocean* (eds. R. Stein and R. W. Macdonald). Springer-Verlag, pp. 33–55.
- Rhoads DC, Germano JD. 1982. Characterization of benthic processes using sediment profile imaging: An efficient method of remote ecological monitoring of the seafloor (REMOTS™ System). *Mar Ecol Prog Ser.* 8:115–128.
- Richerol T, Rochon A, Blasco S, Scott DB, Schell TM, Bennett RJ. 2008. Evolution of paleo sea-surface conditions over the last 600 years in the Mackenzie Trough, Beaufort Sea (Canada). *Mar Micropaleont.* 68(1-2):6–20.
- Schubert C, Calvert SE. 2001. Nitrogen and carbon isotopic composition of marine and terrestrial organic matter in Arctic Ocean sediments: Implications for nutrient utilization and organic matter composition. *Deep-Sea Res Part I.* 48(3):789–810.
- Schulze LM, Pickart RS. 2012. Seasonal variation of upwelling in the Alaska Beaufort Sea: Impact of sea ice cover. *J of Geophys Res Oceans.* 117(C6).
- Shimada K, Itoh M, Nishino S, McLaughlin F, Carmack E, Proshutinsky A. 2005. Halocline structure in the Canada Basin of the Arctic Ocean. *Geophysical Research Letters.* 32:L03605, doi:10.1029/2004GL021358, 2005.
- Sperazza M, Moore J, Hendrix M, Sperazza M. 2004. High-resolution particle size analysis of naturally occurring very fine-grained sediment through laser diffractometry. *J of Sed Res.* 74:736–743.

- Steele M, Morison J, Ermold W, Rigor I, Ortmeyer M, Shimada K. 2004. Circulation of summer Pacific halocline water in the Arctic Ocean. *Journal of Geophysical Research*. 109:C02027, doi:10.1029/2003JC002009, 2004.
- Stein R, Grobe H, Wahsner M. 1994. Organic carbon, carbonate, and clay mineral distributions in eastern central Arctic Ocean surface sediments. *Mar Geol*. 119:269–285.
- Taylor KT, Harvey HR. 2011. Bacterial hopanoids as tracers of organic carbon sources and processing across the Western Arctic continental shelf. *Org Geochem*. 42:487–497.
- Volkman J. 1986. A review of sterol markers for marine and terrigenous organic matter. *Organic Geochemistry*. 9(2):83–99.
- Wakeham S, Lee C, Hedges J, Hernes P, Peterson M. 1997. Molecular indicators of diagenetic status in marine organic matter. *Geochimica et Cosmochimica Acta*. 61:5363–5369.
- Yang D, Shi X, Marsh P. 2015. Variability and extreme of Mackenzie River daily discharge during 1973-2001. *Quaternary International*. 380-381:159–168.
- Yunker MB, Macdonald RW, Velthamp DJ, Cretney WJ. 1995. Terrestrial and marine biomarkers in a seasonally ice covered Arctic estuary—integration of multivariate and biomarker approaches. *Mar Chem*. 49:1–50.
- Yunker MB, Belicka LL, Harvey HR, Macdonald RW. 2005. Tracing the inputs and fate of marine and terrigenous organic matter in Arctic Ocean sediments: a multivariate analysis of lipid biomarkers. *Deep-Sea Res. II* 52(24–26):3478–3508.
- Zimmerman CF, Keefe CW, Bashe J. 1997. Method 440.0 determination of carbon and nitrogen in sediments and particulates of estuarine/coastal waters using elemental analysis. U.S. Environmental Protection Agency. Washington, DC, EPA/600/R-15/009.

## **Appendix A: 2015 Post-Cruise Report**

**Post-Cruise Report for Pilot  
Biophysical and Chemical  
Observations Program: Marine  
Arctic Ecosystem Study**

Contract M14PC00008  
Task Order 2 M15PD00012



Prepared for:

Department of the Interior  
Bureau of Ocean Energy  
Management

US Department of Interior  
Bureau of Safety and  
Environmental Enforcement  
Procurement Branch, HQ 45600  
Woodland Road, Sterling, VA  
20166-9216

Prepared by:  
Stantec Consulting Services Inc.  
4500 Daly Drive, Suite 100  
Chantilly, VA 20151-3724

October 16, 2015

POST-CRUISE REPORT FOR PILOT BIOPHYSICAL AND CHEMICAL OBSERVATIONS PROGRAM: MARINE  
ARCTIC ECOSYSTEM STUDY

*Diane T. Ingraham* for:

Francis Wiese, Ph. D.  
Program Technical Director

*Alexandra Eaves*

Alexandra Eaves Ph. D.  
Assistant Technical Director

Reviewed by:

*Diane T. Ingraham*

Diane Ingraham Ph. D., PMP  
Project Manager



**POST-CRUISE REPORT FOR PILOT BIOPHYSICAL AND CHEMICAL OBSERVATIONS PROGRAM: MARINE ARCTIC ECOSYSTEM STUDY**

**Table of Contents**

<b>1.0</b>	<b>INTRODUCTION .....</b>	<b>1</b>
<b>2.0</b>	<b>CRUISE DEPLOYMENT TIMING AND LOCATION .....</b>	<b>1</b>
<b>3.0</b>	<b>MOORING ARRAY SENSORS AND DEPLOYMENT .....</b>	<b>9</b>
<b>4.0</b>	<b>AUTONOMOUS GLIDER SENSORS AND DEPLOYMENT .....</b>	<b>10</b>
<b>5.0</b>	<b>SCIENCE TEAM .....</b>	<b>14</b>
<b>6.0</b>	<b>SUMMARY .....</b>	<b>15</b>
<b>7.0</b>	<b>BIBLIOGRAPHY .....</b>	<b>15</b>

**LIST OF APPENDICES**

**APPENDIX A      MOORING DESIGNS**

# POST-CRUISE REPORT FOR PILOT BIOPHYSICAL AND CHEMICAL OBSERVATIONS PROGRAM: MARINE ARCTIC ECOSYSTEM STUDY

INTRODUCTION  
October 16, 2015

## 1.0 INTRODUCTION

The MARES 2015 Pilot Biophysical and Chemical Observations Program Task Order 3 (M15PD00012) cruise planned for deployment of an autonomous glider for approximately six weeks, and deployment of a mooring array to be retrieved in the summer of 2016. Deployment was planned for the eastern U.S. Beaufort Sea with the objective of testing the latest technology and equipment to acquire biophysical and chemical time series data, and work towards describing the biogeochemical impact of the Mackenzie river plume in that area. For the mooring devices to be deployed during whaling season, BOEM and the Alaskan Eskimo Whaling Commission had agreed on August 21, 2015 to proceed only with mooring deployment once the communities of Nuiqsut and Kaktovik had completed their annual harvest of bowhead whales.

## 2.0 CRUISE DEPLOYMENT TIMING AND LOCATION

The planned cruise deployment timing and location was previously described in Stantec's *Pre-Cruise Report for Pilot Biophysical and Chemical Observations Program: Marine Arctic Ecosystem Study* (Stantec, 2015). The actual cruise deployment timing and location is described below.

### Pre-cruise mobilization

- July 17, 2015, shipment of the mooring devices from Woods Hole Oceanographic Institution (WHOI) (Woods Hole, MA).
- July 23, 2015, shipment of tall mooring devices from ASL Environmental Services (Victoria, BC).
- August 3, 2015, WHOI mooring devices arrived in Cordova, AK.
- August 5, 2015, shipment of the glider from Teledyne Webb Research (TWR) and arrival in Nome, AK on August 17, 2015.
- August 14, 2015, Cruise deployment stand-down to revise schedule to avoid interference with Bowhead whale harvest for the Communities of Kaktovik and Nuiqsut, AK.
- August 21<sup>st</sup>, 2015 ASL mooring devices arrived in Cordova, AK.
- August 21, 2015, mooring cruise timeline was postponed for twelve days to September 7, 2015 to accommodate commencement of the bowhead whale harvest for the communities of Kaktovik and Nuiqsut, AK.
- August 24, 2015, the MARES mooring devices were loaded aboard the *U.S. Coast Guard Cutter Sycamore* (WLB-209) (225ft long), in Cordova, AK. The vessel departed for Nome on August 26, 2015.
- September 1, 2015, Donglai Gong (VIMS) arrived in Nome AK for pre-deployment field testing of the glider which had been stored at UAF since its shipment to Alaska from the manufacturer TWR in Virginia.



# POST-CRUISE REPORT FOR PILOT BIOPHYSICAL AND CHEMICAL OBSERVATIONS PROGRAM: MARINE ARCTIC ECOSYSTEM STUDY

CRUISE DEPLOYMENT TIMING AND LOCATION  
October 16, 2015

- September 2, 2015, the glider was powered on, the vacuum pressure in the internal compartments held, and there were no obvious issues following shipment from the manufacturer. The glider was not opened again after assembling and testing at TWR.
- September 3, 2015, both glider compass calibrations and a submersion test were performed from shore in Nome, AK (Figure 1). The glider was deemed fully prepared and tested, as of September 4, 2015, and ready for loading aboard the *USCG Sycamore*.
- September 7, 2015, the first two members of the pilot cruise Science team, Principal Investigator, Robert Pickart, and Software Architect, Carolina Nobre, (both from Woods Hole Oceanographic Institute (WHOI)), boarded the *USCG Sycamore*. The glider and calibrated mooring ADCP sensors were loaded and stowed, the large mooring components were already aboard (Figure 2).



**Photo 1** Dr. Donglai Gong, from the Virginia Institute of Marine Science on shore in Nome Alaska with the autonomous glider during pre-deployment testing September 3, 2015.

# POST-CRUISE REPORT FOR PILOT BIOPHYSICAL AND CHEMICAL OBSERVATIONS PROGRAM: MARINE ARCTIC ECOSYSTEM STUDY

CRUISE DEPLOYMENT TIMING AND LOCATION  
October 16, 2015



**Photo 2** MARES mooring devices on deck aboard the USCG Sycamore in Nome AK, September 7, 2015. Shown here are the WHOI tripod and tall moorings intended for the 50 m and 120 m isobaths respectively.

## Cruise Timeline and Details

- September 7, 2015, the *USCG Sycamore* departed from Nome, AK, to start the mooring cruise and headed towards Point Hope where the USCG conducted its outreach activities on Friday, September 11, 2015, AK.
- Due to inclement weather conditions, the Community Observer, Ray Kious, was delayed in arriving from Nome in time for vessel departure. He therefore was re-directed to join the vessel in Barrow, AK.
- September 8, 2015, glider team (VIMS) returned to Virginia.
- Mooring technician, Jim Ryder, who was to depart WHOI to meet the ship in Barrow, had a death in his immediate family. Another experienced mooring technician from WHOI, Steve Murphy, was sent in his stead.
- September 8, 2015, the Science crew aboard the *USCG Sycamore* was informed that Barrow intended to begin their hunt earlier than planned and that the *USCG Sycamore* could not enter port on September 15, for the scheduled rendezvous in Barrow. The rendezvous was rerouted to Kotzebue, AK. The remaining Science crew personnel and equipment were diverted to Kotzebue. The partnering program at UAF, providing a fifth mooring device for the MARES array, was also notified to redirect their mooring device to meet the vessel.
- September 9, 2015, Kaktovik whaling season began.



## POST-CRUISE REPORT FOR PILOT BIOPHYSICAL AND CHEMICAL OBSERVATIONS PROGRAM: MARINE ARCTIC ECOSYSTEM STUDY

CRUISE DEPLOYMENT TIMING AND LOCATION  
October 16, 2015

- September 11, 2015, Environmental factors that could affect the deployment mission were favorable; the weather was improving at the deployment location, and the target location for the mooring array line was ice-free. The community of Nuiqsut, AK had already completed their harvest. Even though the community of Kaktovik, AK, approximately 60 miles to the east of Nuiqsut, AK, had started their hunt, they were weathered-out and did not achieve any of the three allotted strikes they needed to make up their annual subsistence harvest. Historically, the community of Kaktovik has completed their harvest by September 12.
- September 13, 2015, the *USCG Sycamore's* bathymetric system was ground-truthed by repeating a part of a Kotzebue section that was done in NASA's multi-year ship borne study of the Impacts of Climate on the Eco-Systems and Chemistry of the Arctic Pacific Environment (ICESCAPE) program. The comparison was excellent, within about 1 m of the calculated bottom from ICESCAPE.
- September 14, 2015, a review of the latest International Bathymetric Chart of the Arctic Ocean (IBCAO) (version 3.0) in the MARES region revealed a bathymetric feature near the outer-shelf or shelf break where the planned MARES mooring line was to be positioned. This feature was not apparent in previous bathymetric survey resources including the National Oceanic and Atmospheric Administration's 2-Minute Gridded Global Relief Data (ETOPO2) and the two previous versions of IBCAO. To avoid the array measuring anomalous hydrographic conditions due to local topography, it was moved approximately 40 km west of the original longitude in the eastern US Beaufort Sea (Figure 3). Final deployment location would still be subject to change when bathymetric survey is conducted on-site.



**POST-CRUISE REPORT FOR PILOT BIOPHYSICAL AND CHEMICAL OBSERVATIONS PROGRAM: MARINE ARCTIC ECOSYSTEM STUDY**

CRUISE DEPLOYMENT TIMING AND LOCATION  
 October 16, 2015

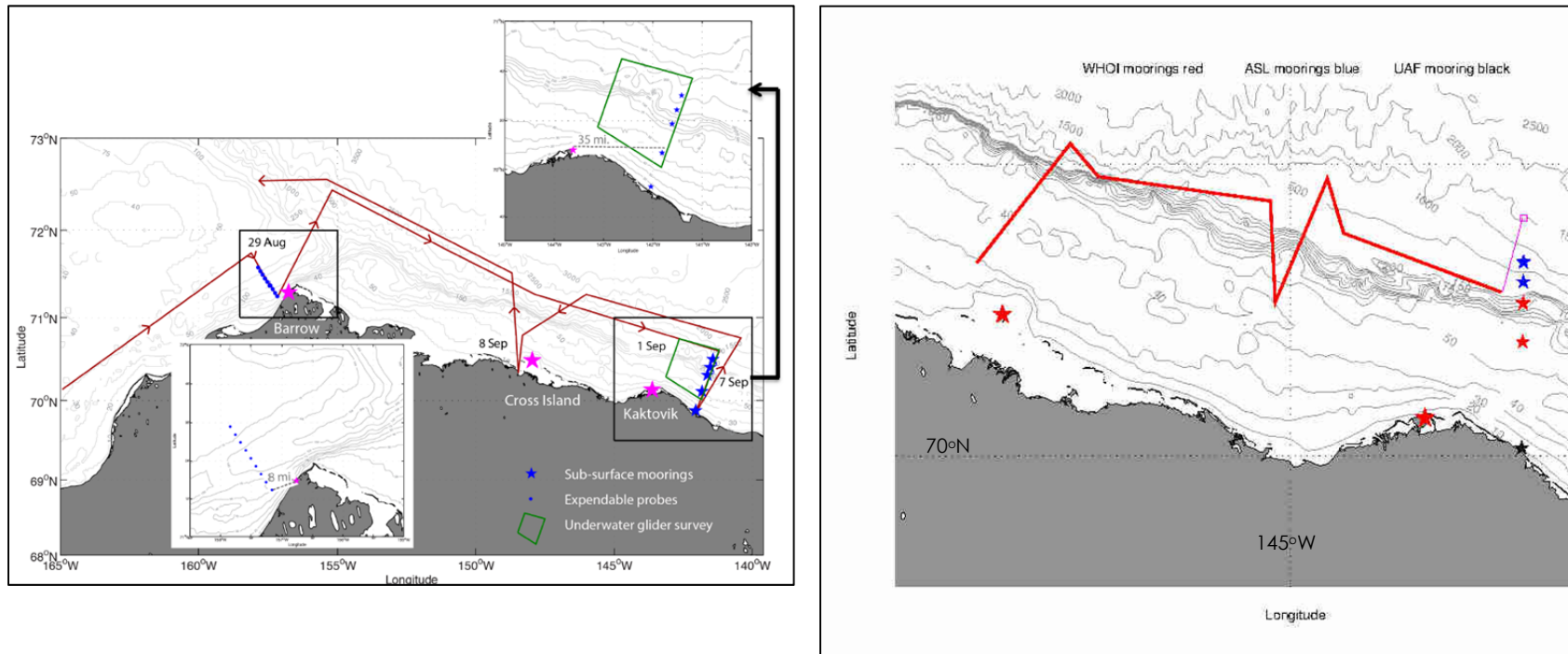


**Figure 2-1** Revised study area and proposed deployment locations of MARES mooring array and autonomous glider flight path (right chart). The left chart (included for reference from (Stantec, 2015)) shows the original pre-cruise planned study area with proposed deployment locations. Mooring devices were revised to be deployed on the shelf break along ~ 50, 140, 350 and 650 meter isobaths (blue stars). Red line indicates the *USCG Sycamore* tract, magenta line indicates intended *USCG Sycamore* tract to glider deployment location, magenta square, location of glider deployment (1500m isobath), small red stars indicate WHOI Moorings, small blue stars indicate ASL Moorings, large red star nearshore on left indicates Cross Island, and large red star nearshore on right indicates Kaktovik. The partnering UAF mooring (small black star nearshore) was not redirected to Kotzebue in time to be loaded on the *USCG Sycamore*. Therefore the 12 m isobath mooring was not going to be part of this mooring array.



## POST-CRUISE REPORT FOR PILOT BIOPHYSICAL AND CHEMICAL OBSERVATIONS PROGRAM: MARINE ARCTIC ECOSYSTEM STUDY

### CRUISE DEPLOYMENT TIMING AND LOCATION

October 16, 2015

- September 15, 2015, the unloading of both mooring technicians, Steve Murphy (WHOI) and Nikolai Milutinovic, (ASL Environmental Sciences), Community Observer, Ray Kious (UIC), and all remaining MARES mooring equipment was successful.
- The partnering UAF mooring device did not arrive in Kotzebue in time and missed the deployment cruise.
- September 16, 2015, the BOEM Alaska COR notified Stantec of Kaktovik's first whale strike; however, the animal was compromised and was not counted as one of the three subsistence strikes. Stantec relayed this information to the Science Crew aboard the *USCG Sycamore*.
- September 17, 2015, the *USCG Sycamore* arrived at the longitude of Barrow and held position until approval to proceed eastwards towards Kotzebue was received from USCG Command D-17, following communication between the Community Observer Ray Kious, and the AEWG.
- September 19, 2015, the *USCG Sycamore* was holding 50 nautical miles offshore while awaiting the community of Kaktovik to complete their strikes.
- September 20, 2015 Stantec formally requested assistance from BOEM to re-engage with AEWG to allow for coordination between the AEWG and the Community Observer aboard the vessel (Ray Kious) for mooring deployment activities to be conducted during marginal whaling conditions (such as high sea state or low light conditions). Otherwise the vessel would have to leave the area no later than noon on September 25, 2015, due to fuel and food constraints aboard the vessel.
- September 21, 2015, the autonomous glider was deployed, and during its first dive at 200 meters a leak was detected and the glider was immediately recovered by the *USCG Sycamore*. The glider was stored on and not below deck as a precaution in case of interaction between the lithium battery and seawater potentially releasing hydrogen gas.
- September 21, 2015, in response to Stantec's formal request to BOEM, BOEM responded that the agreement between BOEM and AEWG would remain intact. Briefly, this August 21, 2015 agreement between BOEM and AEWG, stated in an email to James Kendall (BOEM) from Jessica Lefevre on behalf of the AEWG Chairman, Mr. Harry Bower, reinforced: "... assurances provided by BOEM, that the vessel will traverse the Beaufort Sea well offshore (to the extent possible given ice cover) and will remain offshore until the close of fall whaling at Kaktovik and Nuiqsut...".
- September 22, 2015, Stantec informed the BOEM CORs that due to the combined factors of low probability of the whaling community of Kaktovik obtaining three strikes in time for the *USCG Sycamore* to then conduct bathymetric surveys and mooring deployment before needing to return to port (three strikes in one day with few whales in sight), and a deteriorating forecast in the western Beaufort that the vessel would be transiting through it was decided to prioritize the safety of the vessel the mooring deployment cruise was terminated and the *USCG Sycamore* headed for port in Nome, AK.





# POST-CRUISE REPORT FOR PILOT BIOPHYSICAL AND CHEMICAL OBSERVATIONS PROGRAM: MARINE ARCTIC ECOSYSTEM STUDY

CRUISE DEPLOYMENT TIMING AND LOCATION  
October 16, 2015

## Post-Cruise Demobilization

- September 28, 2015, D. Gong (VIMS), Principal Investigator for the autonomous glider portion arrived in Nome, AK to conduct a necessary safety inspection before shipment of the glider would be possible.
- September 29, 2015, Mooring equipment and autonomous glider were offloaded from the USCG Sycamore. Principle Investigator D. Gong, powered on the glider in an outdoor field as a precaution to check if there was any seawater near the lithium battery, and to assess its performance compared to pre-leak detection readings.
- September 30, 2015, D. Gong conducted a preliminary assessment of the condition of the glider's internal components and found evidence of saltwater entry in the forward bay. The glider was then packaged for shipment back to TWR, the manufacturer, who had installed all components on the glider prior to the pilot mission.
- October 2, 2015, glider packed up for shipment to TWR.

A summary of logistical changes to the deployment cruise are included in Table 2.1.

**Table 2.1 Summary of scheduling changes to the 2015 MARES pilot biophysical and chemical oceanography deployment cruise.**

Activity	Original date	Revised date	Final Change
<u>Load mooring gear in Cordova:</u> Date postponed due to deployment cruise stand-down to allow for respectful discussion with MARES program partners and AEWC regarding concerns of proposed pilot mooring cruise activities in proximity to whaling season.	Aug. 13, 2015	Aug. 25, 2015	none
<u>Load remaining gear and vessel departure with part of science party and community liaison in Nome AK and depart the following day:</u> The loading date cannot be delayed further due to unavailability of the pier in Nome, AK.	Aug. 25-26, 2015	Sept. 6-7, 2015	none
Due to adverse weather conditions, the Community Observer could not travel to Nome, AK in time for vessel departure and joined the vessel in Kotzebue, AK.	Sept. 7 <sup>th</sup> , 2015	Sept. 15 <sup>th</sup> , 2015	Community observer and remaining Science crew boarded in Kotzebue.
Mooring technician Jim Ryder had a death in the immediate family and was replaced by another WHOI mooring tech, Steve Murphy.	NA	NA	Replacement Science crew member
<u>Review of latest bathymetric data resource (IBCAO v.3.0) identified an anomaly at target MARES mooring deployment region not present in previous data</u>	NA	Sept. 14 <sup>th</sup> , 2015	Relocation of MARES target line approximately 40 km west of previous area to avoid distortion from bathymetric anomaly.
<u>Embark WHOI tech and remaining WHOI gear in Barrow:</u>	NA	Sept. 15,	Community of Barrow, AK began whale harvest early and the vessel,



## POST-CRUISE REPORT FOR PILOT BIOPHYSICAL AND CHEMICAL OBSERVATIONS PROGRAM: MARINE ARCTIC ECOSYSTEM STUDY

CRUISE DEPLOYMENT TIMING AND LOCATION  
October 16, 2015

Activity	Original date	Revised date	Final Change
Second crew load phase was required to accommodate air shipment logistics from WHOI (MA) that require more lead time, and remaining WHOI mooring technician is not available for Sept 7 2015 loading and departure date. Historically, Barrow does not start whaling until late-September, and Barrow Communications Center had confirmed the USCGC <i>Sycamore</i> could do small boat operations until Sept. 15 <sup>th</sup> , 2015.		2015	remaining Science crew and gear had to be diverted to Kotzebue, AK for secondary onload.
<u>Mooring from partnering UAF program did not arrive in Kotzebue in time</u>	Sept. 15 <sup>th</sup> , 2015	not available	Partnering UAF mooring not loaded aboard USCG <i>Sycamore</i> for deployment
<u>Approximate arrival date at MARES study region in eastern U.S. Beaufort</u> ; Date initially postponed to minimize interference with whaling activities in Kaktovik and Nuiqsut, AK.	Sept. 1, 2015	Sept. 19 <sup>th</sup> , 2015	Longer transit from Kotzebue to study region, and vessel had to hold offshore for 1 day while awaiting approval from USCG to proceed East towards study region.
<u>Autonomous glider deployment from USCG <i>Sycamore</i> in MARES study region (approximate date)</u> ; Date initially postponed to accommodate later deployment cruise timeframe.	Sept. 1, 2015	Sept. 21 <sup>st</sup> , 2015	Longer transit from Kotzebue to study region, and vessel had to hold offshore for 1 day while awaiting approval from USCG to proceed East towards study region.
<u>Autonomous glider recovery</u>	Ending 2 <sup>nd</sup> week of Oct. 2015	Sept. 21 <sup>st</sup> , 2015	Early recovery of the autonomous glider was necessary as a leak was detected in the device at a depth of 200m and the condition of the internal components was unknown.
<u>Disembark science party in Barrow, AK</u> ; Date initially postponed to accommodate later deployment cruise timeframe (Sept. 22 <sup>nd</sup> , 2015).	Sept. 8, 2015	Sept. 26 <sup>th</sup> , 2015	Science party disembarked in Kotzebue instead of Barrow (whaling season was underway), there was a longer transit time from study region to Kotzebue, AK.
<u>Unload mooring gear and glider from USCG <i>Sycamore</i></u>	NA	Sept. 29 <sup>th</sup> 2015	Moorings not deployed, require and shipment back to home institutions.
<u>Demobilization of autonomous glider and shipment back to manufacturer for diagnostics and integrity assessment.</u>	Second week of October	Oct. 2 <sup>nd</sup> , 2015	Potential for hydrogen to off-gas from interaction between lithium battery and seawater had to be assessed prior to shipment.



# POST-CRUISE REPORT FOR PILOT BIOPHYSICAL AND CHEMICAL OBSERVATIONS PROGRAM: MARINE ARCTIC ECOSYSTEM STUDY

MOORING ARRAY SENSORS AND DEPLOYMENT  
October 16, 2015

## 3.0 MOORING ARRAY SENSORS AND DEPLOYMENT

To address the objective of acquiring biophysical and chemical time series data a mooring array was to be deployed in the eastern U.S. Beaufort through the end of summer 2016 field season. The MARES mooring array consisted of 4 devices that were to be deployed along the 50 m, 140 m, 350 m and 650 m isobaths to measure temperature, salinity, current velocity, fluorescence, abundance of fish and zooplankton, acoustics, photosynthetically active radiation, dissolved oxygen and turbidity. The approximate coordinates were revised to accommodate the detection of a bathymetric anomaly and would need to be finalized according to site-specific bathymetric data acquired on-site. All sensory components of each mooring were loaded aboard the *USCG Sycamore* and ready for deployment as described below, and drawings of each mooring are included in Appendix A. In partnership with UAF, ANIMIDA (PI Jeremy Kasper, the mooring array was to include a fifth device (second tripod) on the shelf at the 12m isobaths, however, it did not arrive at the revised secondary vessel loading site in Kotzebue, AK and was therefore not aboard the *USCG Sycamore* for the 2015 deployment cruise. A sixth mooring device to be positioned further east in the Mackenzie trough at around 1000 m in partnership with Martin Fortier at ArcticNet was independent of the MARES deployment mission. The mooring components are now being shipped back to home institutions (WHOI and ASL).

### **MARES mooring device specifications that were loaded aboard the *USCG Sycamore* (see Appendix A for drawings):**

1. Tripod, ~50m bottom depth, to be positioned at 70.1127 -141.8138 (revised to 70 23.8 (N), 142 36.9 (W), 57m depth), with the following:
  - 300 KHz Acoustic Doppler Current Profiler (ADCP) for measuring ocean currents
  - MicroCAT for measuring conductivity, temperature and pressure
  - Inductive tether with 3 MicroCATs (28m, 22m, 16m)
  - Data logger
  - Dual releases
2. Tall mooring, ~140m bottom depth, to be positioned at 70.3106 -141.6106 (revised to 70 31.7 (N), 142 36.6 (W), 137m depth), with the following:
  - Top float at 35m with the following:
    - Upward Looking Sonar (ULS) for providing under-ice topography data
    - 300 KHz ADCP for measuring ocean currents
    - MicroCAT for measuring conductivity, temperature and pressure
    - Data logger
  - Inductive tether with 3 MicroCATs (28m, 22m, 16m)



## POST-CRUISE REPORT FOR PILOT BIOPHYSICAL AND CHEMICAL OBSERVATIONS PROGRAM: MARINE ARCTIC ECOSYSTEM STUDY

### AUTONOMOUS GLIDER SENSORS AND DEPLOYMENT

October 16, 2015

- McLane Moored Profiler (MMP), record water conditions daily with an acoustic, vector measuring current meter (ACM), dissolved oxygen, turbidity, fluorescence and (photosynthetically active radiation) PAR
  - MicroCAT below bottom stop for measuring conductivity, temperature and pressure
  - 300 KHz Acoustic Doppler Current Profiler (ADCP) below bottom stop for measuring ocean currents
  - Dual releases
3. Tall mooring, ~350m bottom depth, to be positioned at 70.4062 -141.5137 (revised to 70 36.1 (N), 142 36.5 (W), 386 m depth), with the following:
- 1 x ASL Environmental Sciences Ice Profiler (IPS5) for measuring ice draft and surface waves
  - 4 x Sea-Bird Electronics MicroCAT C-T logger (SBE 37-M) for measuring conductivity, temperature and pressure
  - 2 x ASL Environmental Sciences Acoustic Zooplankton and Fish Profiler (AZFP) for bioacoustic backscatter
  - 1 x Teledyne RDI Acoustic Doppler Current Profiler (150kHz QM ADCP) for measuring ocean currents and ice velocity
  - 1 x Teledyne RDI Acoustic Doppler Current Profiler (75kHz ADCP) for measuring ocean currents
  - Dual releases
4. Tall mooring, ~650m bottom depth, to be positioned at 70.5034 -141.4168 (revised to 70 40.1 (N), 142 36.4 (W), 681m depth), with the following:
- 1 x ASL Environmental Sciences Ice Profiler (IPS5) for measuring ice draft and surface waves
  - 4 x Sea-Bird Electronics MicroCAT C-T logger (SBE 37-M) for measuring conductivity, temperature and pressure
  - 1 x Teledyne RDI Acoustic Doppler Current Profiler (150kHz QM ADCP) for measuring ocean currents and ice velocity
  - 1 x Teledyne RDI Acoustic Doppler Current Profiler (75kHz ADCP) for measuring ocean currents
  - Dual releases

## 4.0 AUTONOMOUS GLIDER SENSORS AND DEPLOYMENT

To address the objective of testing the latest technology and equipment to acquire biophysical and chemical time series data, and to gain broader spatial biophysical and chemical data of the mooring array deployment region in the eastern U.S. Beaufort, an autonomous Slocum glider (~5 ft long), was deployed to measure physical, chemical and biological oceanographic



# POST-CRUISE REPORT FOR PILOT BIOPHYSICAL AND CHEMICAL OBSERVATIONS PROGRAM: MARINE ARCTIC ECOSYSTEM STUDY

AUTONOMOUS GLIDER SENSORS AND DEPLOYMENT  
October 16, 2015

properties in a track surrounding the mooring array (Figure 2.1). Specifically, the glider was equipped as follows:

- Seabird pumped CTD, collecting data on Conductivity-Temperature-Depth
- WETLabs ECO Triplet puck (chlorophyll-a fluorescence, CDOM fluorescence, optical backscattering at 700 nm)
- Aanderaa dissolved oxygen optode, measuring dissolved oxygen concentration
- PAR sensor, to measure photosynthetically active radiation
- Imagenex Model 853 scientific echo sounder (120 kHz), for measuring bioacoustic backscattering (acoustic plankton profiling).

An extended buoyancy pump (800 cc vs 460 cc normal) and a hybrid thruster to provide an additional 1000 cc of active buoyancy for freshwater lens penetration. The glider was launched by the Science Team at the 1500m isobaths on the revised mooring deployment longitude. It will go westward initially from the eastern most offshore site, and monitoring and piloting of its initial performance will be conducted remotely (from shore), initially from Nome, AK, then from Virginia Institute of Marine Science. The glider will continually sample counterclockwise along the MARES TO3 glider sampling box with the following coordinates:

Original glider transect coordinates:

70.290 -143.120 (closest to Kaktovik)  
70.013 -141.830  
70.620 -141.200  
70.750 -142.630

## Revised glider deployment coordinates:

The first waypoint was to the west of the mooring array, and following deployment it was to head for the third waypoint on the list and stay out of the whaling region until permission to enter was given.

-142 50.00 70 34.00 Begin waypoint for eastern along-shelf segment  
-144 27.00 70 46.00 End waypoint for eastern along-shelf segment

-144 37.00 70 57.00 Offshore waypoint of central cross-shelf section  
-145 09.00 70 32.00 Mid-shelf waypoint of central cross-shelf section (42 m)

-145 12.00 70 52.50 Begin waypoint for the western along-shelf segment  
-146 58.00 70 57.40 End waypoint for the western along-shelf segment

-147 15.00 71 04.00 Offshore waypoint of the western cross-shelf section

-148 12.50 70 40.00 Inner-shelf waypoint of the western cross-shelf section off Prudhoe Bay, (also glider recovery waypoint).



# POST-CRUISE REPORT FOR PILOT BIOPHYSICAL AND CHEMICAL OBSERVATIONS PROGRAM: MARINE ARCTIC ECOSYSTEM STUDY

AUTONOMOUS GLIDER SENSORS AND DEPLOYMENT  
October 16, 2015

Alternate glider recovery point:  
-147 50.00 70 35.00

Depending on weather and sea conditions the estimated recovery for the glider was planned for the second week of October, at which time a separate charter vessel would have recovered the device. However, the glider had to be recovered by the crew of the *USCG Sycamore* early during its deployment mission as a leak was detected in the forward hull during the first dive at a depth of 200m. The glider crate was shipped from Prudhoe Bay (where it had been sent for the planned recovery), back to Nome, AK to be available for shipping the glider back to the manufacturer.

Following offload from the *USCG Sycamore* there were signs of exterior damage to the glider incurred during recovery and storage on-deck for the steam back to Nome from off the coast of Kaktovik (E.g. broken wings and broken prop from being dragged backwards). However, all the sensors appeared to be intact with no obvious signs of damage.

To assess the condition of the glider and safety for shipping, the manufacturer (TWR) advised that the glider be powered on outdoors to compare the output state of the glider since it was recovered. If only a small amount of water penetrated the glider it should have evaporated inside, and the leak detection voltage would have returned to normal. When the glider was powered on, the leak detect voltage had recovered significantly but was not back to normal, so some dampness was still suspected around near the leak indicator. Furthermore, the internal vacuum pressure held which indicated that the lithium battery was not interacting with seawater and outgassing hydrogen, and the battery appears to be functional as well.

Following this initial assessment and in consultation with the manufacturer (TWR), the glider was opened and there was no sign of water presently in the glider except for a bit of dampness between the science bay and the forward section. Also there appeared to be no obvious signs of damage to any internal glider components, including the battery. However, it was evident that there had been a significant amount of water in the glider at one point. Salt deposits were found inside the nose section and along the bottom of the whole forward section to the science bay (Figure 4-1 A and B). Based on the salt signature, it was estimated there may have been at least 1/8 of the chamber with water lying on the bottom. The bulkhead at the science bay possibly prevented the water from entering the science bay and back section. The inside of the glider was left to dry out indoors to ensure any residual moisture evaporated.





**POST-CRUISE REPORT FOR PILOT BIOPHYSICAL AND CHEMICAL OBSERVATIONS PROGRAM: MARINE ARCTIC ECOSYSTEM STUDY**

AUTONOMOUS GLIDER SENSORS AND DEPLOYMENT  
October 16, 2015

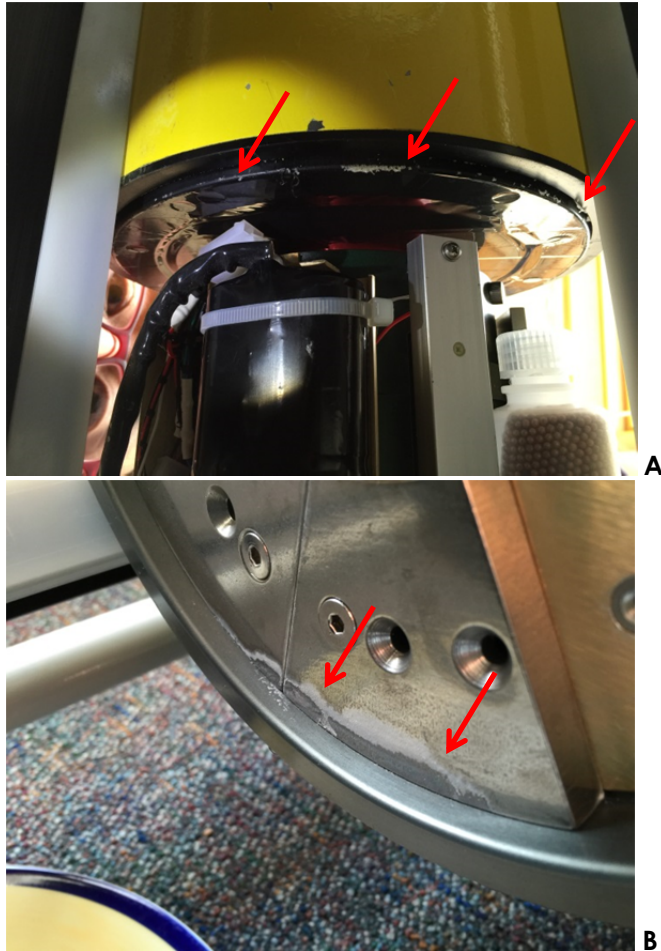


**Photo 3** Internal hull of autonomous glider 417 showing dried saltwater residue (red arrows) in forward hull section, forward (A) and aft (B) bulkheads are shown.

Further inspection of the O-rings revealed they were dirty with sand-like particles. The worst O-ring was found between the forward section and the science bay. It's not clear how the sand got into the glider's O-rings (Figure 4-2 A and B).



# POST-CRUISE REPORT FOR PILOT BIOPHYSICAL AND CHEMICAL OBSERVATIONS PROGRAM: MARINE ARCTIC ECOSYSTEM STUDY

SCIENCE TEAM  
October 16, 2015

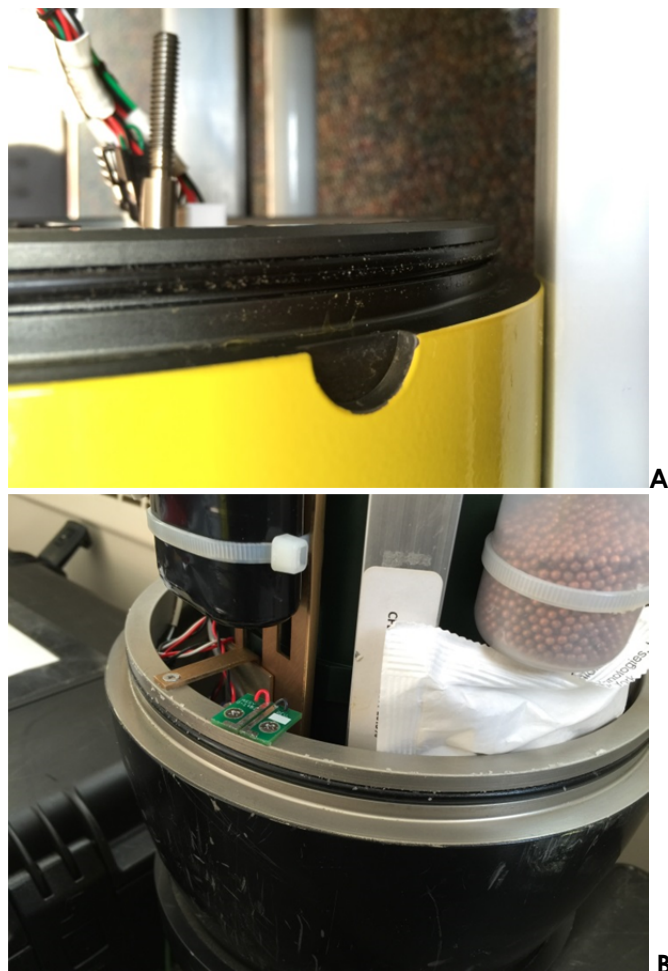


**Photo 4** Close-up of O-rings with indications of salt crystals (A) and sand-like particles (B).

## 5.0 SCIENCE TEAM

The Science Team members, their affiliations and their role for this MARES Pilot Biophysical and Chemical observations cruise were as listed below, changes to the original cruise plan are shown in red:

- Dr. Robert Pickart, Woods Hole Oceanographic Institution, Chief Scientist
- **Steve Murphy, replacement WHOI mooring technician for Jim Ryder (WHOI) who had a death in his immediate family**
- Nikolai Milutinovic, ASL Environmental Sciences, Mooring Technician
- Dr. Carolina Nobre, Woods Hole Oceanographic Institution, Software Technician



# POST-CRUISE REPORT FOR PILOT BIOPHYSICAL AND CHEMICAL OBSERVATIONS PROGRAM: MARINE ARCTIC ECOSYSTEM STUDY

## SUMMARY

October 16, 2015

- Ray Kios, UIC, Community Observer included as part of August 21, 2015 agreement between BOEM and AEWG.
  - Ray Kios was originally going to board the *USCG Sycamore* in Nome, AK along with the Chief Scientist. However, due to fog conditions he could not get to Nome in time for vessel departure. He was re-directed to join the vessel from Barrow then Kotzebue, AK when the Community of Barrow began its whale harvest early.

The autonomous glider was deployed by the cruise Science Team members and monitored from shore:

- Dr. Donglai Gong, Virginia Institute of Marine Science, Principal Investigator
- Haixing (Daniel) Wang, Virginia Institute of Marine Science, Graduate Research Assistant

## 6.0 SUMMARY

All mooring and autonomous glider equipment and sensors were acquired, assembled and loaded aboard the *USCG Sycamore* as proposed for the MARES 2015 Pilot Biophysical and Chemical Observations Program. Several logistical changes were made prior and during the progress of the cruise (summarized in Table 2.1), and the *USCG Sycamore* arrived at the target mooring deployment longitude, and the autonomous glider was deployed. In respect of the August 21, 2015 agreement between BOEM and the AEWG, the *USCG Sycamore* did not approach the mooring deployment target locations as the community of Kaktovik, AK had not obtained its subsistence quota of bowhead whales (historically met by September 12, 2015), and in advance of a worsening sea state in the eastern Beaufort, the *USCG Sycamore* returned to port to prioritize the safety of the vessel and crew without having deployed the mooring devices. The autonomous glider detected a leak in its forward hull and had to be recovered by the *USCG Sycamore* early during its deployment mission on September 21, 2015. None of the equipment was lost, and there were no health and safety incidents reported during the entire pre-mobilization process, during the cruise, and post-cruise mobilization process. A comprehensive Technical Report will be generated with detailed findings from the glider inspection and lessons learned to improve the success of the MARES program going forward.

## 7.0 BIBLIOGRAPHY

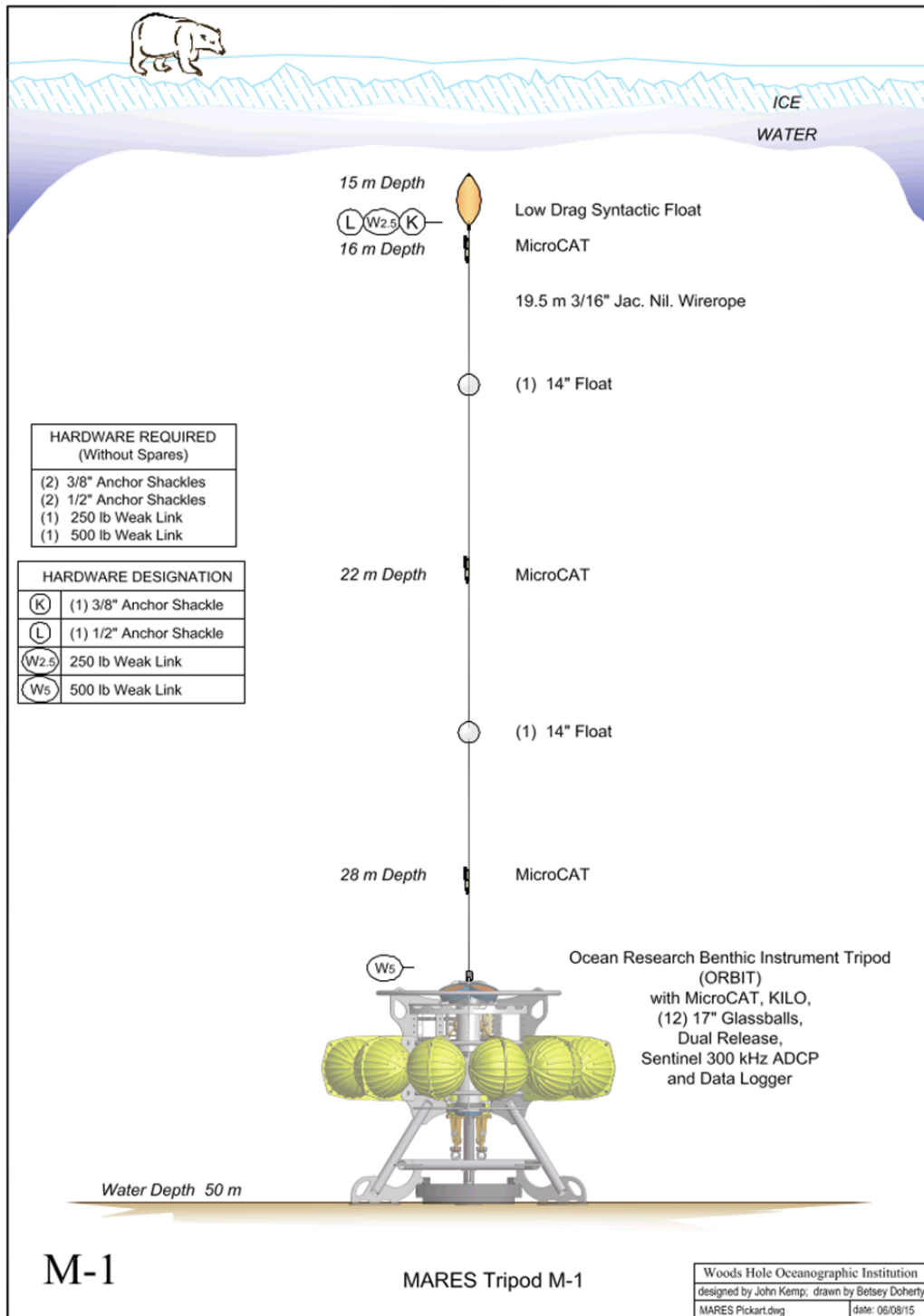
Stantec. (2015). *Pre-Cruise Report for Pilot Biophysical and Chemical Observations Program: Marine Arctic Ecosystem Study*. St. John's NL / Chantilly, VA: Stantec Consulting Services Inc.; August 5, 2015



# APPENDIX A

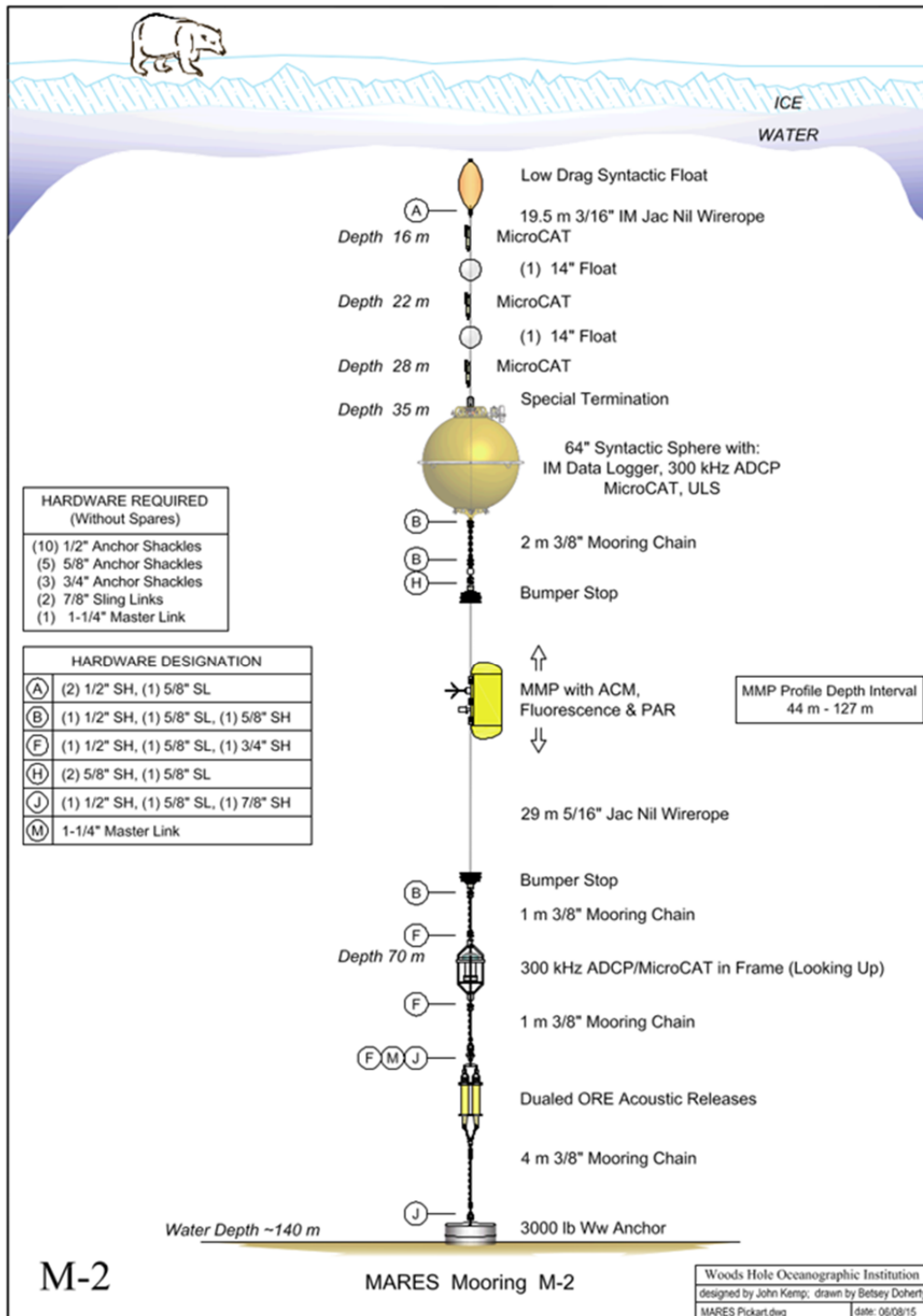
## Mooring Designs

POST-CRUISE REPORT FOR PILOT BIOPHYSICAL AND CHEMICAL OBSERVATIONS PROGRAM: MARINE ARCTIC ECOSYSTEM STUDY



WHOI bottom tripod mooring (depth ~50m)

POST-CRUISE REPORT FOR PILOT BIOPHYSICAL AND CHEMICAL OBSERVATIONS PROGRAM: MARINE ARCTIC ECOSYSTEM STUDY



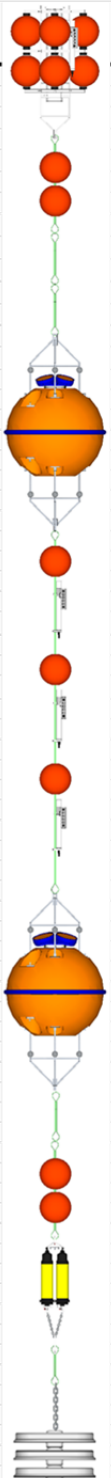
WHOI tall mooring (depth ~140m), the top float will be 35m below the surface

POST-CRUISE REPORT FOR PILOT BIOPHYSICAL AND CHEMICAL OBSERVATIONS PROGRAM: MARINE ARCTIC ECOSYSTEM STUDY

MARES 350 m	
Target Depth (m)	Proposed Instrument
	IPS5 Ice Profiler w/ full battery pack
	ASL Dual cage
70	8 Viny 12B3 floats
	Novatech ARGOS
	Novatech RF Beacon/Flasher
	Seabird CT logger
	6000, 6000, 6000, 2x 6000
	2 Viny 12B3 floats
	6000, 6000, 6000, 2x 6000
	15 degree cage
	AZFP
	6000, 6000, 6000, 2x 6000
100	2x 6000, 6000, 6000, 2x 6000
	150 kHz QM ADCP, upward
	Fiolec M4D 1500m
	2x 6000, 6000, 6000, 2x 6000
	6000, 6000, 6000, 2x 6000
130	Cable Float CF-12
	Seabird CTD with rope clamps
190	Cable Float CF-12
	Seabird CTD with rope clamps
250	Cable Float CF-12
	Seabird CTD with rope clamps
	2x 6000
330	75 kHz ADCP - SC 4 BP
	Fiolec M4D 1500m
	2x 6000, 6000, 6000, 2x 6000
	6000, 6000, 6000, 2x 6000
337	15 degree cage
	AZFP
	ASL dual PORT releases
	ASL dual PORT releases
	6000, 6000, 6000, 2x 6000
	6000
350	6000, 6000, 2x 6000, 2x 6000, 2x 6000, 2x 6000
	3 Train wheels

ASL tall mooring (depth ~350m), the top float of the mooring will be approximately 70m below the surface.

**POST-CRUISE REPORT FOR PILOT BIOPHYSICAL AND CHEMICAL OBSERVATIONS PROGRAM: MARINE ARCTIC ECOSYSTEM STUDY**

MARES 6-700 m		
Target Depth (m)		Proposed Instrument
		IPSS Ice Profiler w/ full battery pack
		ASL Dual cage
70		8 Viny 12B3 floats
		Novatech ARGOS
		Novatech RF Beacon/Flasher
		Seabird CT logger
		1/10", 1/10", 1/10", 2x 1/10"
		2 Viny 12B3 floats
		1/10" Amsted 2, 2/10"
		2x 1/10" shackles
100		150 kHz QM ADCP, upward
		Flotec M40 1500m
		2x 1/10", 1/10", 2x 1/10"
		1/10" Amsted 2 ropes, 2/10"
130		Cable Float CF-12
		Seabird CTD with rope clamps
190		Cable Float CF-12
		Seabird CTD with rope clamps
250		Cable Float CF-12
		Seabird CTD with rope clamps
		2x 1/10"
330		75 kHz ADCP - SC 4 BP
		Flotec M40 1500m
		2x 1/10", 1/10", 2x 1/10"
		Nautilus Vitrovex C2-03
		2x 1/10", 1/10", 2x 1/10"
		dual PORT releases
		1/10" Amsted 2, 2/10"
		1/10"
		1/10", 1/10", 2x 1/10", 2m x 3/8" chain
650		3 Train wheels

**ASL tall mooring (depth ~650m), the top float of the mooring will be approximately 70m below the surface.**

## **Appendix B: Feeding Guilds and Abundance**





**Table B-1. MARES sample feeding guilds and abundance.**

Feeding Guild	Phylum	Class/Subclass	Order	Family	Genus/Species	M1					M2					M3					M4				
						0-1	1-2	2-3	3-4	4-5	0-1	1-2	2-3	3-4	4-5	0-1	1-2	2-3	3-4	4-5	0-1	1-2	2-3	3-4	4-5
	Annelida	Polychaeta				0	0	0	0	0	0	0	0	0	0	4	0	0	0	0	5	0	0	0	0
Surface Deposit				Acrocirridae	nr. Flabelligena cirrata	0	0	0	0	0	0	0	0	0	0	3	0	0	0	0	0	0	0	0	0
Surface Deposit				Ampharetidae		0	0	0	0	0	0	0	0	0	0	0	0	0	1	0	20	4	0	0	0
Head Down Deposit				Capitellidae		0	0	0	0	0	1	2	0	0	0	0	2	9	2	4	1	0	0	4	1
					Mediomastus sp.	0	0	0	0	0	0	0	0	1	1	0	0	0	0	0	0	0	0	0	0
					Barantolla sp.	0	0	0	0	0	0	0	0	0	1	0	0	0	0	0	0	0	0	0	0
Surface Deposit				Cirratulidae		0	0	0	0	0	3	12	0	0	0	12	6	0	0	0	8	1	0	0	0
Surface Deposit				Cossuridae		0	0	0	0	0	0	1	0	0	0	0	0	1	0	0	0	0	0	0	0
Surface Deposit				Hesionidae		0	0	0	0	0	1	0	0	0	0	0	0	0	0	0	1	0	0	0	0
Predatory				Lumbrineridae		0	0	0	0	0	0	0	0	0	0	1	0	0	0	0	1	0	1	0	0
Head Down Deposit				Maldanidae		0	0	0	0	0	0	0	0	0	0	0	0	0	0	0	0	4	2	0	0
Predatory				Nephtyidae		1	0	0	2	1	18	0	0	0	0	17	2	0	0	0	1	0	0	0	0
Predatory				Nereidae		0	1	0	0	0	0	0	0	0	0	0	0	0	0	0	24	0	0	0	0
Scavengers				Onuphidae		0	0	0	0	0	1	0	0	0	0	8	0	0	0	0	7	0	0	0	0
Filter and surface deposit				Oweniidae		0	0	0	0	0	1	0	0	0	0	0	0	0	0	0	0	0	0	0	0
Head Down Deposit				Paraonidae		0	1	0	0	0	3	1	2	0	0	9	14	1	2	2	0	3	0	1	0
Head Down Deposit				Pectinariidae		0	0	0	0	0	3	0	0	0	0	0	0	0	0	0	1	0	0	0	0
Predatory				Pholoidae		0	0	0	0	1	0	0	0	0	0	0	0	0	0	0	0	0	0	0	0
Predatory				Phyllocicidae		0	0	0	0	0	0	0	0	0	0	10	0	0	0	0	3	0	0	0	0
Filter				Sabellidae		0	0	0	0	0	0	2	0	0	0	8	0	1	0	0	2	0	0	0	0
Head Down Deposit				Scalibregmidae		0	0	0	0	0	0	0	0	0	0	1	0	0	0	0	0	0	0	0	0
Predatory				Sigalionidae		2	0	1	0	0	0	0	0	0	0	0	0	0	0	0	2	0	0	0	0
Surface Deposit				Sphaerodoridae		0	0	0	0	0	0	0	0	0	0	5	1	0	0	0	0	0	0	0	0
Surface Deposit				Spionidae		4	4	0	1	4	2	0	0	0	0	2	3	0	1	0	8	0	0	0	0
					Polydora sp.	0	3	2	0	0	0	0	0	0	0	0	0	0	0	0	0	0	0	0	0
Predatory				Syllidae		15	3	1	0	0	9	0	0	0	0	2	2	3	0	0	14	2	0	0	0
Surface Deposit				Terebellidae		0	0	0	0	0	1	0	0	0	0	1	0	0	0	0	0	0	0	0	0
Surface Deposit				Trichobranchidae		0	0	0	0	0	1	0	0	0	0	4	0	0	0	0	1	0	0	0	0
		Oligochaeta				1	0	0	0	0	0	0	0	0	0	0	0	0	0	0	0	0	0	0	0
	Arthropoda					0	0	0	0	0	0	0	0	0	0	1	0	0	0	0	1	0	0	0	0
Predatory		Acari				0	0	0	0	0	0	0	0	0	0	0	0	0	0	0	3	0	0	0	0
Surface Deposit		Ostracoda				0	0	0	0	0	0	0	0	0	0	8	1	1	0	0	3	0	0	0	0
Surface Deposit and Filter		Malacostraca	Tanaidacea	Akanthophoreidae		0	0	0	0	0	0	0	0	0	0	0	0	0	0	0	2	0	0	0	0
					Stenotanais sp.	0	0	0	0	0	0	0	0	0	0	0	0	0	0	0	1	0	0	0	0
					Akanthophoreus nr. gracilis	1	0	0	0	0	0	0	0	0	0	4	0	0	0	0	0	0	0	0	0
Surface Deposit and Filter				Anarthruridae		0	0	0	0	0	1	0	0	0	0	0	0	0	0	0	0	0	0	0	0
Surface Deposit and Filter				Paratanoidea incerta sedis	Leptognathioides nr. polita	0	5	0	0	0	0	0	0	0	0	0	0	0	0	0	0	0	0	0	0
Surface Deposit and Filter				Pseudotanaididae	Pseudotanais sp.	0	0	0	0	0	1	0	0	0	0	0	0	0	0	0	0	0	0	0	0
Surface Deposit and Filter				Typhlotanaididae	Peraeospinosus sp.	0	0	0	0	0	5	0	0	0	0	0	0	0	0	0	0	0	0	0	0
Surface Deposit and Filter			Amphipoda	Aoridae	Lembos sp.?	0	0	0	0	1	0	0	0	0	0	0	0	0	0	0	0	0	0	0	0
				Corophiidae	Leptocheirus sp.	0	2	0	0	0	0	0	0	0	0	0	0	0	0	0	0	0	0	0	0

Feeding Guild	Phylum	Class/Subclass	Order	Family	Genus/Species	M1					M2					M3					M4				
						0-1	1-2	2-3	3-4	4-5	0-1	1-2	2-3	3-4	4-5	0-1	1-2	2-3	3-4	4-5	0-1	1-2	2-3	3-4	4-5
				Isaeidae		1	0	0	1	0	0	0	0	0	0	0	0	0	0	0	0	0	0		
				Lysianassidae		0	0	0	0	0	1	0	0	0	0	0	0	0	0	0	0	0	0		
				Oedicerotidae		0	0	0	0	0	0	0	0	0	2	0	0	0	0	0	0	0	0		
				Phoxocephalidae		0	0	0	0	0	1	0	0	0	0	1	0	0	0	0	0	0	0		
				Stenothoidae		1	0	0	0	0	0	0	0	0	0	0	0	0	0	0	0	0	0		
Surface Deposit and Filter			Isopoda	Desmosomatidae	Eugerda sp.	0	0	0	0	0	0	0	0	0	1	0	0	0	0	0	0	0	0		
					Chelator sp.	0	0	0	0	0	0	0	0	0	3	0	0	0	0	1	0	0	0		
Surface Deposit and Filter				Gnathiidae		0	0	0	0	0	0	0	0	0	0	0	0	0	1	0	0	0	0		
					Gnathia nr. triloba	0	0	0	0	1	0	0	0	0	0	0	0	0	0	0	0	0	0		
					Gnathia sp.	0	0	0	0	1	0	0	0	0	0	0	0	0	0	0	0	0	0		
Surface Deposit and Filter				Munnidae	Munna stephenseni	1	0	0	0	0	0	0	0	0	0	0	0	0	0	0	0	0	0		
Surface Deposit and Filter				Paranthuridae		0	0	0	0	0	0	0	0	0	1	0	0	0	0	0	0	0	0		
Surface Deposit and Filter			Cumacea	Diastylidae	Ehtonodiastylis nr. nimia	0	0	0	0	0	0	0	0	0	5	0	0	0	0	1	1	0	0		
Surface Deposit		Copepoda	Harpacticoida			6	5	1	3	0	164	1	0	0	247	2	3	2	0	95	5	1	0		
Filter	Chordata	Ascidiacea				0	0	0	0	0	7	0	0	0	2	0	0	0	0	17	0	0	0		
Filter	Cnidaria	Anthozoa	Hexacorallia	Actiniaria		0	0	0	0	0	0	0	0	0	0	1	0	0	0	0	0	0	0		
Photosynthetic	Ochrophyta	Bacillariophyceae	Diatoms			0	0	0	0	0	210	49	0	0	115	250	0	0	0	80	0	0	0		
Predatory	Foraminifera					45	44	41	52	69	157	105	24	111	96	249	190	123	71	18	422	115	149	62	
Predatory	Kinorhyncha					0	0	0	0	0	12	0	0	0	60	1	0	0	0	14	0	0	0		
Filter	Mollusca	Bivalvia				0	0	0	0	0	1	0	0	0	13	2	0	0	0	4	0	0	0		
				Mytilidae		0	0	0	0	0	0	0	0	0	0	1	0	0	0	0	0	0	0		
				Pectinidae		0	0	0	0	0	0	0	0	0	1	0	0	0	0	0	0	0	0		
				Thyasiridae		0	0	0	0	0	0	0	0	0	1	0	0	0	0	0	0	0	0		
					Mendicula ferruginosa	0	0	0	0	0	0	0	0	0	1	2	0	0	0	0	0	0	0		
					Thyasira nr. cygnus?	0	0	0	0	0	0	0	0	0	0	0	2	0	0	0	8	1	0		
				Yoldiidae	Yoldiella spp.	0	0	0	0	0	3	0	0	0	1	0	0	0	0	4	0	0	0		
					Portlandia intermedia	0	0	0	0	0	0	0	0	0	3	0	0	0	0	0	0	0	0		
Predatory		Solenogastres				0	0	0	0	0	0	0	0	0	0	0	0	0	3	0	0	0	0		
Surface Deposit and Predatory	Nematoda					0	5	0	5	0	47	0	2	1	163	140	10	18	3	107	126	27	12		
Predatory	Nemertea					7	2	0	0	0	7	0	0	0	3	1	0	0	0	2	2	0	0		
		Heteronemertea				0	0	0	0	0	0	0	0	0	2	0	0	0	0	0	0	0	0		
Surface Deposit, non-parasitic	Platyhelminthes					0	0	0	0	0	1	0	0	0	0	0	0	0	0	0	0	0	0		
Predatory	Priapulida					0	0	0	0	0	0	0	0	0	11	0	0	0	0	3	0	0	0		
Surface Deposit	Sipunculidae					0	0	0	0	0	0	0	0	0	1	0	0	0	0	9	1	0	0		
Total Abundance						348					1074				1885					1607					



### **Department of the Interior (DOI)**

The Department of the Interior protects and manages the Nation's natural resources and cultural heritage; provides scientific and other information about those resources; and honors the Nation's trust responsibilities or special commitments to American Indians, Alaska Natives, and affiliated island communities.



### **Bureau of Ocean Energy Management (BOEM)**

The mission of the Bureau of Ocean Energy Management is to manage development of U.S. Outer Continental Shelf energy and mineral resources in an environmentally and economically responsible way.

### **BOEM Environmental Studies Program**

The mission of the Environmental Studies Program is to provide the information needed to predict, assess, and manage impacts from offshore energy and marine mineral exploration, development, and production activities on human, marine, and coastal environments. The proposal, selection, research, review, collaboration, production, and dissemination of each of BOEM's Environmental Studies follows the DOI Code of Scientific and Scholarly Conduct, in support of a culture of scientific and professional integrity, as set out in the DOI Departmental Manual (305 DM 3).